Angulins and the Tricellular Tight Junction: Role in Inflammatory Bowel Diseases

Inaugural-Dissertation

to obtain the academic degree

Doctor rerum naturalium (Dr. rer. nat.)

submitted to the Department of Biology, Chemistry, Pharmacy

of Freie Universität Berlin

by

Jia-Chen E. Hu

Berlin, 2020

The dissertation was carried out from October 1st, 2017 to December 31st, 2020 under the supervision of PD Dr. Susanne M. Krug and Prof. Dr. Michael Fromm in the Institut für Klinische Physiologie / AB Ernährungsmedizin, Charité – Universitätsmedizin Berlin, Campus Benjamin Franklin.

1st Reviewer: PD Dr. Susanne M. Krug

Institut für Klinische Physiologie / AB Ernährungsmedizin

Charité – Universitätsmedizin Berlin, Campus Benjamin Franklin

2nd Reviewer: Prof. Dr. med. Rudolf Tauber

Institut für Laboratoriumsmedizin, Klinische Chemie und Pathobiochemie

Charité – Universitätsmedizin Berlin, Campus Virchow-Klinikum

I hereby declare that I have written this doctoral thesis independently. The figures or resources that were taken from other sources are duly cited in the text. The contents of this thesis, either in full or in part, have never been submitted at this or any other university.

Date of defence: 19.04.2021

Acknowledgement

First and foremost, I would like to thank PD Dr. Susanne Krug and Prof. Dr. Michael Fromm for offering the opportunity to perform my doctoral thesis in their labs, which were funded by the Deutsche Forschungsgemeinschaft Research Training Group "TJ-Train", GRK 2318.

My primary supervisor, PD Dr. Susanne Krug provided not only an attractive project, but also constant help to all kinds of questions. She acted as an extraordinary role model of scientist to me, who had started with little experience in the scientific area.
A gratitude also belongs to my secondary supervisor, Prof. Dr. Michael Fromm, for his continuous advice and help and for sharing his knowledge as well as his resources.

I would also like to thank Prof. Dr. Rudolf Tauber for the kind willingness of supervising this work. My mentor, Prof. Dr. Geoffrey Sandle, I want to thank not only for his great suggestions to this work, but also for enlightening me the essence of PhD.

My thanks must go to the central endoscopy department of Campus Benjamin Franklin, Charité – Universitätsmedizin Berlin, especially Dr. Federica Branchi, PD Dr. Christian Bojarski, Dr. med. Michael Schumann and Dr. med. Christoph Treese. Without their help this work would undoubtedly never have been accomplished.

I would like to thank PD Dr. Rita Rosenthal for her dedication as the scientific coordinator of the Research Training Group 2318 and for her meaningful discussion during group meetings.

Furthermore, I want to thank In-Fah Lee, Anja Fromm, and Britta Jebautzke for their methodological support and experiential suggestions. The entire group is also what I would like to thank for the constant cooperation and delightful atmosphere.

Last but not least, I would like to thank my family for their understanding and support. I want to thank my friends, Dr. Rain and Dr. Yan Liu, for their immediate responsiveness to my technical problems and literature requests. Special thanks belong to my beloved friend who accompanied me into darkness through this whole way, but more importantly who showed me the genuineness and beauty of life and restored my faith to humanity.

Content

1 Introduction

1.1 Tight junctions

As one of the four basic tissue types, epithelia are the interface of inner and outer environment of the body. In this, they function both as a protective barrier and transport-mediators across the cell layer. For molecules, there are two ways of passing through epithelia: transcellular transport by specific transmembrane proteins and paracellular transport which is a passive movement across the space between adjacent cells (**Figure 1a**).

Based on the proportion of transepithelial flux via the paracellular route, epithelia could be classified as tight epithelia, in which transcellular transport behaves as a major pathway for example in distal segments of the intestine, and leaky epithelia as typically found in the proximal intestine, in which the paracellular pathway becomes a path of greater importance (Claude and Goodenough, 1973).

The function of the paracellular route is mainly achieved by the junctional complex between polarized epithelial cells (Denker and Nigam, 1998), comprising four structures, from the basal to the apical side in order, desmosomes, gap junctions, adherens junctions and tight junctions (TJ, Zonula occludens) (**Figure 1b, c**). Desmosomes are small contact regions between lateral membranes of neighbouring cells. Gap junctions are connections between contiguous cells, which allow the exchange of molecules smaller than 1000 Da. Adherens junctions are connected to the actin skeleton and attach neighbouring cells to each other.

Of all these four components of the junctional complex, the TJ holds the most apical position between the lumen and the intracellular space and is considered as determinant of the paracellular transport. Therefore, on one hand, it behaves as a “fence” that divides the apical membrane from the basolateral membrane of polarized cells and regulates the movement of membrane constituents from apical side to basolateral domain (Diamond, 1977), and on the other hand, the TJ also has a “gate function” that controls the passage of water, ions, small water-soluble molecules and – under certain circumstances – macromolecules into intercellular spaces (Farquhar and Palade, 1965).

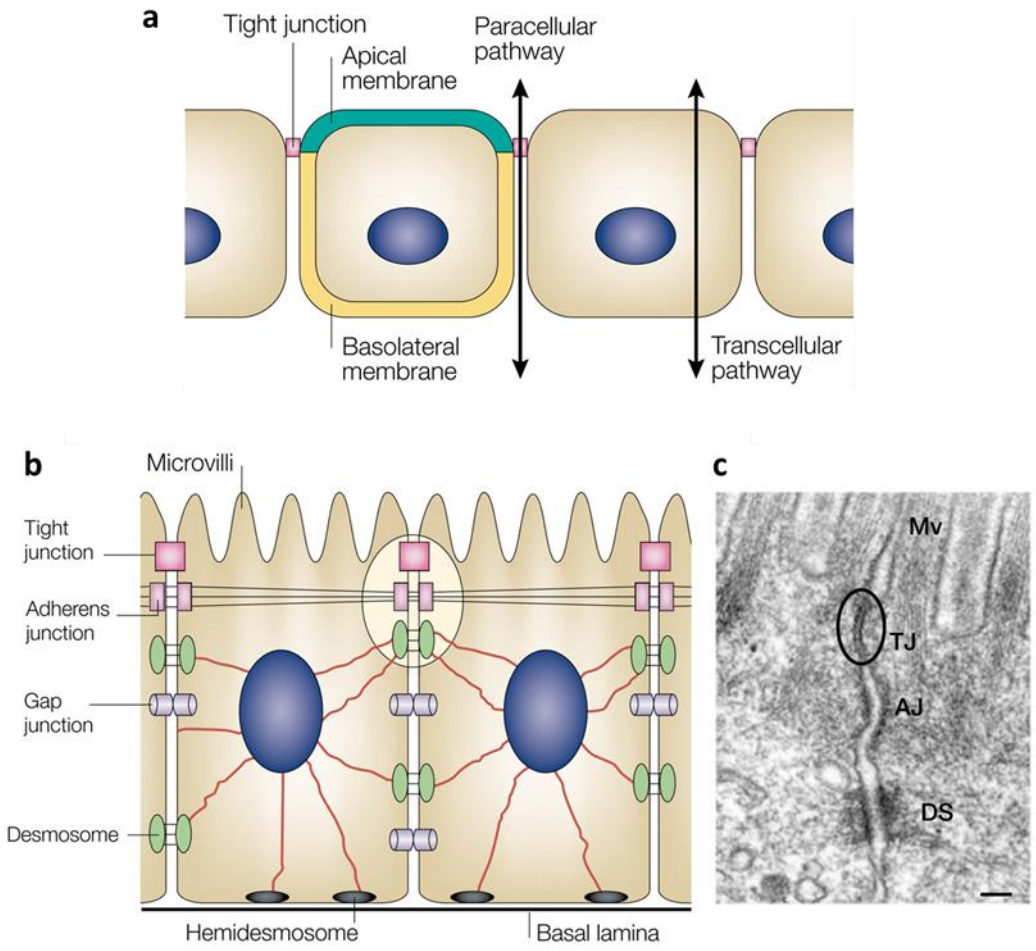

Figure 1 *Transport pathways and junctional complex.* ***(a)*** *Schematic diagram of the transcellular and paracellular pathway through epithelia.* ***(b)*** *Schematic representation of intestinal epithelial cells.* ***(c)*** *Electron micrograph of the junctional complex in murine intestinal epithelial cells. Scale bar = 200 nm. Mv = microvilli, TJ = tight junction (circled), AJ = adherens junction, DS = desmosome. (Tsukita et al., 2001).*

The morphological structure of the TJ was first described over half a century ago as fused outer membranes of adjacent cells (Farquhar and Palade, 1963). With the application of freeze fracture electron microscopic technique, the belt-like meshwork strands of TJs were exhibited (Staehelin et al., 1969), which should refer to the TJs between two epithelial cells, namely the bicellular TJ (bTJ) (as marked in **Figure 2**). In the region where three or more cells meet, TJ strands are differently organized and termed the tricellular TJ (tTJ). Here the most apical bTJs converge and extend to the

basal direction forming a 10 nm wide and 1 µm long central tube (Staehelin, 1973) (**Figure 2**, arrow heads), which since then has been considered to be a structural weak point of the paracellular barrier.

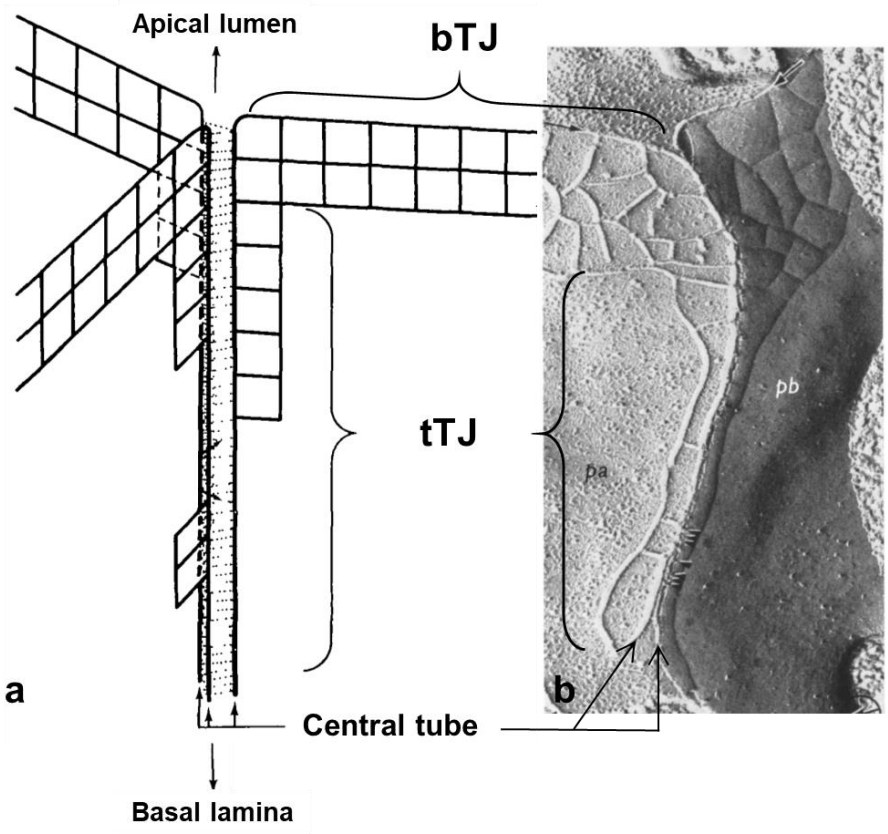

Figure 2 *Schematic drawing* ***(a)*** *and freeze fracture electron micrograph* ***(b)*** *of the bTJ (transverse bracket) and the tTJ (vertical bracket). The central tube is pointed by a group of arrow heads. (modified from Staehelin, 1973).*

Until now, a number of TJ proteins have been discovered and are grouped into four families: (1) the claudin family including 27 members in mammals (Mineta et al., 2011), (2) junctional adhesion molecules (JAM) (Martin-Padura et al., 1998), (3) TJ-associated MARVEL proteins (TAMP) comprising three members, occludin (Furuse et al., 1993), tricellulin (Ikenouchi et al., 2005), and myelin and lymphocyte and related proteins for vesicle trafficking and membrane link (MARVEL) D3 (Steed et al., 2009, Raleigh et al., 2010), and (4) the angulin family containing three members (Higashi et al., 2013).

Functionally, claudins could be roughly divided into four sub-groups: (i) cation-selective channel-forming claudins (e.g. claudin-2, -10b, -15), (ii) anion-selective channel-forming claudins (e.g. claudin-10a, -17), (iii) water-channel-forming claudins (claudin-2, -15) and (iv) barrier-forming claudins (e.g. claudin-1, -3, -4, -8) (Krug et al., 2014). Depending on combination and proportion, they enable different barriers to have distinct function. For example, in the duodenum the overall expression of barrier-forming claudins is lower than in the colon, whereas the cation and water channel-forming protein, claudin-2, has an abundant expression in small intestine but only remote amounts in crypts of colon (Markov et al., 2010). This increase of tightening claudins from proximal to distal intestine fits to the diverse function of these intestinal segments that most of the ion and water transport takes place in the small intestine whereas the large intestine performs a fine tuning. Dysregulation of TJ proteins could cause or be caused by corresponding diseases due to altered paracellular passage of water, solute, and macromolecules (Krug et al., 2014). As an example, upregulation of claudin-2 under intestinal inflammatory conditions results in an increased diffusion of cations and water, leading to a so-called leak-flux diarrhoea (Sandle, 2005).

1.2 Tricellular tight junction proteins

At the region where three or more cells meet, the closely gathered bTJ strands elongate towards the basal lamina in parallel instead of fusing together, which would consequently leave an extra space in between of the vertical strands (Wade and Karnovsky, 1974). That is to say, the central tube, as an assumed weak spot, could serve as a potential route for transepithelial fluxes.

As for molecular composition, there are two major components of tTJs, tricellulin comprising four transmembrane domains and the angulin family which passes the cell membrane only once (Masuda et al., 2011, Higashi et al., 2013) (**Figure 3**). Tricellulin is the first component found to have a predominant localization at tTJs (Ikenouchi et al., 2005). Six years later, a novel role of lipolysis-stimulated lipoprotein receptor (LSR) was identified as a tTJ protein (Masuda et al., 2011), followed by the discovery of its two homologous-gene-encoded proteins forming the angulin family and also mainly localizing at tTJs (Higashi et al., 2013).

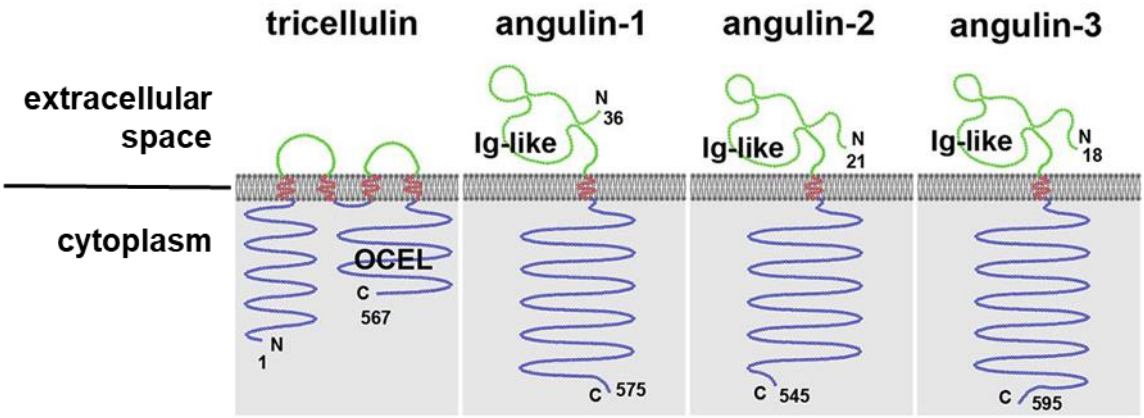

Figure 3 *Molecular comparison of tTJ proteins. OCEL = occludin ELL-like domain, Ig-like = immunoglobulin-like domain. (modified from Higashi and Miller, 2017).*

1.2.1 Tricellulin

Tricellulin, also known as MARVEL D2, is a tetraspan membrane protein with an N-terminal and a C-terminal cytoplasmic region, first described in 2005 (Ikenouchi et al., 2005). It localizes primarily at tTJs and has a ubiquitous expression in epithelial cells (Ikenouchi et al., 2005).

Tricellulin is essential for maintaining an intact TJ structure as well as barrier function. Knockdown of tricellulin induces, on one hand, morphological reconstruction characterizing by the disorganization of bTJs and tTJs, and on the other hand, functional change representing by a decrease of transepithelial resistance (TER) and an increase flux of 4 kDa fluorescein isothiocyanate-dextran (FITC-dextran, FD) (Ikenouchi et al., 2005). Reversely, overexpression experiments indicated that tricellulin was responsible for regulating the passage of macromolecules (Krug et al., 2009b). When tricellulin was overexpressed only at tTJs, the permeability for small ions was unaltered, however, there was an extensive reduction of the permeability for macromolecules up to 20 kDa. As a direct evidence, fluorescence live-cell imaging visualized the passage of macromolecules as 3 kDa dextran at tTJs (Krug et al., 2009b).

Previous studies showed that bacteria and their products could disturb the paracellular barrier by targeting or regulating tricellulin (Nomura et al., 2014, Morampudi et al., 2016, Markov et al., 2019, Eum et al., 2014). Given the assumption that tTJs presumed to be

the break point of the overall TJ barrier, it is plausible to speculate that tricellulin acts a crucial part in preventing the crack of pathogens and immunogens.

1.2.2 Angulins

Angulins are the most recently identified protein family of TJs, composed of three proteins known before as (i) LSR, (ii) immunoglobulin-like domain-containing receptor 1 (ILDR1), and (iii) ILDR2 (Higashi et al., 2013). Angulins are defined as a protein family in consideration of their homology and localization at tTJs. Functionally, they share the capability of recruiting tricellulin to tTJs.

Angulin-1 (also known as LSR) was initially recognized as a rate-limiting step in the progress of lipid clearance (Yen et al., 1994). Later, using a retrovirus-based cDNA screening, angulin-1 was identified to have a primary localization at tricellular contacts, which was then verified to be tTJs by immunofluorescence co-staining and immune-freeze-fracture replica electron microscopy (Masuda et al., 2011).

Angulin-1 could recruit tricellulin to tTJs, evidenced by a serial of experiments: 1) when tricellulin was knockdown, the localization of angulin-1 at tTJs was unaffected; 2) oppositely, tricellulin was no longer concentrated at tTJs after extremely suppressing angulin-1 expression; and 3) with re-expression of angulin-1, tricellulin regained its position at tTJs (Masuda et al., 2011). Furthermore, this recruitment effect could not be reproduced with the absence of C-terminal cytoplasmic domain of tricellulin or the cytoplasmic region of angulin-1 (Masuda et al., 2011).

As for barrier function, knockdown of angulin-1 led to an increased permeability to fluorescein and macromolecules up to 40 kDa and a decreased TER, which could be retrieved by its re-expression (Masuda et al., 2011, Higashi et al., 2013), indicating that angulin-1 was also essential for sustaining the epithelial barrier.

Up to date, angulin-1 has been linked to lipid metabolic abnormality (El Hajj et al., 2019, Xie et al., 2018b, Akbar et al., 2016), Alzheimer's disease (Xie et al., 2018a), and various cancers including gastric (Sugase et al., 2018), ovarian (Hiramatsu et al., 2018), endometrial (Shimada et al., 2017b, Shimada et al., 2017a, Shimada et al., 2016b), breast (Reaves et al., 2017, Reaves et al., 2014), and colon cancer (García et al., 2007). For example, angulin-1 expression could serve as a potential prognostic biomarker for colon cancer (García et al., 2007) and a decreased angulin-1 level was

related to enhanced cell invasion (Shimada et al., 2017b). Like tricellulin, bacteria also targeted angulin-1 in order to get through the apical barrier. *Clostridium perfringens*-produced iota toxin could bind to N-terminal of angulin-1 and transport via endosomal trafficking leading to cytotoxicity (Nagahama et al., 2018). *Clostridium difficile* is an enteric pathogen which could cause serious diarrhoea. *Clostridium difficile* transferase (CDT) is a frequent toxin produced by hypervirulent strains and could target angulin-1 as a host cell receptor by directly bounding to its extracellular immunoglobulin-like (Ig-like) domain contributing to the invasion of host cells and the collapse of cytoskeleton (Hemmasi et al., 2015).

Angulin-2 (also known as ILDR1) was first identified in 2004 with a 30 % homology to angulin-1 and a membranal localization of its two of three variants (Hauge et al., 2004). Apart from an large involvement in hearing loss (Borck et al., 2011, Diaz-Horta et al., 2012, Nagtegaal et al., 2019), angulin-2 has been reported to be controversial in regulating paracellular water transport (Gong et al., 2017, Hempstock et al., 2020). Knock-out of *Ildr1* in mouse kidney resulted in an increased permeability to water causing renal concentrating defect and subsequently polyuria, while overexpression of *Ildr1* in renal epithelial cells led to a decreased paracellular water permeability (Gong et al., 2017). However, a more recent study where the localization of angulin-1 and -2 were also investigated showed that shifted localization of angulin-1 might have compensated for the barrier function and therefore the overall water transport was not affected (Hempstock et al., 2020).

Angulin-3 (also known as ILDR2) was related to type 2 diabetes at first (Dokmanovic-Chouinard et al., 2008). Using single-cell RNA sequencing technique, the deficiency of angulin-3 gene was identified to be involved in the injury of cytoskeleton (Lu et al., 2017). Angulin-3 was also presented an increased expression in inflamed inflammatory bowel disease patients' tissues by immunohistochemistry (IHC) and a beneficial react in rheumatoid arthritis model by inhibiting T cell activation (Hecht et al., 2018).

Regarding localization, angulin-1 and -2 are complementarily expressed in various epithelia in spite of a couple of overlap, whereas angulin-3 could be found mainly surrounding neural tissues (Higashi et al., 2013). Furthermore, in each epithelium, there was at least one angulin localizing at tricellular contacts (Higashi et al., 2013).

As for the barrier function, both angulin-2 and -3 exhibited the ability to recruit tricellulin to the tTJ, yet their barrier functions are not identical to angulin-1 representing by different recovery levels of TER as well as permeability to flux tracers (Higashi et al., 2013).

1.3 Inflammatory bowel disease (IBD)

Inflammatory bowel disease (IBD), consisting of ulcerative colitis (UC) and Crohn's disease (CD), is a group of chronic idiopathic relapsing and remitting gastrointestinal conditions. Up to 21st century, although the incidence of IBD in western countries has stabilized, its prevalence remains climbing and has already exceeded 0.3 %; meanwhile in developing regions like Asia and South America on the other hand, an increasing incidence of IBD has emerged (Ng et al., 2017, Kaplan and Ng, 2017).

Although IBD could occur almost at any age, most patients get their diagnosis between 30s and 40s, even five to ten years earlier for CD patients (Burisch and Munkholm, 2015). As for mortality, patients with CD were reported to have a higher standardized mortality ratio (SMR) of 1.14 to 1.52 than the general population (Canavan et al., 2007, Duricova et al., 2010, Manninen et al., 2012, Bewtra et al., 2013, Aniwan et al., 2018), whereas in UC the all-cause SMR showed no difference in comparison to the general population (0.71 to 1.17) (Jess et al., 2007, Manninen et al., 2012, Bewtra et al., 2013, Aniwan et al., 2018). Due to the lack of cure, the treatment for IBD aims at controlling to gain and remain remission and to prevent complications. Taken together, the developing prevalence, rather low mortality, early disease onset, and short of cure for IBD pose a heavy burden to every health system of the world.

As the matter of aetiology, genetic predisposition, environmental factors, and intestinal microbiota are believed to contribute to the occurrence of IBD with the interaction of aberrant immune system (**Figure 4**). Until now, over 200 IBD-associated loci have been identified through Genome-wide association studies (GWAS). Studies in first-degree relatives of IBD (Roth et al., 1989) and in twins of CD (Keita et al., 2018) supported the primary defect due to genetic predisposition. Environmental determinants involve factors in multiple aspects of life influencing the occurrence and development of the disease, such as smoking (Sutherland et al., 1990, To et al., 2016a, To et al., 2016b), medicaments (Cornish et al., 2008, Moninuola et al., 2018, Zou et al., 2020),

and diet (Persson et al., 1992, Jantchou et al., 2010, Ananthakrishnan et al., 2013). Regarding the microbiome, numerous studies provided convincing evidence of the involvement. Colonic bacteria were essential for inducing colitis in genetically susceptible mice (Veltkamp et al., 2001). Faecal transplantation has become an effective management of CD, and specific microbiota were reported to be an influencer of the course of IBD as well as a biomarker in therapy response prediction and the risk of recurrence (Ananthakrishnan et al., 2017, Yilmaz et al., 2019, Sokol et al., 2020). However, none of the factors seems to be indispensable and the exact mechanisms of pathogenesis of IBD still need to be explored.

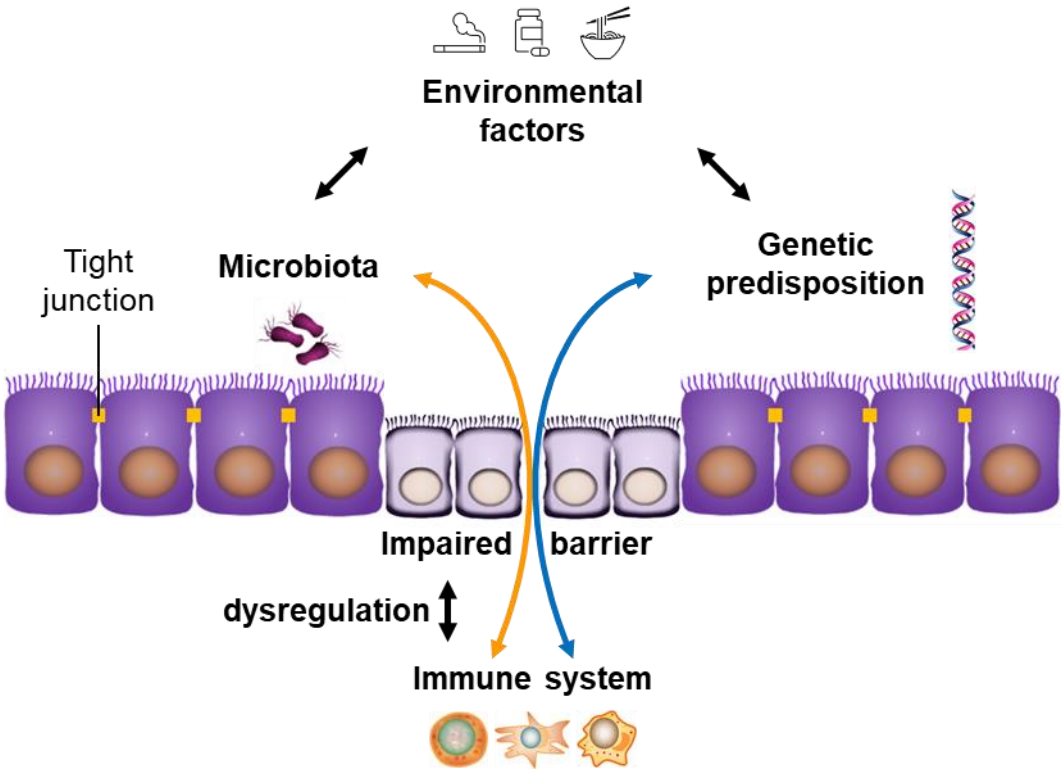

Figure 4 *Risk factors of the pathogenesis of IBD. The occurrence of IBD is assumed to be the leverage of genetic, environmental, and microbial factors with complex interactions with the immune system miscommunicated with the intestinal epithelial barrier.*

Intestinal epithelial cells are constantly in the process of shedding and replenishing, proliferating, and differentiating, as well as absorbing necessary elements while preventing unwanted entering. As the source of nutrients, the gastrointestinal tract has to fulfil the function of digestion and absorption when facing a surfeit of antigens and toxic substrates within the lumen, which indubitably requires an intact and functional barrier to hold in between.

The TJ is considered to be a critical component of the physical barrier. In IBD, the TJ changed in ultrastructure, expression, and localization. In active CD, freeze fracture analysis showed that TJ strands alone with the depth of its main meshwork were reduced, and the breaks or interruptions of the strands greatly were increased (Zeissig et al., 2007). At protein expression level, channel-forming claudin-2 was observed to be upregulated in both UC (Heller et al., 2005, Oshima et al., 2008) and CD (Zeissig et al., 2007). Claudin-4 and -7 were downregulated in UC (Oshima et al., 2008) while claudin-3, -5 and -8 in CD (Zeissig et al., 2007). The TAMP family member occludin was also found to be lower in both types of IBD (Zeissig et al., 2007, Heller et al., 2005) while tricellulin was found to be reduced in active UC (Krug et al., 2018). Regarding localization, in CD, claudin-5 was delocalized from the TJ to the lateral cell membrane (Zeissig et al., 2007) and tricellulin was shifted from depth of crypts to the surface epithelium (Krug et al., 2018). These changes of TJ fall into the impacts described above: (i) increased paracellular passage of water and solutes leading to classical leak flux diarrhoea and (ii) increased paracellular passage of macromolecules causing an enhancement of antigen uptake.

However, whether the barrier dysfunction inclines to be the trigger or the consequence of IBD is difficult to define and using this monogenesis to explain seems also unrealistic. A recent hypothesis suggested a dysregulation between immune system and intestinal epithelial cells which on one hand reacted to microbiome and then communicated with immune system, and on the other hand adjusted epithelial barrier according to instructions from immune cells (Martini et al., 2017). Therefore, the molecular factors in between are of great importance to discover.

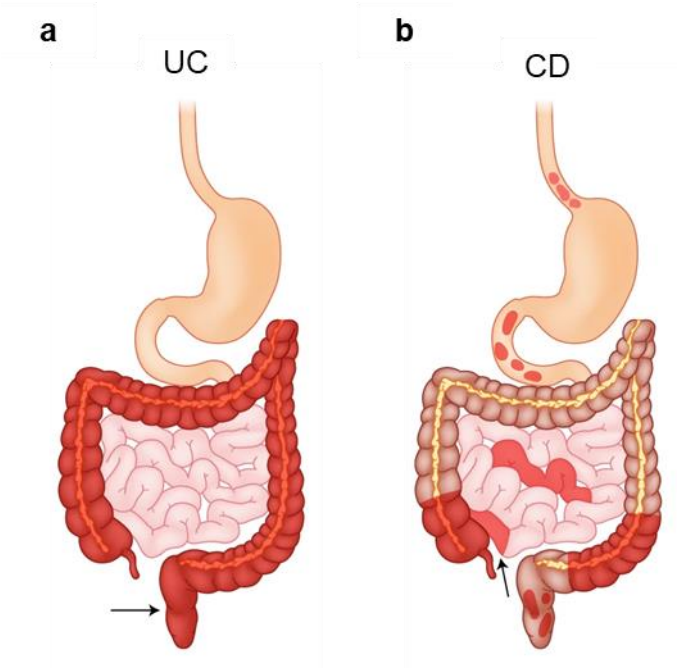

Figure 5 *Clinical features of IBD.* ***(a)*** *Continuous inflammation in UC starting from the rectum (arrowhead, the most common affected segment) until farthest terminal ileum.* ***(b)*** *Segmental inflammation in CD with the possible emergence in the whole digestive tract. The arrowhead pointed the frequent region, the terminal ileum. (Neurath, 2019).*

1.3.1 Ulcerative colitis (UC)

As one major type of IBD, ulcerative colitis (UC) was first reported in late 1800s, describing as idiopathic colitis with superficial ulcers of the colon and discharge of blood and mucus (Wilks and Moxon, 1889). This concept of UC up to now has developed to colonic inflammation that initiates from the rectum and continuously affects the proximal segments (**Figure 5a**). Based on the involved region in colon, UC could be classified as proctitis which is limited to rectum, left-sided colitis which compromises until splenic flexure, and extensive colitis which could affect the whole colon (Silverberg et al., 2005). The most common symptom is bloody diarrhoea, with more affected intestinal duct, patients with UC may suffer from abdominal cramping and even constitutional symptoms such as fever and fatigue.

In spite of a slight preference of male (Murakami et al., 2019) or female (Selvaratnam et al., 2019) in the occurrence of UC reported, there is no significant gender difference

on the whole (Ungaro et al., 2017). Most of UC patients gets diagnosed at their 30s and a second peak was reported at 60s to 70s (Carroll et al., 2019, Jones et al., 2019, Mak et al., 2019, Ciapponi et al., 2020). The risk factors of the disease include familial predisposition (Moller et al., 2015), smoking (Ananthakrishnan, 2015), certain drug uses like current use of oral contraceptives (Wang et al., 2019) and hormone replacement therapy (Khalili et al., 2012), while on the contrary appendectomy (Sahami et al., 2016) and breastfeeding (Xu et al., 2017) seem to have a protective effect.

The intestinal epithelial barrier is one of the targets of the inflammation and in theory also plays a role in initiating the disease. As the interface of the internal body and external environment, the intestinal epithelial barrier on one hand absorbs and digests variants nutrients and on the other hand prevents unwanted entering of antigens and toxic substrates within the intestinal lumen. In order to fulfil these functions, there is no doubt that the barrier has to be intact and fully functional. As described above, tTJ protein tricellulin is not only critical for the maintaining the overall TJ structure and barrier function, but also plays a crucial role in the passage of macromolecules (Krug et al., 2009a).

In active UC, tricellulin was shown to be downregulated and an impaired intestinal barrier function exhibited as a decreased epithelial resistance along with an increased permeability for fluorescein and FD 4 kDa was observed in a recent study (Krug et al., 2018).

These findings raised the classical hen-or-egg question in the pathogenesis of UC: whether the downregulation of tricellulin is the reason of an increased luminal antigens uptake which succeedingly activates and supports the immune reaction or, the other way around, is only the consequence of the impaired barrier. To elucidate this relation between the downregulated tricellulin and the impaired barrier function might provide an insight to the pathophysiology of UC and potentially imply the upcoming relapse. Meanwhile, in CD, the other major type of IBD, a shift of the localization of tricellulin was demonstrated with an unchanged expression level of tricellulin (Krug et al., 2018), and angulin-1 which is responsible for the correct localization of tricellulin was downregulated in CD and could endamage the barrier function (Hu et al., 2020). In this context, whether angulins are also involved in the relapse of UC needs to be investigated.

In UC, studies have also demonstrated the role of pro-inflammatory cytokines, especially produced by T helper (T_h) 2 cells, during the pathogenesis of the disease. For example, lamina propria mononuclear cells (LPMCs) from UC patients release a significant higher amount of pro-inflammatory cytokine interleukin-13 (IL-13) compared with controls, which could then alter TJs, represented by the upregulation of claudin-2 that leads to a raise of solute and water passage and subsequently results in leak-flux diarrhoea (Heller et al., 2005). Latter research exhibited a decreased level of tTJ protein tricellulin and an increased passage of macromolecules, which could be induced by IL-13 through signaling pathways extracellular signal-regulated kinases (ERK) 1/2, c-Jun N-terminal kinases (JNK), and their common transcription factor activator protein 1 (AP-1) (Krug et al., 2018).

IL-13 is a cytokine discovered by a rich production of T_h2 cells in inflammatory conditions (Brown et al., 1989) and later it was revealed that innate immune cells such as eosinophils (Woerly et al., 2002), basophils (Smithgall et al., 2008), mast cells (Toru et al., 1998), natural killer (NK) cells and NK T cells (Fuss et al., 2004) were able to produce IL-13 as well. IL-13 is involved in a variety of mucosal inflammation, including UC (Heller et al., 2005), asthma (Huang et al., 1995), and several fibrotic disease like idiopathic pulmonary arterial hypertension (Daley et al., 2008) and systemic sclerosis (Hasegawa et al., 1997). Physiologically IL-13 is a supportive factor in antigen expulsion (Urban et al., 1998), but under pathological condition, the overwhelming of the cytokine becomes a damaging agent.

There are two receptors for IL-13 that have been reported. The IL-13 receptor α1 (IL-13Rα1) usually dimerizes with IL-4 receptor α (IL-4Rα), a receptor of IL-4 which is structurally resembling to IL-13, and signals mainly through signal transducer and activator of transcription (STAT) 6. The type 2 receptor IL-13Rα2 on the contrary functions as a monomer and has a higher affinity to IL-13 compared with type 1 receptor. Therapeutic biologicals regarding IL-13 include Pitrakinra, Anrukinzumab, and Tralokinumab. Pitrakinra, instead of being an antibody, is in fact a mutated human recombinant IL-4 protein that could prevent receptor complex formation between IL-4Rα and IL-13Rα1, which exerts negative effects on colitis (Palamides et al., 2016). Anrukinzumab, a monoclonal antibody that inhibits the binding between IL-13 and IL-4Rα, presents no improvement on active UC patients (Reinisch et al., 2015). Tralokinumab is a human IL-13-neutralizing IgG4 monoclonal antibody that has the capacity to block the

binding to both IL-13 receptors. The promising point was that clinical remission rate after Tralokinumab treatment increased from 6 % to 18 %, however, neither clinical response rate nor mucosal healing rate significantly improved (Danese et al., 2015). Inhibitory experiments of these two types of receptor in preceding research showed that IL-13 mediated claudin-2 upregulation through IL-13Rα1 while it downregulated tricellulin via IL-13Rα2 (Krug et al., 2018), which might explain the unsatisfactory results of the IL-13-related biologicals.

1.3.2 Crohn's disease (CD)

Crohn's disease (CD) is the other major type of IBD first reported as regional ileitis in 1932 (Crohn et al., 1932). Unlike UC which affects principally only colon, CD can involve the whole gastrointestinal tract, with terminal ileum being the most common affected segment (**Figure 5b**). Clinical presentation of CD could differ in patients, depending on involved location, severity of inflammation, and the presence and type of complications. Most frequent symptoms are right lower quadrant abdominal pain, chronic diarrhoea, and weight loss. CD has a higher incidence of extra-intestinal manifestation and complications compared with UC. A cohort study reported a ratio of perforated or stenosed complication within three months after diagnosis being nearly one fifth and a cumulative risk of complication at 20 years after diagnosis being over 50 % (Thia et al., 2010). Perianal diseases could be seen in almost one third of CD patients, onset ranging from 18 years pre-diagnosis to 33 years post-diagnosis (Eglinton et al., 2012). Endoscopically compared with UC, inflammation in CD is segmental instead of continuous, and lesions are rather transmural than superficial. According to disease location, CD could be classified as ileal, colonic, and ileocolonic disease, with isolated or combined upper gastrointestinal disease (Silverberg et al., 2005).

A complicated interaction between genetic predisposition, environmental exposure, and intestinal microbiota could eventually give rise to CD by disordered immune responses and impaired epithelial barrier function. The expression and morphology changes of bTJs in CD has been described above. About tTJ proteins, tricellulin was left unchanged in CD compared with healthy controls. Nevertheless, its predominant localization seemed to have increased in the surface epithelium and extended from apical areas to more basolateral domains (Krug et al., 2018). Although the regulatory mechanisms behind this shifting and the underlying components are still unexplored,

a reasonable hypothesis would be that the displacement of tricellulin might result from elements responsible for its correct localization.

1.3.3 Cytokines in CD

Cytokines consist of hundreds of small molecular proteins involved in miscellaneous immunological regulations not only under pathological conditions like IBD, but also in healthy individuals. Cytokines play a vital role in balancing immune function, but when excessively produced they can also exert pathological effects on immune system. The involvement of cytokines in IBD could date back to 1980s when IL-2 was described to have a reduced level correlating to a diminished response of T cells to cell surface antigens (Ebert et al., 1984). GWAS identifying susceptible loci concerning IL-6, IL-12, IL-17, IL-21, IL-23, tumour necrosis factor (TNF)-α, interferon (IFN)-γ and so on spot-lighted an indispensable character of cytokines in pathogenesis of IBD (Jostins et al., 2012). Additionally, multiple genetically modified animal colitis models, such as IL-2-deficient mice (Sadlack et al., 1993), IL-7 transgenic mice (Samaridis et al., 1991), IL-10-deficient mice (Kühn et al., 1993), supplemented the evidence of cytokines understanding in IBD. Regarding to the two subtypes of IBD, UC relates primarily to T_h2-related cytokines, while CD bounds closer to cytokines produced by T_h1 and T_h17 cells. This different profile of inflammatory cytokines between CD and UC may also explain their clinical heterogeneity and distinct pathological characteristics.

As for the source of cytokines, there are numerous immune and non-immune cells possessing the capability to respond to various antigen stimuli and produce abundant pro- or anti-inflammatory cytokines, including epithelial cells, adipocytes, stromal cells, dendritic cells (DCs), macrophages, neutrophils, fibroblasts, innate lymphoid cell (ILCs), and a variety of T cells. These cells, along with their cytokine products, build a sophisticated interlaced network through every course of IBD (**Figure 6**). Disruption of the existing homeostasis possibly triggers the initiation of the inflammation which could turn into a chronic stage when the balance fails to re-establish.

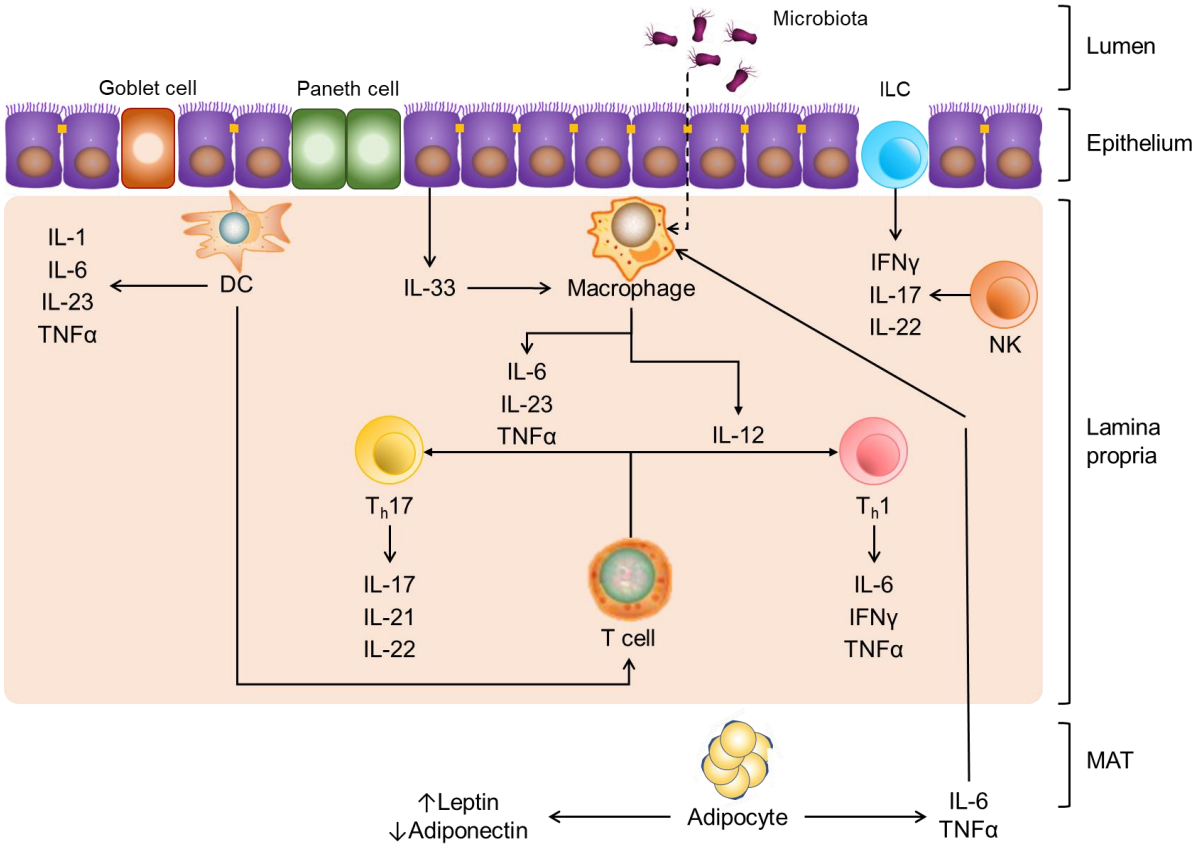

Figure 6 *Pro-inflammatory cytokine network in IBD. Cytokines from both innate immunity and adaptive immunity (specifically T_h1 and T_h17 cytokines) are involved in Crohn's disease. DC = dendritic cell, ILC = innate lymphoid cell, MAT = mesenteric adipose tissue, NK = natural killer cell. (For generation of the scheme, data from Trayhurn and Wood (2004) and Neurath (2017) were used).*

1.3.3.1 TNF-α

TNF-α has been deeply studied in IBD and the anti-TNF agent is the most classic biologic treatment for IBD. It is mostly produced by DCs, macrophages and differentiated T cells. Once produced, TNF-α is also capable of activate macrophages to produce other pro-inflammatory cytokines in return. CD patients was reported to have an elevated TNF-α level (Sartor, 2006). Exposure to TNF-α resulted in a shifting of occludin and increased paracellular permeability to FD 4 kDa via apoptosis and cell shedding (Juuti-Uusitalo et al., 2011).

1.3.3.2 The IL-1 family

The IL-1 family is a cytokine family of 11 members largely involved in innate immunity, of which seven are pro-inflammatory cytokines including IL-1α, -1β, -18, -33, -36α, -36β, and -36γ whereas four have anti-inflammatory properties (IL-1 receptor antagonist, IL-36Ra, IL-37 and IL-38). IL-1β plays a prominent role which does not have a general expression in healthy condition but could be rapidly induced through Toll-like receptor (TLR) signaling causing fever and immune activation (Piccioli and Rubartelli, 2013). Mucosal IL-1Ra to IL-1 ratio was declined and IL-1β was augmented in CD promoting innate immune system, both of which were correlated to the disease activity (Reinecker et al., 1993, Casini-Raggi et al., 1995, Dosh et al., 2019).

1.3.3.3 IL-6

IL-6 is another proinflammatory cytokine produced by lamina propria macrophages and $CD4^+$ T cells increasingly secreted in CD (Reinecker et al., 1993). After binding to its soluble receptor sIL-6R, the cytokine-receptor complex could bind to transmembrane protein gp130 and then activate antigen presenting cells (APCs) or T cells. A neutralizing protein to sIL-6R was able to ameliorate colitis activity and to induce apoptosis in adoptive transfer mice model, suggesting that one of the mechanisms of maintaining chronic inflammation in CD could be through prevention of T cell apoptosis (Atreya et al., 2000).

1.3.3.4 The IL-12 family

The IL-12 family consists of five members, IL-12, -23, -27, -35, and -39. IL-12 is a heterodimeric cytokine of p40 and p35 subunits, which could induce polarization of T cells and stimulate ILCs. It had a upregulated expression in LPMCs of CD compared with UC and controls (Monteleone et al., 1997). Resembling results were demonstrated with IL-23 which was a cytokine sharing the p40 subunit with IL-12 but also involved in T_h17 pathway and suppressing the activity of regulatory T cell (T_{Reg}) (Liu et al., 2011). In T cell transfer model of colitis, IL-23 tended to be the initiating factor contributing to inflammation and motivated the production of IL-6 and IL-17 by memory $CD4^+$ T cells (Yen et al., 2006).

1.3.3.5 IFN-γ

Interferons, besides their antiviral function, play a part in immunomodulation by promoting the activity of T_{Reg} and NK cells. In human, there are three types of interferons: type I contains the most members, IFN-α, -β, -ε, -ω, and -κ; type II and III are IFN-γ and IFN-λ respectively. IFN-γ is capable of catalysing major histocompatibility complex (MHC) on APCs and stimulating macrophages and lymphocytes to produce cytokines. In CD, lamina propria T lymphocytes secrete a remarkable amount of IFN-γ (Ghosh et al., 2006). It was reported that IFN-γ could lead to a decrease of transepithelial resistance, an increase of paracellular permeability to FD 3 kDa, and additionally the localization of occludin, claudin-1 and claudin-4 were redistributed (Bruewer et al., 2003).

1.3.3.6 T_h17 cytokines

In addition to T_h1 and T_h2 cells, T_h17 cells have also been identified as a latest T cell subset with the capability of IL-17A, IL-17F, IL-21, IL-22, and part of IFN-γ production. T_h17 cells are the major source of IL-17 family which comprises of six members, IL-17A to IL-17F. The prominent members of IL-17 are IL-17A and IL-17F that display 50 % sequence similarity and that are expressed as homodimers or co-expressed as heterodimer (Wright et al., 2007). IL-17 was also found to be increased in CD (Sartor, 2006). In dextran sulphate sodium (DSS)-induced colitis model, IL-17A knockout caused severer disease activity whereas IL-17F knockout moderated the symptoms (Yang et al., 2008), which might explain the disappointed outcome of IL-17 antibody treatment in CD patients.

IL-21, a cytokine belonging to the IL-2 family, is produced by T_h17 cells and in reciprocal is also able to stimulate the differentiation of T_h17 cells (Korn et al., 2007). IL-21-induced phosphorylation of STAT 1 and STAT 3 is essential for the differentiation of human naïve B cells (Recher et al., 2011). In CD, IL-21 was shown to have an increased expression regardless of subtypes of the disease when compared with UC and controls (Monteleone et al., 2005), which made IL-21 a potential target of new therapeutic strategy. Neutralizing IL-21 in adoptive transfer mice model showed an ameliorative effect resulting from decreased infiltration of neutrophils (Holm et al., 2018).

IL-22 comes from multiple sources in intestine, including ILCs, T cells, and NK cells, with a distinct expression in colon and small intestine (Mizoguchi, 2012). As a double agent in intestinal inflammation, on one hand, IL-22 promotes the production of mucus (Sugimoto et al., 2008), another character of intestinal barrier, stimulates regeneration of intestinal epithelial cells contributing to mucosal healing (Pickert et al., 2009); on the other hand, T cell-derived IL-22 was proven to be the pathogenesis of colitis in mice transfer model (Kamanaka et al., 2011). In active CD, IL-22 was found to have an elevated serum level (Zhang et al., 2017).

1.3.3.7 Leptin

Leptin is a special kind of cytokine secreted largely by white adipose tissue (WAT), therefore also classified as an adipokine. In terms of histology, there are two major types of adipose tissue, WAT and brown adipose tissue (BAT). BAT takes charge of thermoregulation whereas WAT is involved in energy storage as well as being a dynamic organ involved numerous physiological and metabolic processes. With excessive nutrition, adipocytes grow hypertrophic and become hyperplasia, which leads to cell apoptosis, hypoxia, macrophages infiltration and pro-inflammatory cytokines releasement (i.e. TNF-α, IL-1β and IL-6) (Trayhurn and Wood, 2004). Moreover, the WAT also possesses additional endocrine ability, secreting adipocytokines mainly leptin and adiponectin.

The adipose tissue could also be categorised anatomically into subcutaneous adipose tissue (SAT) and visceral adipose tissue (VAT), the latter being of greater importance in CD. Mesenteric adipose tissue (MAT) is the peri-intestinal part of VAT, which under pathological condition could change its morphology. For example, in CD, a particular characteristic was described from the beginning termed as creeping fat – the thickened mesenteric fat tissue adjacent to inflamed intestinal segments (Crohn et al., 1952) – which could be an important source of additional adipokines.

Leptin takes a part in both innate immunity by suppressing NK cells and activating monocytes, and adaptive immunity by promoting T cell proliferation and stimulating the production of cytokines (Abella et al., 2017). Under inflammatory condition, intestinal epithelial cells created an increasing amount of leptin which could then lead to the damage of epithelial wall and the infiltration of neutrophils (Sitaraman et al., 2004).

Interestingly, the existing data concerning serum leptin level in CD is highly inconsistent. Compared to controls, all possible regulatory directions have been reported, namely increased (Kahraman et al., 2017), unchanged (Frivolt et al., 2018, Valentini et al., 2009, Rodrigues et al., 2012), and decreased (Waluga et al., 2014, Karmiris et al., 2006). Nevertheless, the elevated tissue expression of leptin was quite identical between studies (Barbier et al., 2003, Paul et al., 2006). In mice *in vivo* experiment, administration of intrarectal leptin was able to induce inflammation after 48 h (Sitaraman et al., 2004). *In vitro* experiment in mouse liver and human endometrial cell lines, leptin showed the ability to downregulate angulin-1 at pathological dosage (Stenger et al., 2010, Shimada et al., 2016a). In addition, leptin has been linked to decreased TER and altered morphology of Zonula Occludens 1 (ZO-1), a typical representation for TJs, in human intestinal cell line (Le Drean et al., 2014).

2 Aims

IBD is a group of chronic relapsing and remitting gastrointestinal inflammations, whose exact pathogenesis remains to be elucidated. A recent hypothesis of miscommunication between intestinal epithelial cells and immune system enlightens the importance of recognition of molecular interactions in between to decrypt the disease. CD and UC are the two major types of IBD.

TJs are critical in maintaining intestinal barrier function, the ultrastructure, expression, and localization of which are altered in IBD. The central tube formed by tTJs has been assumed to be a weak spot of the paracellular barrier. Tricellulin, one of the major components of tTJs essential for an intact TJ structure as well as the regulation of the passage of macromolecules, was shown to be downregulated in active UC and shifted in CD despite unchanged expression level.

(1) The central aim of this work was to investigate the involvement of angulins in CD and to further unravel the regulating mechanisms behind. Angulins, as the other components of tTJs, are responsible for the correct localization of tricellulin. Therefore, a more sophisticated alteration of tTJs involving the upstreaming regulator of tricellulin was hypothesized. For this purpose, the mRNA and protein expression of angulins were analysed using intestinal biopsies from CD patients and healthy controls. Further exploration of responsible cytokines, signaling pathways, and barrier function was performed in human intestinal epithelial cell lines.

(2) As a decrease of tricellulin expression enhanced macromolecule uptake in active UC, this part of the study was to explore the role of tricellulin downregulation during inflammation by analysing tricellulin expression levels, electrophysiological data, and flux changes in remission UC.

(3) IL-13-mediated tricellulin downregulation was reported to signal via AP-1. Clarification of the regulatory promotor elements involved was thus another aim of this thesis. Promoter activity analysis on wild type tricellulin promoter and mutations of potential binding sites (jun and fos) were performed.

3 Materials and Methods

3.1 Materials

3.1.1 Equipment

7500 Fast Real-Time PCR System	Thermo Fisher, Rockford, USA
AccuBlock Digital Dry bath	Labnet, Edison, USA
Agarose gel electrophoresis chamber	Corning, Kaiserslautern, Germany
Biological safety cabinet HS 15	Heraeus, Hanau, Germany
Centrifuge	Qualitron DW-41, Artisan, Champaign, USA PerfectSpin 24R, Peqlab, Erlangen, Germany Universal 320R, Hettich, Tuttlingen, Germany
Confocal laser scanning microscope	Carl Zeiss, Jena, Germany
FastPrep-24 Classic Instrument	MP Biomedicals, Illkirch, France
Ice flaker Scotsman AF 80	Scotsman, Ipswich, UK
Imaging system	Fusion FX 7, Vilber Lourmat, Eberhardzell, Germany Azure, Biozym, Hessisch Oldendorf, Germany
Incubator Binder CB 150	Binder, Tuttlingen, Germany
Inverted microscope CK 2	Olympus, Tokyo, Japan
Light source KL 1500 LCD	Schott, Mainz, Germany
Magnetic stirrers IKAMAG RCT	IKA, Staufen, Germany
Microplate Luminometer Centro LB 960	Berthold, Bad Wildbad, Germany
Microplate reader Infinite M 200/Spectra classic	Tecan, Switzerland
Mini-PROTEAN® Tetra Vertical Electrophoresis Cell	Bio-rad Laboratories, Feldkirchen, Germany
Pipetboy acu 2	Integra, Biebertal, Germany

PowerPac power supply	Bio-rad Laboratories, Feldkirchen, Germany
Resistance measuring device	Institut für Klinische Physiologie, CBF, Charité Berlin
Rocking Platform WT 15	Biometra, Göttingen, Germany
Secuflow fume cupboard	Waldner, Wangen, Germany
SevenCompact pH meter S 220	Mettler-Toledo, Singapore
Thriller Thermoshaker incubator	Peqlab, Erlangen, Germany
Tissue Floatation Bath TFB 45	Medite, Burgdorf, Germany
Ussing chamber	Institut für Klinische Physiologie, CBF, Charité Berlin
Vortexer RS-VA 10	Phoenix, Garbsen, Germany
Water Purification System arium pro	Sartorius, Göttingen, Germany

3.1.2 Consumables

10 ml serological pipet	Corning, Kaiserslautern, Germany
10 µL pipet tip	Sarstedt, Nümbrecht, Germany
100 µL pipet tip	Sarstedt, Nümbrecht, Germany
1000 µL pipet tip	Sarstedt, Nümbrecht, Germany
12-well plate	Corning, Kaiserslautern, Germany
15 ml polystyrene conical tube	Corning, Kaiserslautern, Germany
25 ml serological pipet	Greiner Bio-One, Frickenhausen, Germany
5 ml serological pipet	Corning, Kaiserslautern, Germany
50 ml polystyrene conical tube	Corning, Kaiserslautern, Germany
Cell culture flask (25 cm^2)	Corning, Kaiserslautern, Germany
Cell culture flask (96 cm^2)	Corning, Kaiserslautern, Germany
Cover glass	VWR, Darmstadt, Germany
Cryotubes	Sarstedt, Nümbrecht, Germany
Eppendorf tubes (1.5 mL)	Eppendorf, Wesseling-Berzdorf, Germany

Lysing matrix tube type D	MP Biomedicals, Illkirch, France
MicroAmp Fast Optical 96-Well Reaction Plate	Thermo Fisher, Rockford, USA
MicroAmp Optical Adhesive film	Thermo Fisher, Rockford, USA
Microscope slides	R. Langenbrinck, Emmendingen, Germany
Millicell-PCF insert (0.4 µm pore size)	Merck Millicell, Darmstadt, Germany
Millicell-PCF insert (3 µm pore size)	Merck Millicell, Darmstadt, Germany
Pipet (0.5 – 10 µL, 10 – 100 µL, 100 – 1000 µL)	Eppendorf, Wesseling-Berzdorf, Germany
PolyScreen PVDF transfer membrane	Perkin Elmer, Rodgau, Germany
Safe seal tube (1.5 mL)	Sarstedt, Nümbrecht, Germany
Single-cap PCR tube	Biozym, Oldendorf, Germany
Stirring rod (120 mm)	Sarstedt, Nümbrecht, Germany
Syringe Filter (25 mm, sterile)	Th.Geyer, Renningen, Germany

3.1.3 Chemicals

50 x Tris-acetate/EDTA (TAE) buffer	Serva, Heidelberg, Germany
Acrylamide	Carl Roth, Karlsruhe, Germany
Agarose Basic	Applichem, Darmstadt, Germany
Albumin	Thermo Fisher, Rockford, USA
Alexa fluor antibody	Molecular Probes MoBiTec, Göttingen, Germany
Ammonium persulfate (APS)	Sigma-Aldrich, Steinheim, Germany
Ampicillin	Ratiopharm, Ulm, Germany
Bacto agar	BD, MD, USA
Bicinchoninic acid (BCA) protein assay reagent A + B	ThermoFisher, Rockford, USA
Bovine serum albumin (BSA)	BIOMOL, Hamburg, Germany
Bromphenol blue	Sigma-Aldrich, Steinheim, Germany
DAPI	Roche Diagnostics, Mannheim, Germany

Dextran 4 kDa	Serva, Heidelberg, Germany
Dimethyl sulfoxide (DMSO)	Carl Roth, Karlsruhe, Germany
dNTPs	NEB, Frankfurt am Main, Germany
Dithiothreitol (DTT)	Merck, Darmstadt, Germany
Dual-Luciferase Reporter Assay System	Promega, Walldorf, Germany
Dulbecco's PBS with Mg/Ca (PBS $^{+/+}$)	ThermoFisher, Rockford, USA
Dulbecco's PBS without Mg/Ca (PBS $^{-/-}$)	ThermoFisher, Rockford, USA
Dulbecco's modified eagle medium (DMEM): F-12 Medium	Sigma-Aldrich, Steinheim, Germany
Ethanol (100 %)	Merck KGaA, Darmstadt, Germany
Ethanol (80 %)	Th. Geyer, Renningen, Germany
Ethidium Bromide (EtBr)	Serva, Heidelberg, Germany
Ethylene Diamine Tetra Acetic Acid (EDTA)	Merck, Darmstadt, Germany
Ethylene Glycol Tetra Acetic Acid (EGTA)	Carl Roth, Karlsruhe, Germany
Fetal bovine serum (FBS)	ThermoFisher, Rockford, USA
FITC-labelled Dextran 4 kDa	TdB Labs, Uppsala, Sweden
Fluorescein	Sigma-Aldrich, Steinheim, Germany
Glucose	Carl Roth, Karlsruhe, Germany
Glycerol	Serva Electrophoresis, Heidelberg, Germany
Glycine	Carl Roth, Karlsruhe, Germany
High Capacity cDNA Reverse Transcription kit	Thermo Fisher, Rockford, USA
Horseradish peroxidase (HRP)	Sigma-Aldrich, Steinheim, Germany
Hydrochloric acid (32 %)	Carl Roth, Karlsruhe, Germany
LB Medium Powder	MP Biomedicals, Illkirch, France
Lipofectamine 2000	Thermo Fisher, Rockford, USA
Methanol	Merck KGaA, Darmstadt, Germany
Milk Powder	Carl Roth, Karlsruhe, Germany
Minimum Essential Medium (MEM) with glutamax	Sigma-Aldrich, Steinheim, Germany
Molecular weight marker (1 kb)	Bioline, Luckenwalde, Germany
Molecular weight marker (100 bp)	Bioline, Luckenwalde, Germany
NEB 10-beta Competent *E. coli*	NEB, Frankfurt am Main, Germany

NEBuilder HiFi DNA assembly cloning kit	NEB, Frankfurt am Main, Germany
NucleoSpin Gel and PCR Clean-up Midi kit	Macherey-Nagel, Düren, Germany
NucleoSpin Plasmid Mini kit	Macherey-Nagel, Düren, Germany
NucleoSpin RNA/Protein kit	Macherey-Nagel, Düren, Germany
PageRuler	Thermo Fisher, Rockford, USA
Paraformaldehyde (PFA, 16 %)	EMS, PA, USA
Passive lysis buffer	Promega, Walldorf, Germany
Polyvinylpyrrolidone (PVP, wt 40.000)	Sigma-Aldrich, Steinheim, Germany
Protease inhibitor cocktail tablets	Roche, Mannheim, Germany
QIAGEN Plasmid Midi Kit	Qiagen, Hilden, Germany
Quantablu™ Fluorogenic Peroxidase Substrate Kit	Thermo Fisher, Rockford, USA
Roswell Park Memorial Institute (RPMI) 1640 Medium	Sigma-Aldrich, Steinheim, Germany
Sodium Dodecyl Sulfonate (SDS)	Carl Roth, Karlsruhe, Germany
Stable outgrowth medium	NEB, Frankfurt am Main, Germany
Super Signal™ West Pico PLUS Luminal Enhancer solution/Stable Peroxide Solution	Thermo Fisher, Rockford, USA
SuperSignal West Pico PLUS Chemiluminescent Substrate	Thermo Fisher, Rockford, USA
T4 DNA Ligase	NEB, Frankfurt am Main, Germany
TaqMan Universal PCR Master Mix	Thermo Fisher, Rockford, USA
Tetramethyl ethylenediamine (TEMED)	Carl Roth, Karlsruhe, Germany
Tissue glue	B Braun, Melsungen, Germany
Tric-HCl 0.5M, pH 6.8	Bio-rad Laboratories, Feldkirchen, Germany
Tris	Carl Roth, Karlsruhe, Germany
Tris-HCl 1.5M, pH 8.8	Bio-rad Laboratories, Feldkirchen, Germany
Triton X-100	Sigma-Aldrich, Steinheim, Germany
Trypsin	Sigma-Aldrich, Steinheim, Germany
Tween 20	Acros Organics, Geel, Belgium

Water	Millipore, MA, USA
Xylol	Carl Roth, Karlsruhe, Germany
β-Mercaptoethanol	Carl Roth, Karlsruhe, Germany

3.1.4 Cell lines

For cell culture experiments, the following three cell lines were used.

3.1.4.1 HT-29/B6 cells

HT-29 (ATCC® HTB-38™) is an intestinal epithelial cell line that originated from a colorectal adenocarcinoma of a 44-year-old Caucasian female in 1964 (Fogh and Trempe, 1975). Its subclone HT-29/B6 was selected under glucose-free condition (Kreusel et al., 1991) and served as a model to explore the functions and mechanisms of intestinal epithelium. The basic properties of colonic epithelial cells are present in this cell clone as the cells possess a transepithelial resistance comparable to a tight colonic epithelium, exhibit polarity and secret mucus. This cell line was used for the previous IL-13-regulated tricellulin study (Krug et al., 2018), and therefore was also chosen for the follow-up experiments in this thesis, namely the transient transfection of tricellulin promoter as well as cytokines treatment.

3.1.4.2 T84 cells (ATCC® CCL-248™)

The T84 cell line is also a human intestinal carcinoma cell line that originally derived from a site of lung metastasis of a 72-year-old male diagnosed with primary colon carcinoma and that afterwards transplanted in nude mice (Murakami and Masui, 1980). The expression of tight junction proteins and peptide hormones receptors made this cell line also suitable for mimicking epithelial barrier. T84 cells was used for cytokines treatments and electrophysiological measurements.

3.1.4.3 Caco-2 cells (ATCC® HTB-37™)

Caco-2 (Cancer coli-2) cells are another well-known epithelial cell line that was obtained from a grade II colorectal adenocarcinoma of a 72-year-old Caucasian male (Fogh et al., 1977). They are characterized by the spontaneous property of differentiation into a polarized adherent monolayer with a decreased colonocyte character and an increased enterocyte feature starting from 13 days after confluence (Engle et al.,

1998). In this thesis, this cell line was used for cytokine treatments as well as electrophysiological measurements.

3.1.5 Buffers and solutions

For Western Blot:

Total lysis buffer

Tris-Cl, pH 7.5	10 mM
NaCl	150 mM
Triton X-100	0.5 %
SDS	0.1 %
Protease inhibitor cocktail tablets	1 pill for every 10 mL before use

Membrane lysis buffer

1 M Tris-Cl, pH 7.4	2 mL
1 M $MgCl_2$	500 µL
0.5 M EDTA	200 µL
0.5 M EGTA	120 µL
H_2O	add to 100 mL
Protease inhibitor cocktail tablets	1 pill for every 10 mL before use

5× Laemmli buffer

SDS	2 g
DTT	1.54 g
0.5 M Tris, pH 6.8	5 mL
Bromphenol blue	20 mg
Glycerol	10 mL
H_2O	add to 20 mL

The solution needs to be filtrated after preparation.

Separation gel (8.5 %)

30 % Acrylamide	5.7 mL
1.5 M Tris, pH 8.8	7 mL
H_2O	6.9 mL
10 % SDS	200 µL
10 % APS	200 µL
TEMED	10 µL

Separation gel (12.5 %)

30 % Acrylamide	8.2 mL
1.5 M Tris, pH 8.8	7 mL
H_2O	4.7 mL
10 % SDS	200 µL
10 % APS	200 µL
TEMED	10 µL

Premixed solution for stacking gel

30 % Acrylamide	85 mL
0.5 M Tris, pH 6.8	125 mL
H_2O	290 mL

The solution needs to be kept in dark.

Stacking gel

Premixed solution for stacking gel	9.8 mL
10 % SDS	100 µL
10 % APS	100 µL
TEMED	10 µL

10× West buffer

Glycine	144 g
Tris	30.4 g
H_2O	add to 1 L

Electrophoresis buffer for Western Blot

10× West buffer	500 mL
10 % SDS	50 mL
H_2O	add to 5 L

Transfer buffer

10× West buffer	100 mL
Methanol	100 mL
H_2O	add to 1 L

10× tris-buffered saline (TBS)

NaCl	400 g
Tris	60.5 g
H_2O	add to 4.5 L

The solution is first titrated to pH of 7.3 by HCl and then filled with H_2O to 5 L.

TBS/Tween

10× TBS	500 mL
Tween-20	5 mL
H_2O	add to 5 L

BSA blocking solution

BSA	5 g
2.5 % Sodium azide	0.8 mL
TBS/Tween	add to 100 mL

For Ussing chamber experiments:

Ringer's solution

Solution I	225 g
Solution II	525 g
Solution III	25 mL
H_2O	add to 5 L

The solution needs to be gassed with Carbogen until clear. For cell culture experiments, 0.1 g Glucose per 100 mL Ringer solution should be supplemented; for intestinal tissues, 2.14 g Substrates mix needs to be added to 500 mL Ringer solution.

20× Solution I for Ringer solution

$NaHCO_3$	35.28 g
H_2O	add to 1 L

10× Solution II for Ringer solution

NaCl	66.4 g
$Na_2HPO_4 \cdot 12\ H_2O$	8.6 g
$NAH_2PO_4 \cdot H_2O$	0.82 g
KCl	4.05 g
$MgCl_2 \cdot 6\ H_2O$	2.44 g
H_2O	add to 1 L

50× Solution III for Ringer solution

$CaCl_2 \cdot 2\ H_2O$	35.2 g
H_2O	add to 1 L

Substrates mix for Ringer's solution

Hydroxybutyrate	3.78 g
L-Glutamine	21.924 g
D-Mannose	108.12 g
Glucose	118.8 g
Imipenem	0.6 g
Piperacillin	3.0 g

For mutation construction:

LB liquid medium

LB Medium Powder	25 g
H_2O	add to 1 L

The solution needs to be autoclaved after preparation. 100 mg/mL Ampicillin need to be added before use.

LB medium for agar plate

Bacto agar	4.5 g
LB liquid medium	300 mL

The solution needs to be autoclaved after preparation. Before plating, it should be microwaved until solved and 100 mg/mL Ampicillin need to be added when the solution is cooled down to 50 °C.

Electrophoresis buffer for agarose gel

50× TAE	100 mL
EtBr	250 µL
H_2O	add to 5 L

3.2 Methods

3.2.1 Patients and study criteria

IBD patients and patients without intestinal diseases visited at the endoscopy center of Department of Gastroenterology, Rheumatology and Infectious Diseases, Charité – Universitätsmedizin were enrolled to the study with prior consent. The diagnosis of IBD was based on the standard criteria (Gomollon et al., 2017, Ungaro et al., 2017) and the endoscopic activity was evaluated using endoscopy subscore of the Mayo score (Schroeder et al., 1987) or simple endoscopic score for CD (SES-CD) (Daperno et al., 2004) for UC or CD respectively.

Exclusion criteria were: age below 18 or above 80 years, pregnancy, presence of other major diseases (neoplastic diseases, other immunological diseases, and chronic inflammatory diseases), biotic treatment, presence of fistula or perforation, need of surgery, lack of consent to the study.

Healthy controls were free of gastrointestinal diseases (e.g., IBD, irritable bowel syndrome, diarrhoea, previous gastrointestinal surgery) and other major conditions described above. The study was approved by the local ethics committee (No. EA4/015/13).

For CD study, paraffin embedded tissues in stocking as well as fresh biopsies taken from sigmoid colon were used in the study. For UC study, biopsies were taken from 10 cm, 30 cm, and 60 cm from anus. All samples were collected in disposable plastic containers filled with saline. The specimens for protein expression and mRNA analysis were stored in liquid nitrogen until analysis whereas those for Ussing chamber experiments were carefully handled and glued as described in 3.2.4.

3.2.2 Cell culture

All three human intestinal cell lines, HT-29/B6, T84, and Caco-2, were cultured at 37 °C in a 5 % CO_2 in air atmosphere. For cultivating cells, 25 cm^2 culture flasks were used and complete growth mediums for these three cell lines are listed as follow:

Cell line	Basic medium	Supplements
HT-29/B6	RPMI 1640 medium	10 % FBS 100 U/mL penicillin 100 µg/mL streptomycin
T84	DMEM: F-12 medium	10 % FBS 100 U/mL penicillin 100 µg/mL streptomycin
Caco-2	MEM with glutamax	15 % FBS 100 U/mL penicillin 100 µg/mL streptomycin

Medium was renewed every two to three days.

3.2.2.1 Subculture of the cells

In order to remove FBS traces which contain trypsin inhibitor in culture vessels, culture medium within flasks that needed to be passage was removed. Flasks were then rinsed with PBS $^{-/-}$ and pre-incubate with 3 mL of Trypsin-EDTA solution at 37 °C. After 5 min, the content was discarded and replaced with 1 mL of Trypsin-EDTA solution. The flask was then placed at 37 °C and when the cell layer was dispersed, 10 mL of complete growth medium were added to the flask. The cell suspension was aspirated by gently pipetting for five times.

For new flasks, 1.5 mL of the cell suspension and 5.5 mL corresponding medium were added to culture vessels. For filters, cells were first counted using a cell counter and 4 × 10^5 cells were seeded onto 3 µm (HT-29/B6 and T84 cells) or 0.4 µm (Caco-2 cells) pore-sized cell culture inserts.

3.2.2.2 Cytokines and inhibitors experiments

To screen potential responsible cytokine(s), HT-29/B6, T84 and Caco-2 cells were incubated with following cytokines for 24 h (TNFα) or 48 h (all the other cytokines).

Cytokine	Concentration	Source
TNFα	500 U/mL	PeproTech, Hamburg, Germany
IFNγ	1000 U/mL	PeproTech, Hamburg, Germany
Leptin	200 ng/mL	PeproTech, Hamburg, Germany
IL-1β	100 ng/mL	PeproTech, Hamburg, Germany
IL-6	10 ng/mL	Miltenyi Biotec, Bergisch Gladbach, Germany
IL-12	100 ng/mL	PeproTech, Hamburg, Germany
IL-13	100 ng/mL	PeproTech, Hamburg, Germany
IL-17A	100 ng/mL	PeproTech, Hamburg, Germany
IL-17F	100 ng/mL	Miltenyi Biotec, Bergisch Gladbach, Germany
IL-21	100 ng/mL	Miltenyi Biotec, Bergisch Gladbach, Germany
IL-22	50 ng/mL	PeproTech, Hamburg, Germany
IL-23	100 ng/mL	PeproTech, Hamburg, Germany
IL-33	100 ng/mL	Miltenyi Biotec, Bergisch Gladbach, Germany

Inhibitors were applied 1 h prior to leptin treatment at listed concentration. For the 96 h of leptin treatment with or without inhibitors, the medium was renewed after 48 h along with the described concentration of leptin and corresponding inhibitors.

Inhibitor	Concentration	Source
U0126	10 µM	Cell signaling Technology, Frankfurt am Main, Germany
LY294002	10 µM	Calbiochem, Darmstadt, Germany
AG490	100 µM	Calbiochem, Darmstadt, Germany
Stattic	20 µM	Calbiochem, Darmstadt, Germany
WP1066	5 µM	Calbiochem, Darmstadt, Germany

3.2.2.3 Transfection

In order to measure the activity of tricellulin promoter activity, Lipofectamine 2000 was applied for transient transfection on HT-29/B6 cells with the constructs described above (WT, jun-mut, fos-mut, and DM tricellulin promoter) along with jun (NM_002228, OriGene, Herford, Germany), fos (NM_005252, OriGene, Herford, Germany). After growth in a 25 cm^2 flask for eight days, HT-29/B6 cells was trypsinized and counted. 4 × 10^5 cells were seeded onto Millicell-PCF inserts (pore size 3.0 µm, effective area 0.6 cm^2, Millipore, Bedford, MA, USA) in a 12-well plate and placed in a 5 % CO_2 environment at 37 °C for 24 h. On the day of transfection, cells were washed with PBS $^{-/-}$ and 800 µL of FBS-free RPMI 1640 medium was added. Following DNAs were diluted separately in 500 µL of RPMI 1640 medium along with additional 250 ng *Renilla* luciferase vector (pGL4.70, Promega, Walldorf, Germany) in each condition.

DNA	**Amount (µg)**
Firefly luciferase vector (pGL4.10, Promega)	2.5
Tricellulin WT promoter on pGL4.10	2.5
Tricellulin jun-mut promoter on pGL4.10	2.5
Tricellulin fos-mut promoter on pGL4.10	2.5
Tricellulin DM promoter on pGL4.10	2.5
Jun (SC118762, Origene, Herford, Germany)	1.25
Fos (SC116873, Origene, Herford, Germany)	1.25

Lipofectamine 2000 reagent was also diluted in 500 µL of RPMI 1640 medium in a DNA to Lipofectamine 2000 ratio of 4 to 1. Then, 500 µL of diluted Lipofectamine 2000 were added to each diluted DNA and the mixture was incubated at room temperature for 15 min. Next, 210 µL of DNA-lipid complex were added to each filter and placed back to 5 % CO_2 atmosphere at 37 °C. After 4 h, 100 µL of FBS with or without IL-13 (200 ng/mL) were applied to each filter followed by a 48-hour incubation at 37 °C.

3.2.3 Molecular biological methods

3.2.3.1 Protein extraction from formalin-fixed paraffin-embedded (FFPE) tissue

To isolate protein from paraffin-embedded sections, Qproteome FFPE Tissue Kit (QIAGEN, Hilden, Germany) was used. FFPE Intestinal biopsies of CD patients were acquired from sample stocks in the Institute for protein preparation. The protein extraction process was carried out according to the instruction the manual:

Five sections with a thickness of around 15 µm of each tissue were cut and collected in one 1.5 mL collection tube. In a fume hood, 1 mL of xylene was pipetted into each tube followed by 10 s of vigorously vortexing, 10 min of incubation, 2 min of centrifugation at top speed, and removal of the supernatant. The application of this step was then repeated twice. 1 mL of 100 % ethanol was pipetted into the same tube, which was subsequently mixed by vortexing, incubated for 10 min, and centrifuged for 2 min at top speed. After discarding the supernatant, this step was repeated once more. The same procedure was applied with 96 % and 70 % ethanol.

To prepare a working solution of extraction buffer, 6 µL of β-mercaptoethanol were added to 94 µL of the EXB Plus buffer supplied by the kit. After pipetting 100 µL of the working solution, each tube was properly sealed using a collection tube sealing clip and incubated on ice for 5 min. In order to reverse formalin crosslinks, these tubes were heated to 100 °C for 20 min, and then agitated at 750 revolutions per minute (rpm) at 80 °C for 2 h to solubilize protein. Afterwards, the tubes were placed on ice for 1 min and the sealing clips were carefully removed. In the end, 15 min of centrifugation at 14,000 × g at 4 °C was applied and the supernatant was transferred to a new 1.5 mL collection tube.

3.2.3.2 Membrane protein extraction

For harvesting membrane proteins from frozen intestinal biopsies, lysing matrix tubes containing ceramic beads were filled with 1.5 mL ice-cold membrane lysis buffer prepared by 1 M pH 7.4 Tris-Cl, 1 M $MgCl_2$, 0.5 M EDTA, 0.5 M EGTA and protease inhibitors. Each sample was put into one tube described above and was homogenized using a FastPrep-24 Classic Instrument (60 s, 4 m/s, MP Biomedicals, USA) for four times until no visible piece of the sample could be seen. After a primary centrifugation

(200 × g, 5 min, 4 °C), supernatants were transferred into new 1.5 mL tubes and again centrifuged at 42,100 × g for 30 min at 4 °C. Afterwards, pellets were resuspended in total lysis buffer (10 mM pH 7.5 Tris-Cl, 150 mM NaCl, 0.5 % Triton X-100, 0.1 % SDS and protease inhibitors) and stored at −80 °C.

3.2.3.3 Total protein extraction

To obtain total protein from cell culture samples, cells were washed with ice-cold PBS $^{-/-}$ and scraped from the Millicell-PCF inserts into a 1.5 mL tube after adding 200 µL of ice-cold total lysis buffer, followed by an incubation on ice for 30 min with intermittent vortex and a centrifugation at 15,000 × g for 15 min at 4 °C. The protein-containing supernatants were stored at −80 °C.

3.2.3.4 RNA and protein extraction (NucleoSpin RNA/Protein kit)

To isolate both RNA and protein in parallel from the same sample, NucleoSpin RNA/Protein kit (Macherey-Nagel, Düren, Germany) was used to minimize the consumption of precious biopsies.

For homogenization of samples, each intestinal biopsy was put into lysing matrix tube containing 350 µL of RP1 buffer and 3.5 µL of β-mercaptoethanol and was then applied four time of the program described in 3.2.2.2 using FastPrep-24 Classic Instrument until no visible piece of sample could be observed. Next, the lysate was retrieved and pipetted onto a NucleoSpin Filter. After centrifugation at 11,000 × g for 1 min, 350 µL of 70 % ethanol was added to the flowthrough and the mixture was loaded to a NucleoSpin RNA/protein column after properly mixing by pipetting up and down. A centrifugation at 11,000 × g for 30 s at this step was applied to separate RNA which was then bound to the column membrane and protein which was soluble within the flowthrough.

To purify RNA, 350 µL Membrane Desalting Buffer was added followed by a centrifugation at 11,000 × g for 1 min. Meanwhile, rDNase reaction mixture was prepared by gently mixing 90 µL Reaction Buffer with 10 µL rDNase for each extraction, 95 µL of which was then pipetted onto the membrane and incubated at room temperature for 15 min. To wash the membrane, 200 µL RA2 buffer and 600 µL RA3 buffer were applied followed by centrifuging at 11,000 × g for 30 s. An additional centrifugation at 11,000 × g for 2 min was performed to dry the silica membrane. In the end, purified

RNA was harvested by applying 50 µL of RNase free H_2O and centrifuging at 11,000 × g for 1 min.

As for protein, the flowthrough was transferred to a new 1.5 mL tube with the same volume of Protein Precipitator. After incubation for 10 min, the mixture was centrifuged for 15 min at top speed. To wash the protein, the supernatant was replaced by 500 µL of 50 % ethanol and centrifuged at 11,000 × g for 1 min. At last, extracted protein was obtained by discarding the supernatant and lysing in corresponding volume of total lysis buffer depending on the size of the pellet within the tube.

3.2.3.5 Protein concentration measurement (BCA protein assay)

The determination of protein concentration in this thesis is based on the colorimetric detection of Cu^{1+} reduced from Cu^{2+} by protein in an alkaline environment using BCA. For calibration, the concentration of 0.2 mg/mL, 0.8 mg/mL, and 1.2 mg/mL of BSA was prepared using a standard BSA solution of 2 mg/mL. The working solution of BCA assay was prepared by 50 parts of reagent A and 1 part of reagent B. 10 µL of BSA at above concentration along with H_2O, corresponding lysis buffer, and each sample were then pipetted to a transparent 96-well plate, prior to adding 190 µL of the prepared BCA working solution. After incubation at 37 °C for 30 min, the absorbance of the plate was measured at 562 nm using a Tecan Spectra microplate reader. The protein concentration of unknown samples was calculated based on the linear relationship between BSA standard and its known concentration.

3.2.3.6 SDS-polyacrylamide gel electrophoresis (SDS-PAGE)

PAGE is a typical protein electrophoresis method in use to analyse proteins. The pore structure of the polyacrylamide gel allows a size-selective (within the range of 5 to 250 kDa) movement of protein in an electric field. SDS is introduced to the PAGE system to overcome its limitation of multi-subunit complexes formation and unpredictable movement, so that data interpretation of the gel based on the size of protein becomes feasible.

Gels for SDS-PAGE are composed of separation gel and stacking gel. The separation gel is made from H_2O, 30 % Acrylamide, Tris-HCl (pH 8.8), 10 % SDS, TEMED, and

APS. Depending on the size of the targeted protein, 8.5 % and 12.5 % gels were prepared in this thesis. The gel was poured until around 3 cm distance left to the top of the glass chamber. 1 mL of 100 % ethanol were then gently distributed to the top of the gel to get rid of bubbles and to prevent the gel from drying out. After complete polymerization of the separation gel (approximately 20 to 30 min), ethanol was discarded, and the remaining traces were absorbed using filter paper.

The stacking gel contains 4 % of Acrylamide, and is mixed additionally with H_2O, Tris-HCl (pH 6.8), 10 % SDS, TEMED, and APS. After pouring the gel on top of the separation gel, a comb was placed in to form the shape of wells. The whole gel was clamped into a vertical electrophoresis apparatus filled with electrophoresis buffer after fully polymerized. Prepared protein samples with 5× Laemmli buffer were heated to 95 °C for 5 min and then loaded along with protein molecular mass marker. The electrophoresis was carried out at 100 V until the region of targeted size was well separated.

3.2.3.7 Western blot

For Western Blot, a wet transfer method using polyvinylidene fluoride membrane (PVDF) was performed. To start with the transfer, transfer buffer containing methanol, Tris and glycine was freshly prepared and pre-cooled at 4 °C. After SDS-PAGE, the gel was equilibrated in transfer buffer for 5 min, as well as the PVDF membrane which was activated in methanol until semi-transparent. Sponges were rinsed with transfer buffer to avoid air bubbles. To make a transfer sandwich, a gel holder cassette was first placed with the black side down in a container filled with enough transfer buffer to sink the whole sandwich. Then, a layer of sponge, a piece of filter paper, gel, PVDF membrane, a second piece of filter paper and sponge were carefully laid to within the cassette in this exact order while any air bubble was tried to avoid. Next, the sandwich was put into a transfer unit in the correct electrical direction. The wet transfer was taken place at 100 V for 60 min with an ice box inside the chamber and a magnetic stirrer constantly spinning.

After transferring the protein from the gel to the membrane, the antibody binding process starts. The blot was first blocked in blocking solution (1 % PVP-40 and 0.05 %

Tween-20) at room temperature for 1 h and then incubated overnight in the corresponding primary antibody at 4 °C. Antibodies used in this thesis were diluted in 5 % BSA plus 0.02 % sodium azide in TBST and dilution ratios refer to the table below.

Antibody	**Dilution ratio**	**Source**
Rabbit anti-Tricellulin	1:2000	Abfinity, Invitrogen
Rabbit anti-Angulin-1	1:3000	Sigma
Mouse anti-β-actin	1:10000	Invitrogen
Rabbit anti-Claudin-2	1:1000	Invitrogen
Mouse anti-Claudin-4	1:1000	Invitrogen
Rabbit anti-STAT3	1:1000	Cell signaling
Rabbit anti-phosphorylated STAT3	1:1000	Cell signaling

Next, the blot was washed 3 times for 10 min with TBST, followed by an incubation at room temperature for 1 h in the HRP-conjugated secondary antibody against corresponding primary antibody. The secondary antibody was diluted to 1:10,000 in 1 % non-fat milk powder in TBST. After incubation, the blot was again washed 3 times for 10 min with TBST.

As for image detecting, SuperSignal West Pico Plus chemiluminescent substrate was prepared by one volume of Luminol/Enhancer solution and one volume of Stable Peroxide solution. The blot was rinsed in the mixed solution at room temperature for 2 min, quickly sealed within two transparent film foils, and immediately detected by Fusion FX7. In the end, densitometric analysis was performed using Multi Gauge V2.3 software (FujiFilm, Japan). Intensities of the bands of the respective protein of interest were normalized using β-actin as loading control.

3.2.3.8 Polymerase chain reaction (PCR)

PCR is one of the most common methods in molecular biology for rapidly amplifying DNA, which is achieved by three consecutive steps. Denaturation is the first step to start a PCR process. The double strands of DNA are separated by heating at certain temperature. The second step is annealing that primers bind to their complementary sequences on single DNA strand. In the end, the DNA polymerase comes into play for

extension from the end of the primer along the template DNA strand in the direction of 5’ to 3’.

As a critical role during PCR, different DNA polymerases possess diverse characteristics leading to distinct amplifying behaviours from the prospect of thermostability, fidelity and processivity. In order to construct mutants of tricellulin promoter, KAPA HiFi HotStart (Roche) polymerase was used in this reaction. For the five PCRs performed, following primers were used, respectively. In order to introduce mutations on wild type tricellulin promoter on luciferase vector (**Figure 7**), primers containing jun mutation were used in PCR jun-1, -2 and PCR jun-fos whereas primers with fos mutation in PCR fos-1, -2 and PCR jun-fos.

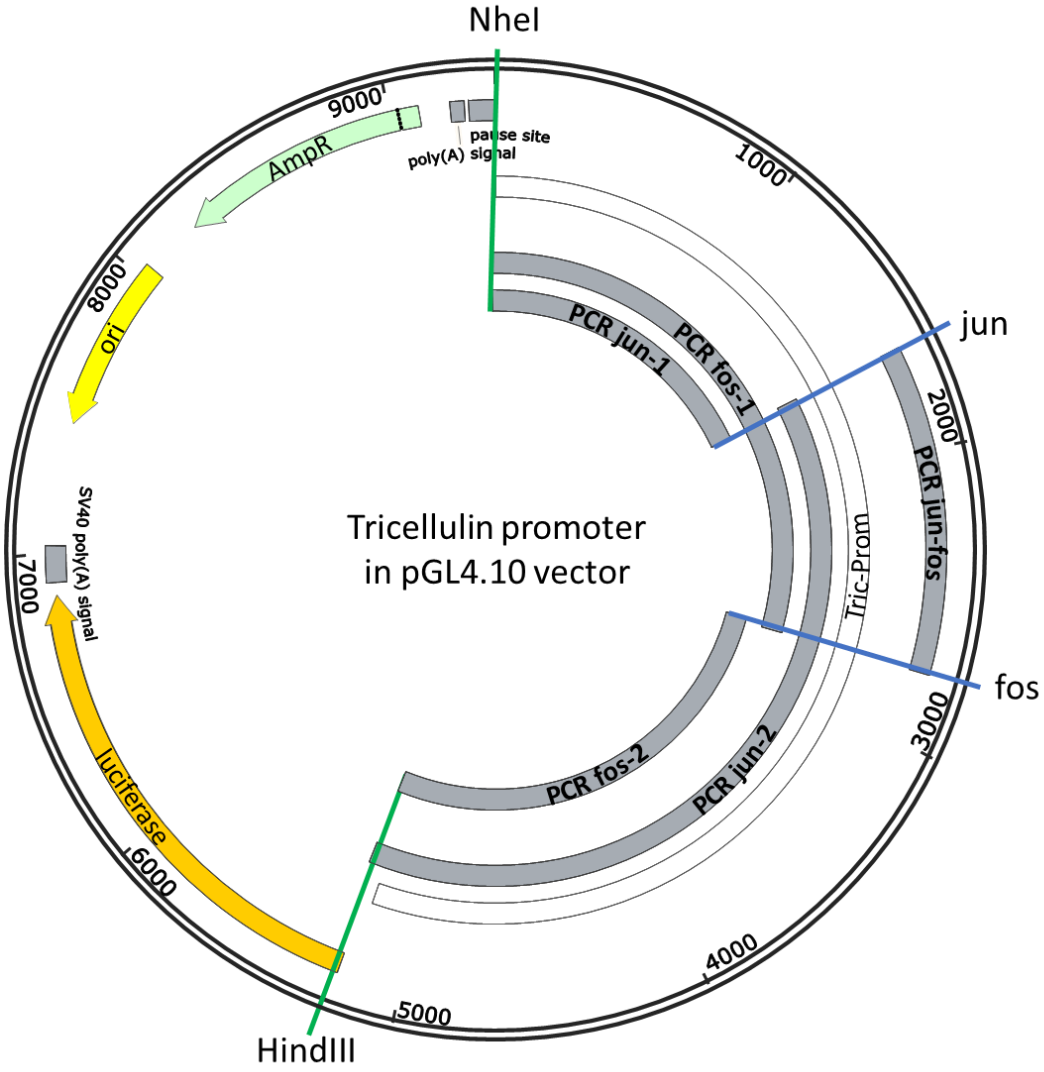

Figure 7 *Plasmid map and information (AP-1 binding site jun and fos, multiple cloning site NheI and HindIII, and PCR products used for mutation construction) of tricellulin promoter on pGL4.10 vector (Promega).*

PCR jun-1:

Forward primer jun-1 (T_m = 66.5 °C):

5’-AGTGCAGGTGCCAGAACATTTCTCTGG-3’

Reverse primer jun-1 (Tm = 66.8 °C):

5’-CCCCTAATGTCTTTCAAGATGATCCTGAGAG-3’

PCR jun-2:

Forward primer jun-2 (Tm = 66.8 °C):

5’-CTCTCAGGATCATCTTGAAAGACATTAGGGG-3’

Reverse primer jun-2 (Tm = 64.0 °C):

5’-TGGCGCTGGGCCCTTCTTAATG-3’

PCR fos-1:

Forward primer fos-1 (Tm = 66.5 °C):

5’-AGTGCAGGTGCCAGAACATTTCTCTGG-3’

Reverse primer fos-1 (Tm = 68.0 °C):

5’-CTGAGGCCATCTGAATATCGTAGGGCC-3’

PCR fos-2:

Forward primer fos-2 (Tm = 63.2 °C):

5’-GGCCCTACATGATTCAGATGGCCTCAG-3’

Reverse primer fos-2 (Tm = 64.0 °C):

5’-TGGCGCTGGGCCCTTCTTAATG-3’

PCR jun-fos:

Forward primer jun-fos (Tm = 66.8 °C):

5’-CTCTCAGGATCATCTTGAAAGACATTAGGGG-3’

Reverse primer jun-fos (Tm = 68.0 °C):

5’-CTGAGGCCATCTGAATATCGTAGGGCC-3’

PCR reaction setup:

Component	**Volume (µL)**
Nuclease-free H_2O	16.5
5× KAPA HiFi Fidelity Buffer	5
10 mM dNTPs	0.75
10 µM forward primer	0.75
10 µM reverse primer	0.75
Template DNA	0.75
KAPA HiFi HotStart DNA Polymerase	0.5
Total	25

PCR thermocycling condition:

Step		**Temperature (°C)**	**Time**
Initial denaturation		95	3 min
25 Cycles	Denaturation	98	20 s
	Annealing	60	15 s
	Extension	72	4 min
Final extension		72	5 min
Hold		4	∞

3.2.3.9 Agarose gel electrophoresis

Agarose gel electrophoresis is a widely used method in molecular biology to separate DNA molecules according to the size. In an electric field, DNA moves towards the anode due to its negative charge. The agarose gel during this process acts like a sieve because of its micropore structure. As a result, smaller DNA fragments travel faster than larger ones, and the compact form of plasmid DNAs also migrates more rapidly.

Ethidium Bromide (EtBr) is a known carcinogen which could interact with DNA and fluoresce under ultraviolet (UV) light. Therefore, EtBr is a common dye added to the electrophoresis system to visualize the separated DNA.

For gel preparation, 1 % agarose gel was solved in 1× TAE buffer and microwaved until the solution appeared clear without floating particles. After cooling down to around 50 °C, EtBr was added into the solution to a final concentration of 0.5 µg/mL. The solution was mixed by gently spun and then poured to an assembled electrophorese chamber inserted with a comb to form wells for samples. After polymerization, the gel was placed into a electrophoreses tank filled with 1× TAE buffer with 0.5 µg/mL EtBr, and the comb was carefully removed. Next, samples mixed with loading buffer were loaded into each well, along with the marker in the correct range of samples. The gel was run until the needed distance at 60 or 90 V depending on the size of the chamber. For detection, the gel was placed in an Azure instrument. Under UV light, the DNA was detectable, and size of samples were compared to the marker.

3.2.3.10 Restriction enzyme digestion

Restriction digestion is also a usual process in molecular biology used for digesting DNA strands by restriction enzyme to generate paired ends, so that afterwards two molecules of DNA are able to ligate together. Restriction enzymes are a group of enzymes that recognize and cut at a specific multiple cloning site of DNA. For firefly luciferase vector pGL4.10 (Promega, Walldorf, Germany) and tricellulin promoter, NheI-HF (NEB, Frankfurt am Main, Germany) and HindIII-HF (NEB, Frankfurt am Main, Germany) were introduced to the digestion system.

Restriction enzyme digestion setup:

Component	**Volume (µL)**
Nuclease-free H_2O	15
10× Cutsmart buffer (NEB)	2
DNA (pGL4.10 or tricellulin promoter)	1
Restriction enzyme NheI-HF	1
Restriction enzyme HindIII-HF	1
Total	20

The reaction above was incubated at 37 °C for 1 h and inactivated by heating to 80 °C for 20 min. The samples were then checked and purified by 1 % agarose gel and DNA clean-up kit.

3.2.3.11 DNA extraction (from agarose gels)

To extract DNA from an agarose gel, the band of interest was slice off under UV light, and the gel piece was collected in a 1.5 mL tube which was weighed with and without the gel. For each 100 µg of gel, 200 µL of NTI buffer from NucleoSpin Gel and PCR Clean-up Midi kit (Macherey-Nagel, Düren, Germany) was added into the reaction tube. Then, the sample was heated at 50 °C for around 10 min with intermittent vortex. After complete dissolution, the sample was loaded to a column provided by the kit and centrifuged at 11,000 × g for 30 s. The silica membrane was washed with 700 µL NT3 buffer, centrifuged at 11,000 × g for 30 s, and dried by another centrifugation step at 11,000 × g for 2 min. In the end, the DNA sample was eluted with 20 µL of NE buffer by centrifuging 11,000 × g for 1 min.

3.2.3.12 Ligation

For constructing wild type (WT) tricellulin promoter on a firefly luciferase reporter vector pGL4.10, the digested (described in 3.2.2.14) and purified (as in 3.2.2.15) tricellulin promoter and pGL4.10 vector were connected together through their cohesive ends using T4 DNA Ligase (NEB, Frankfurt am Main, Germany).

Ligation setup:

Component	**Volume**
Tricellulin promoter	50 ng
pGL4.10 vector	50 ng
10× T4 DNA Ligase Buffer (NEB)	1 µL
T4 DNA Ligase	1 µL
Nuclease-free H_2O	add to 10 µL

The reaction was incubated at 16 °C overnight and inactivated at 65 °C for 10 min.

3.2.3.13 DNA assembly (NEBuilder HiFi DNA assembly cloning kit)

Tricellulin promoter with jun-, fos-, and double-mutation in pGL4.10 vector were structured together using NEBuilder HiFi DNA assembly cloning kit (NEB, Frankfurt am Main, Germany) which was an emerging method for effectively assembling multiple

DNA fragments via an overlap of 15 to 80 base pair (bp). The assembly system works based on the synergistic effect of the exonuclease which generates a 3’ overhang, the polymerase which fills the vacancy digested by the exonuclease during annealing and the DNA ligase which seals the notch left.

DNA assembly setup:

Tricellulin jun-mutation promoter in pGL4.10:

Component	**Volume (μL)**
2× NEBuilder HiFi DNA Assembly Master Mix (NEB)	4
PCR jun-1	1
PCR jun-2	2
Digested pGL4.10	1
Total	8

Tricellulin fos-mutation promoter in pGL4.10:

Component	**Volume (μL)**
2× NEBuilder HiFi DNA Assembly Master Mix (NEB)	4
PCR fos-1	1
PCR fos-2	2
Digested pGL4.10	1
Total	8

Tricellulin double-mutation promoter in pGL4.10:

Component	**Volume (μL)**
2× NEBuilder HiFi DNA Assembly Master Mix (NEB)	6
PCR jun-1	1
PCR fos-2	2
PCR jun-fos	2
Digested pGL4.10	1
Total	12

Assembly thermocycling condition:

Temperature (°C)	Time
37	15 min
50	2 h
4	∞

3.2.3.14 Transformation

Transformation is a process of gene transfer, in detail the uptake of foreign DNA by bacteria. The eligible bacteria for transformation have the capability to take up extracellular DNAs, therefore such bacteria are also termed as competent cells. In this thesis, NEB 10-beta Competent *E. coli* was utilized for the transformation of WT, jun mutated, fos mutated and double mutated tricellulin promoter in pGL4.10 vector.

Antibiotic selection acts like a first-line screen during cloning, which is carried out on account of the existence of an additional antibiotic gene in the vector used for transformation. Therefore, when these specific antibiotics (i.e., ampicillin) are added during the preparation of culture plates, the growth of unwanted bacteria will be inhibited, as only positive clones contain the antibiotic resistance gene and are able to grow on the selection plate.

The competent cells were first thawed on ice for 10 min. 5 µL of each DNA mentioned above was pipetted into the competent cells mix and gently mixed. After 30 min rest on ice, the mixture went through heat shock at 42 °C for 30 s and was placed on ice for 5 min. 950 µL of stable outgrowth medium (NEB) was added to the cell mixture which was then shook (250 rpm) at 37 °C. After 60 min, each mixture was spread onto a pre-warmed (37 °C) ampicillin selection plate (100 mg/mL) and incubated at 37 °C overnight.

3.2.3.15 Plasmid isolation

Plasmids are important extrachromosomal genetic source of bacteria, which allow the endowment of certain properties back to the bacteria. Therefore, plasmids provide

countless possibilities in recombinant DNA technology, and the isolation of plasmids paves the way to cloning, sequencing, transfection, etc.

After transformation, when there were colonies grown on selection plates on the following day, several single colonies were picked with pipet tips and each was cultured in 2 mL Lysogeny broth (LB) liquid medium containing 100 mg/mL ampicillin at 37 °C overnight. The *E. coli* LB culture was used to harvest corresponding plasmid by NucleoSpin Plasmid Mini kit (Macherey-Nagel).

1.5 mL of the *E. coli* LB culture were added into a 1.5 mL tube which was centrifuged at 11,000 × g for 30 s. The pellet was then completely solved in 250 µL Buffer A1 by vigorously vortexing. 250 µL of Buffer A2 was the next added into the tube which was mixed by gently inverting 6 times and incubated at room temperature for 5 min until the solution turned clear. 300 µL of Buffer A3 was pipetted into the tube after incubation and again mixed by lightly inverting the tube for 6 times until the solution appeared colourless. Next, the tube was centrifuged at 11,000 × g for 10 min and the supernatant was loaded to a column provided by the kit. After centrifuging at 11,000 × g for 1 min, the column was washed with 500 µL Buffer AW and 600 µL Buffer A4 accompanied by a centrifugation at 11,000 × g for 1 min for each washing. The traces of ethanol were removed by additional centrifugation at 11,000 × g for 2 min. The plasmid DNA was eluted in 50 µL of Buffer AE after centrifuging at 11,000 × g for 1 min.

The isolated plasmid DNAs were first checked by 1 % agarose gel and when confirmed by correct band size, the DNAs were further examined for jun and fos mutation by sequencing with following primers.

Primer for jun sequencing:

5’-GTGAAGTGGCTTATTTGAATCAAACCACCC-3’

Primer for fos sequencing:

5’-ATTTCAATGGCCTAGCCAGTCTTCCTGTT-3’

When the results came back positive for corresponding mutation site, 500 µL of the *E. coli* LB culture matched to that sample was further cultivated in 50 mL LB liquid medium on a thermoshaker incubator at 225 rpm at 37 °C overnight. To isolate a larger volume

of plasmid DNAs, Qiagen plasmid Midiprep kit was applied with relatively similar extraction steps to what described above in Miniprep. Afterwards, the plasmid DNAs were again verified by 1 % agarose gel and sequenced thoroughly using the primers below.

Primer sequencing 1:

5‘-CTAGCAAAATAGGCTGTCCC-3’

Primer sequencing 2:

5‘-GTGAAGTGGCTTATTTGAATCAAACCACCC-3’

Primer sequencing 3:

5‘-AACAGGAAGACTGGCTAGGCCATTGAAAT-3’

Primer sequencing 4:

5‘-CATGCCATTCTCCTGCCTCA-3’

Primer sequencing 5:

5‘-CAAGTAGAGTCATTTCCTCAAACATCTAAAT-3’

Primer sequencing 6:

5‘-TGGCGCTGGGCCCTTCTTAATG-3’

3.2.3.16 Glycerol stocks

For long-term storage, the bacterial cultures are preserved in medium with glycerol to be protected from ice crystal formation within the medium. 800 µL of the *E. coli* LB culture were mixed with 800 µL of sterile glycerol in a cryotube, which was then stored at −80°C.

3.2.3.17 Promoter activity measurement

Luciferase Reporter Assays are a common tool to study promoter activity. By applying two individual reporters within one single system, one as experimental and the other as internal control, could minimize the experimental variability, for example transfection efficiency, to a great degree. In the dual luciferase reporter (DLR) assay system, the firefly and *Renilla* luciferase are measured using one sample, which means, after a

stabilized luminescent signal from the firefly luciferase is generated and recorded, the firefly luminescence is quenched and a signal from the *Renilla* luciferase starts to accumulate. In this thesis, tricellulin promoter mutants were constructed on the firefly luciferase vector pGL4.10 while the *Renilla* luciferase vector pGL4.70 was co-transfected as an internal control.

At the end of 48 h of IL-13 treatment after transfection, the filters were rinsed with PBS $^{-/-}$, and 250 µL of passive lysis buffer (Promega) were added onto the filters, from which the cells were next scraped off and collected in a 1.5 mL tube. The sample was then frozen by liquid nitrogen and thawed at 37°C twice, followed by centrifuging at top speed for 30s.

For luciferase activity measurement, the supernatant was carefully taken into a new 1.5 mL tube. 20 µL of obtained sample were pipetted onto a white 96-well plate and measured by a microplate luminometer Centro LB 960 (Berthold) after 10 s of incubation with 50 µL of luciferase assay reagent II (Promega) for firefly luciferase activity and subsequently 10 s incubating with 50 µL Stop & Glo (Promega) to acquire *Renilla* luciferase value.

For additional protein expression analysis, 100 µL of total lysis buffer were added and mixed by pipetted up and down. Then, the same procedure was performed as described in total protein extraction.

3.2.3.18 RNA extraction from intestinal biopsies

To obtain RNA, intestinal biopsies were collected and frozen using liquid nitrogen as soon as possible because of the instability of RNA. At the time of extraction, each sample was put in a lysing matrix tubes containing ceramic beads filling with 0.5 mL RNAzol (WAK-Chemie) and homogenized using a FastPrep-24 Classic Instrument (60 s, 4 m/s, MP Biomedicals, USA) for four times until no visible piece of the sample could be seen. The solution was then transferred into a new Eppendorf tube followed by addition of 50 µL of chloroform. After 15 s of thoroughly vortex, the sample was incubated at 4 °C for 5 min and centrifuged at 4 °C for 15 min at 12,000 × g. The aqueous phase was then carefully transferred into a new Eppendorf tube and mixed with same volume of isopropanol for RNA precipitation. After 30 min of incubation at 4 °C, the sample was again centrifuged at 4 °C for 15 min at 12,000 × g. Next, the supernatant

was discarded, and the RNA pellet was washed with 70 % ethanol. A centrifugation at 4 °C for 10 min at 12,000 × g was then carried out and the supernatant was again discarded. The pellet was dried for around 5 min and then resuspended in 50 µL of nuclease-free water at 4 °C for 30 min. The sample was stored at −80 ° C.

3.2.3.19 cDNA synthesis (High capacity cDNA reverse transcription kit)

To synthesize cDNA from extracted RNA, a 2× Reverse Transcription Master Mix was first prepared on ice. For each reaction, the volume needed for each component is listed as follow:

Component	**Volume (µL)**
Nuclease-free H_2O	3.2
10× RT Buffer	2.0
10× RT Random Primers	2.0
25× dNTP Mix	0.8
RNase Inhibitor	1.0
MultiScribe Reverse Transcriptase	1.0
Total	10.0

After pipetting 10 µL of the master mix to each single-cap PCR tube, 10 µL of RNA which was equilibrated to the same concentration were added into the tube. Air bubbles were then eliminated by briefly centrifugation. In the end, reaction tubes were placed to a pre-programmed thermal cycler (settings as below).

Temperature (°C)	**Time (min)**
25	10
37	120
85	5
4	∞

Synthesized cDNAs were stored afterwards at −80 °C.

3.2.3.20 Real-time PCR (RT-PCR)

RT-PCR is a method that allows the detection of the amount of cDNA reflected by the intensity of fluorescent signal. A comparative quantification could be carried out when a gene of interest is compared to a housekeeper gene (i.e., GAPDH) which is expressed uniformly in all measured samples.

A master mix of PCR was prepared using the following setting:

Component	**Volume per reaction (µL)**
2× TaqMan Universal PCR Master Mix	10
20× gene of interest probe mix	1
20x GAPDH probe mix	1
Nuclease-free H_2O	6

18 µL of the master mix were then pipetted into a MicroAmp Fast Optical 96-Well Reaction Plate, following by 2 µL of the cDNA sample (containing same concentrations) as well as nuclease-free H_2O as negative control. The plate was sealed with a layer of MicroAmp Optical Adhesive film and briefly centrifuged to eliminate air bubbles and to collect contents to the bottom. Next, the plate was loaded in the RT-PCR instrument, and the listed program was pre-set and applied.

Stage	**Temperature (°C)**	**Time**
Hold	95	10 min
40 Cycles	95	15 s
	60	1 min

To analyse the data, the difference cycle number between the gene of interest and GAPDH within one sample was first calculated as ΔC_t. Each ΔC_t value was then calculated by subtracting the ΔC_t value of a calibrator sample within the control group, expressed by $\Delta\Delta C_t$. The fold difference was interpreted therefore as $2^{-\Delta\Delta Ct}$.

3.2.3.21 Immunofluorescent staining

For cell culture, cells growing on 0.4 µm-pore-size Millicell-PCF inserts were treated with corresponding cytokines and/or inhibitors as described in the part cytokines and inhibitors experiments. After the treatment, the cell monolayers were rinsed with PBS $^{+/+}$, fixed with 2 % PFA in PBS $^{+/+}$ at room temperature for 20 min, quenched with 25 mM glycine in PBS $^{+/+}$ at room temperature for 15 min to reduce autofluorescence, and permeabilized using 0.5 % Triton X-100 in PBS $^{+/+}$ at room temperature for 7 min. Next, the cells were blocked with 5 % goat serum in PBS $^{+/+}$ at room temperature for 20 min, followed by an incubation with primary antibodies (listed in the table below) at 4 °C overnight.

Antibody	**Dilution ratio**	**Source**
Rabbit anti-Tricellulin	1:1000	Invitrogen
Rabbit anti-Angulin-1	1:1000	Sigma-Aldrich
Mouse anti-ZO-1	1:200	Invitrogen

On the following day, an incubation with secondary antibodies (Alexa Fluor 488 goat anti-mouse or Alexa Fluor 594 goat anti-rabbit, 1:500, Molecular Probes MoBiTec) and 4',6-diamidino-2-phenylindole (DAPI, 1:1000) was carried out at 37 °C for 1 h after two times washing with blocking solution. Then, the filter layer was shortly rinsed with H_2O, cut off from the filter holder, and placed on the middle of an object slide. A single drop of mounting solution was dripped onto the filter layer which was in the end covered with coverslip. Confocal laser scanning microscope (LSM, Zeiss) were utilized for obtaining fluorescence images.

3.2.4 Electrophysiological measurements

3.2.4.1 Ussing chamber

The Ussing chamber is a device invented more than half a century ago (Ussing and Zerahn, 1951) used for measuring transport properties as well as the barrier function of epithelium. The chamber is assembled by two hemi chambers which are continuously gassed with carbogen to equilibrate O_2 and CO_2, and which are circulated with temperature-controlled water (**Figure 8a**). A polarized epithelial layer could be

mounted between the two hemi chambers with the modification of the sample container for cell culture (Kreusel et al., 1991) or intestinal biopsy (Stockmann et al., 1999) (**Figure 8b, c**).

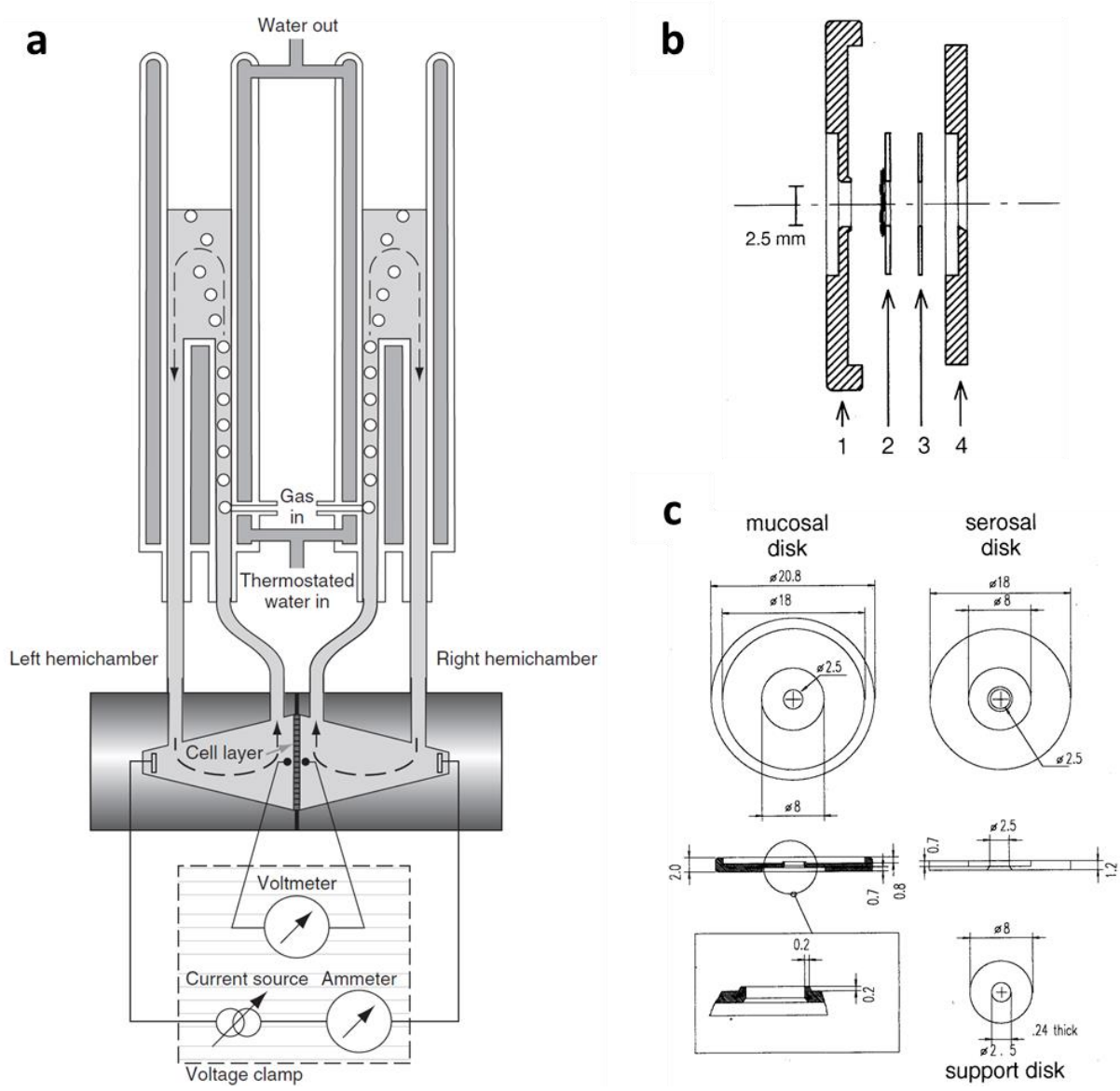

Figure 8 *Schematic drawing of an Ussing chamber and the biopsy container.* ***(a)*** *Representative diagram of an Ussing chamber (Günzel et al., 2010).* ***(b)*** *Working scheme of a sample container for intestinal biopsies (Stockmann et al., 1999). 1 = mucosal side of the polyacrylic disk, 2 = support disk for gluing specimen, 3 = silicone rubber ring, 4 = serosal bipartite polyacrylic disk.* ***(c)*** *Sketch map of the biopsy container in detail according to DIN (Deutsches Institut für Normung) standards. The silicone ring has the same diameters as the support disk but is 0.19mm thick. All measures in the drawings are in millimetres (Stockmann et al., 1999).*

3.2.4.2 Transepithelial resistance measurement

The electrophysiological data like transepithelial resistance (TER) could be acquired by connecting the Ussing chamber to various apparatus, including a voltmeter, an ammeter, a current source, an amplification device, and a computer. In order to eliminate the influence of the bath solution as well as the chamber compartments, the resistance of chamber filled with the same Ringer's solution is measured before inserting the sample. This value will be subtracted in later calculation.

In principle, the two electrodes at the outer edge provide a current applied on the epithelial layer area, which generates a voltage change measured by the other two electrodes close to the sample. The transepithelial resistance could be then calculated using Ohm's law (R = U/I).

3.2.4.3 Impedance measurement

The transepithelial resistance measured as described above has a limitation due to the indiscrimination between different compartments of the sample, for example between epithelial resistance (R^{epi}) and subepithelial resistance (R^{sub}), the sum of which is equivalent to the tissue resistance (R^{t}). This difference between R^{epi} and R^{sub} does not always matter, however in IBD, the thickened subepithelial tissues increase the measured resistance value leading to an unchanged total transepithelial resistance in spite of a decreased resistance from the epithelial layer (Zeissig et al., 2004, Krug et al., 2018), which could bring about inaccurate understanding of the barrier function under this circumstance. Therefore, the impedance measurement is introduced.

Measuring the impedance relies on the resemblance between the cell membrane and a capacitor. The electric circuit of the sample is consisting of this capacitor and the epithelial resistance in parallel, which is then connected to the subepithelial resistance in series (**Figure 9a**) (Fromm et al., 1985, Günzel et al., 2010). The impedance is therefore measured at different alternating current (AC) frequencies (ω). At a very low frequency ($\omega \rightarrow 0$), the current would flow entirely through the epithelial resistor instead of the capacitor, which means the measured value represents the total resistance; at a very high frequency ($\omega \rightarrow \infty$), the epithelial resistor would be short circuited and hence the measured resistance would reflect the subepithelial resistance (**Figure 9b**).

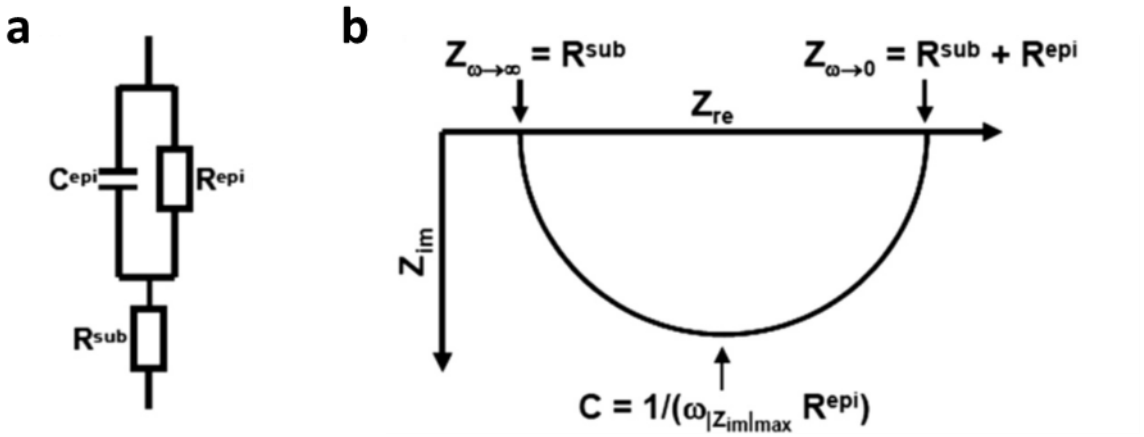

Figure 9 *Schematic diagram of impedance measurement.* ***(a)*** *Electric model of intestinal biopsies.* ***(b)*** *Nyquist diagram (plot of the real Z_{re} and the imaginary Z_{im} portion of the impedance) for model shown in* ***(a)****. (Krug et al., 2009c).*

3.2.4.4 Paracellular flux measurement

Paracellular permeability properties could be reflected by tracers of different molecular size with the label of measurable substrate, such as fluorescein and FITC-labelled dextran. Adding equilibrium solution to both side of the chambers makes the measurement of passive transport possible, since the osmotic and gradient difference are eliminated.

For fluorescein measurement, the two hemi chambers were filled with 10 ml of Ringer's solution after the sample was mounted in. After the resistance of the sample reached stable, 300 µL of basolateral solution was taken into a 1.5 mL tube as the blank sample and the hemi chamber was then filled with 300 µL of fresh Ringer's solution. 10 µL of 100mM fluorescein was pipetted apically and samples were taken at the time of 15 min, 30 min, 45 min and 60 min, respectively. In order to determine the concentration, 10 µL of the 100 mM fluorescein solution was diluted to 1 µM, 0.5 µM, 0.1 µM, 0.05 µM, 0.01 µM, 0.005 µM and 0.001 µM for standard curve. 130 µL of each sample from Ussing chambers as well as from standard curve were measured at 520 nm by a spectrometer (Tecan Infinite M200). The calculation of the flux was performed as follow:

$$J = \frac{(c_2 - c_1) \times V_{chamber}}{(t_2 - t_1) \times A}$$

J	Flux
c_1, c_2	Concentration of the time point 1 and 2
$V_{chamber}$	Volume of the added Ringer's solution
V_{sample}	Volume of the sample
t_1, t_2	Time of the sample taken

Due to the concentration dependence of the flux, the value was then converted to permeability to facilitate the comparison.

$$P = \frac{J}{c}$$

P	Permeability
c	Concentration of the substrate in Ussing chamber

For FITC-dextran measurement, the procedure for determining the permeability was similar to that for fluorescein. The FITC-dextran was dialyzed before the experiment to avoid the disturbance by disjointed FITC fragments. For the experiment, the chambers were filled with 5 mL of Ringer's solution. After the empty sample was taken, 25 µL of 40 mM dextran was added to the basolateral side while 25 µL of 40 mM FITC-dextran to the apical chamber. The time points for FITC-dextran experiment were 0 min, 30 min, 60 min, 90 min and 120 min. The measurement of the concentration as well as the calculation of the flux and the permeability were identical to what described for fluorescein above.

3.3 Statistical analysis

Data are expressed as mean values ± standard error of the mean (SEM). Statistical analyses were performed using Student's t-test for comparison between two groups or one-way ANOVA in the occasion of more than two groups (multiple testing) and $p < 0.05$ was considered significant.

4 Results

4.1 Shifted localization of tricellulin in CD

4.1.1 Patients features

From 2017 to 2020, 19 CD patients as well as 24 control patients described as in 3.2.1 were recruited to the study and underwent colonoscopy (**Table 1**). The disease activity was evaluated based on the clinical manifestation and simple endoscopic score for CD (SES-CD). SES-CD is a commonly used scoring system for assessing endoscopic activity of CD, including the following aspects: mucosal ulcers, surface involved by CD or ulceration, and the presence of narrowing (Daperno et al., 2004).

Table 1 Characteristics of the enrolled CD population.

Characteristic	**Control** (n = 24)	**CD** (n = 19)
Age (median, range)	54 (24-66)	35 (25-64)
Gender (male/female)	8/16	5/14
SES-CD, n		
Remission (0-2)	-	5
Active (> 2)	-	14

4.1.2 Expression of angulins in intestinal biopsies

To investigate the expression of angulins, intestinal biopsies were collected from the enrolled patients with prior consent. First, on mRNA level, angulin-1 was downregulated in active CD (CD_{Active}) compared with controls (Ctrl) and remission patients (CD_{Rem}) (**Figure 10a**, $*p < 0.05$). The expression of angulin-2 demonstrated a resembling pattern but statistically unsignificant (**Figure 10b**). Angulin-3 was within the similar range in CD as in Ctrl (**Figure 10c**).

In order to be comparable with previous studies (Zeissig et al., 2007, Krug et al., 2018), the mRNA expression of TJ proteins tricellulin, claudin-2 (Cldn-2) and claudin-4 (Cldn-4) were also analysed. Tricellulin did not change in CD compared with Ctrl (**Figure 10d**). Cldn-2 showed an upregulation in CD_{Active} in comparison with Ctrl (**Figure 10e**,

$p < 0.01$) and CD_{Rem} (Figure 10e**, *$p < 0.05$). Cldn-4 was unaltered in CD and in Ctrl (**Figure 10d, f**).

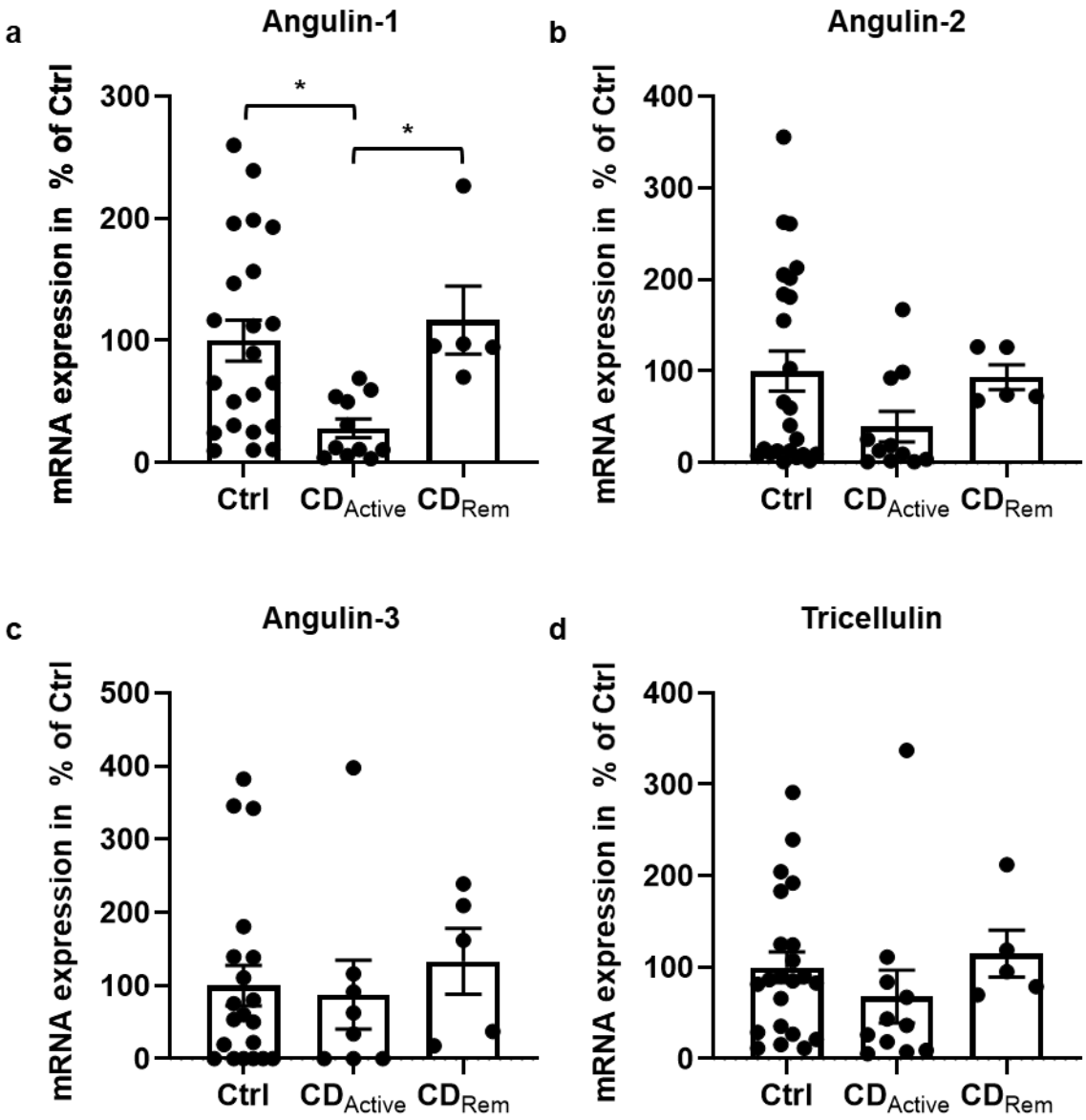

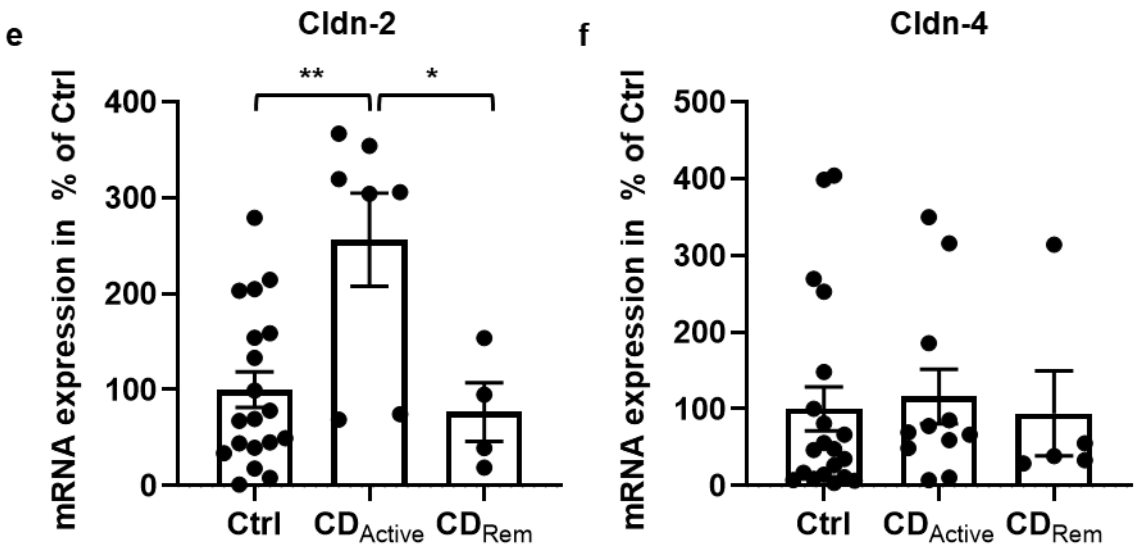

Figure 10 *Scatterplot with bar of mRNA expression of TJ proteins in human intestinal tissues. Mean value of Ctrl is set to 100 %.* ***(a)*** *Angulin-1 was down-regulated in active CD (28.26 ± 7.62 %, n = 11) compared to Ctrl (100 ± 16.81 %, n = 22, *p* < 0.05*) and remission patients (116.86 ± 27.87 %, n = 5, *p* < 0.05*).* ***(b)*** *Angulin-2: Ctrl = 100 ± 21.85 %, n = 24; CD_{Active} = 37.63 ± 16.14 %, n = 11; CD_{Rem} = 97.44 ± 12.52 %, n = 5).* ***(c)*** *Angulin-3: Ctrl = 100 ± 27.54 %, n = 20; CD_{Active} = 87.76 ± 46.96 %, n = 8; CD_{Rem} = 133.09 ± 44.91 %, n = 5.* ***(d)*** *Tricellulin: Ctrl = 100 ± 16.75 %, n = 22; CD_{Active} = 67.87 ± 28.82 %, n = 11; CD_{Rem} = 114.90 ± 25.69 %, n = 5.* ***(e)*** *Cldn-2 showed an increasement in CD_{Active} (256.28 ± 48.51 %, n = 7) in comparison with Ctrl (100 ± 18.61 %, n = 19, **p* < 0.01*) and remission CD (76.67 ± 30.36 %, n = 4, *p* < 0.05*).* ***(f)*** *Cldn-4: Ctrl = 100 ± 28.64 %, n = 20; CD_{Active} = 127.67 ± 39.31 %, n = 11; CD_{Rem} = 68.33 ± 29.68 %, n = 5.*

Next, the protein expression of angulin-1 was analysed using intestinal biopsies in FFPE sections and showed a downregulation in CD compared to Ctrl (**Figure 11a, b**, **p* < 0.05). Due to the potential heterogeneous distribution of epithelial cells within FFPE sections, intestinal biopsies which were directly frozen in liquid nitrogen and did not underwent fixation or embedding were then investigated for the avoidance of sample selection bias. Angulin-1 protein expression was also downregulated in CD_{Active} and recovered in CD_{Rem} (**Figure 11c, d**, ***p* < 0.01), similar to the findings at mRNA level.

As controls, the protein expression of tricellulin and Cldn-4 were also analysed and found to be unaltered as previously demonstrated (Krug et al., 2018) (**Figure 11e-h)**.

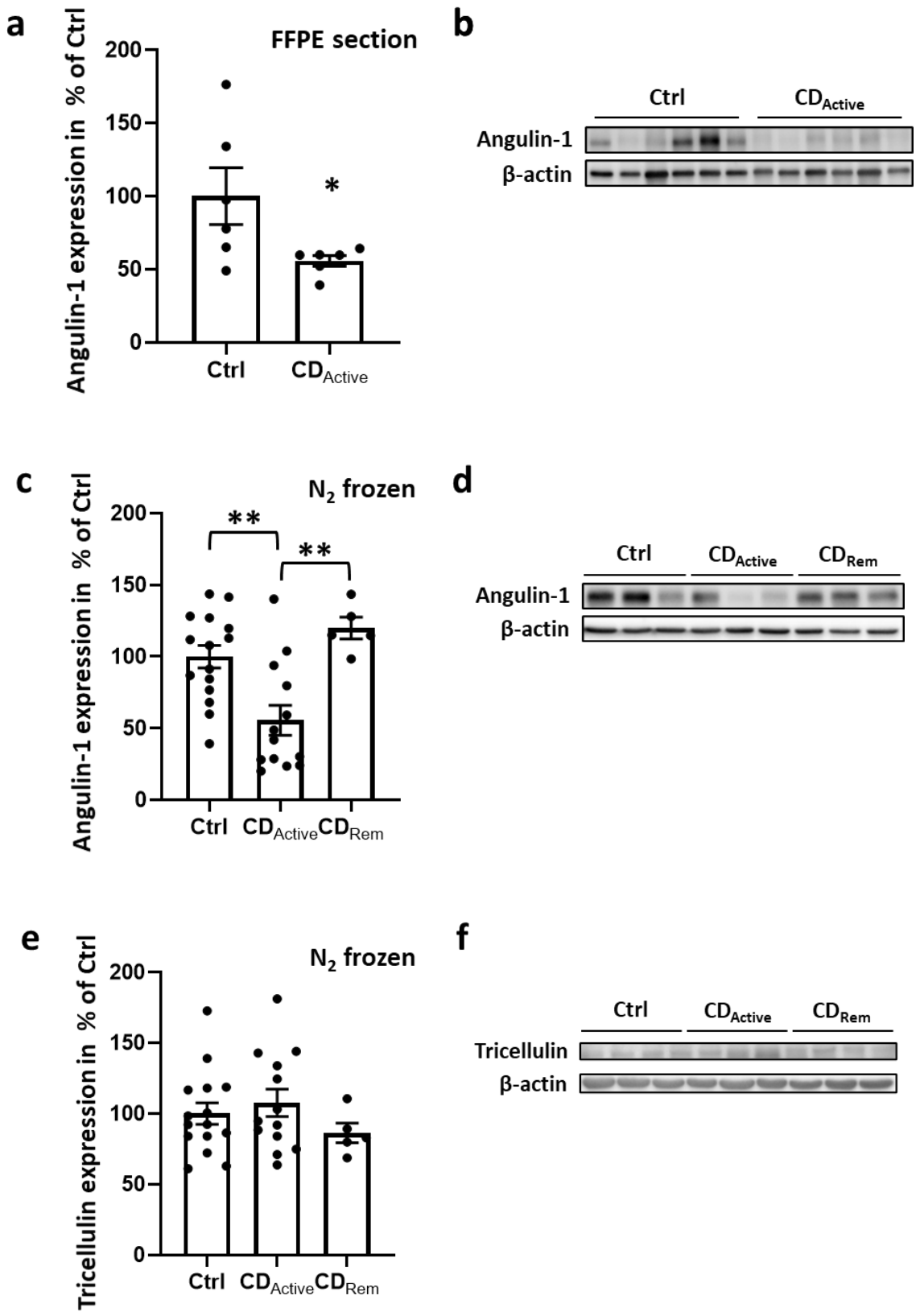

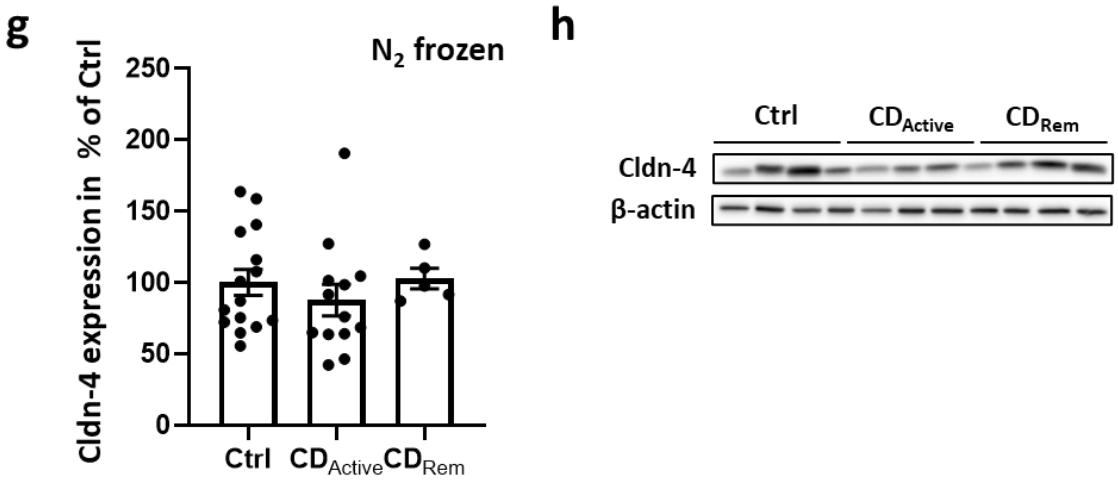

Figure 11 *Analysis of TJ protein expression in human intestinal tissues. Mean value of Ctrl is set to 100 %.* ***(a)*** *Scatterplot with bar of Angulin-1 in FFPE section of Ctrl and CD. Angulin-1 was downregulated in CD (Ctrl: 100 ± 19.42 %, n = 6; CD: 55.82 ± 3.67 %, n = 6, *p < 0.05).* ***(b)*** *Representative western blots of FFPE sections from Ctrl and CD.* ***(c)*** *Scatterplot with bar of Angulin-1 in biopsies directly frozen after colonoscopy from Ctrl, CD_{Active}, and CD_{Rem}. Angulin-1 was downregulated in CD_{Active} (49.43 ± 11.13 %, n = 13) compared with Ctrl (Ctrl: 100 ± 11.34 %, n = 15, **p < 0.01) and CD_{Rem} (131.00 ± 12.21 %, n = 5, **p < 0.01).* ***(d)*** *Representative western blots of fresh intestinal biopsies from Ctrl, CD_{Active}, and CD_{Rem}.* ***(e)*** *Scatterplot with bar of tricellulin in biopsies directly frozen after colonoscopy from Ctrl, CD_{Active}, and CD_{Rem}. Ctrl: 100 ± 7.64 %, n = 15; CD_{Active}: 107.60 ± 9.70 %, n = 13; CD_{Rem}: 86.31 ± 6.93 %, n = 5.* ***(f)*** *Representative western blots of tricellulin.* ***(g)*** *Scatterplot with bar of Cldn-4 in biopsies directly frozen after colonoscopy from Ctrl, CD_{Active}, and CD_{Rem}. Ctrl: 100 ± 9.24 %, n = 15; CD_{Active}: 85.23 ± 10.80 %, n = 13; CD_{Rem}: 101.98 ± 7.41 %, n = 5.* ***(h)*** *Representative western blots of Cldn-4.*

4.1.3 Cytokine effects of angulins in human intestinal epithelial cell lines

To explore the underlying mechanisms of angulin-1 downregulation in CD, twelve pro-inflammatory cytokines (TNF-α, IFN-γ, Leptin, IL-1β, IL-6, IL-12, IL-17A, IL-17F, IL-21,

IL-22, IL-23 and IL-33) that were commonly involved in the disease were applied to three human intestinal epithelial cell lines (T84 and Caco-2, HT-29/B6).

In T84 cells, angulin-1 was only downregulated by leptin (**Figure 12c**, ***$p < 0.001$), while none of the other cytokines had an effect on angulin-1 protein expression level (**Figure 12**). Tricellulin was increased by IL-6 (**Figure 12e**, *$p < 0.05$) and decreased by IL-22 (**Figure 12j**, ***$p < 0.001$). The upregulation of Cldn-2, which was a typical TJ change in CD (Zeissig et al., 2007), was able to be induced with the treatment of TNF-α, IL-6, IL-12, IL-17A, and IL-22 (**Figure 12a, e, f, g, j**, ***$p < 0.001$). On the contrary, the reduction of Cldn-2 could be caused by IFN-γ, IL-17F and IL-33 (**Figure 12b, h, l**, ***$p < 0.001$). Cldn-4 was elevated after incubation with (**Figure 12e**, **$p < 0.01$), IL-12 (**Figure 12f**, ***$p < 0.001$), IL-17A (**Figure 12g**, *$p < 0.05$), or IL-22 (**Figure 12j**, **$p < 0.01$). As for TER, leptin showed no effect after treatment (**Figure 13c**). A reduced TER was observed when T84 cells were treated with TNF-α, IL-6 or IL-22 (**Figure 13a, e, j**, ***$p < 0.001$).

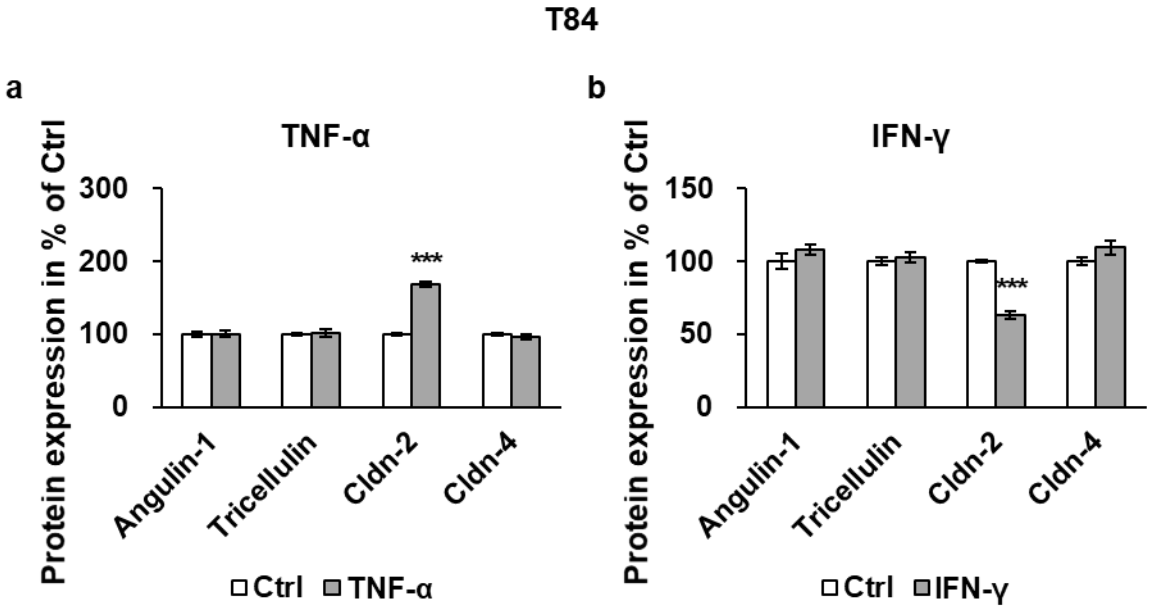

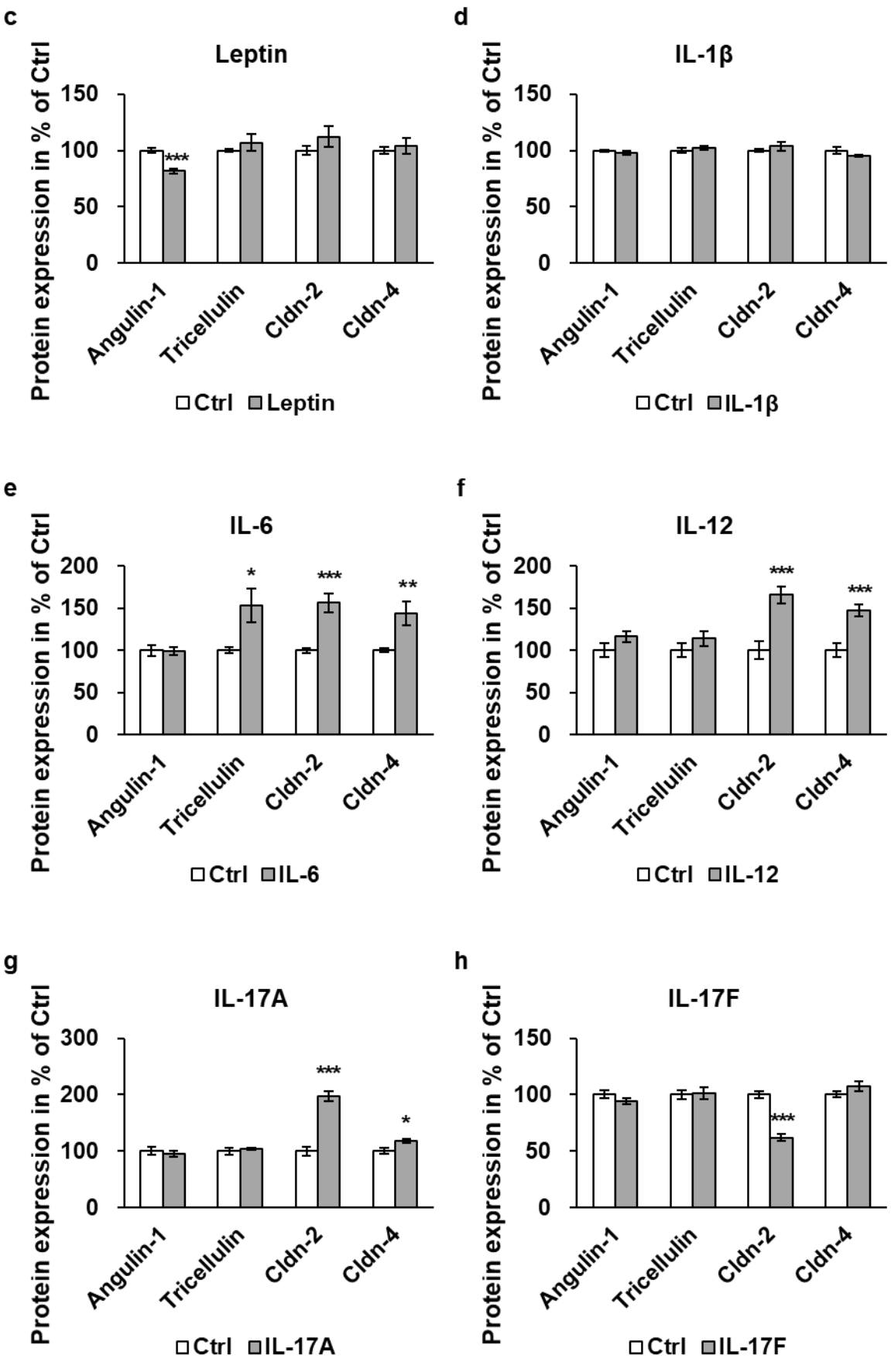
c
Leptin
Protein expression in % of Ctrl
150
100
50
0
***
Angulin-1
Tricellulin
Cldn-2
Cldn-4
Ctrl
Leptin
d
IL-1β
Protein expression in % of Ctrl
150
100
50
0
Angulin-1
Tricellulin
Cldn-2
Cldn-4
Ctrl
IL-1β
e
IL-6
Protein expression in % of Ctrl
200
150
100
50
0
*
***
**
Angulin-1
Tricellulin
Cldn-2
Cldn-4
Ctrl
IL-6
f
IL-12
Protein expression in % of Ctrl
200
150
100
50
0
***
***
Angulin-1
Tricellulin
Cldn-2
Cldn-4
Ctrl
IL-12
g
IL-17A
Protein expression in % of Ctrl
300
200
100
0
***
*
Angulin-1
Tricellulin
Cldn-2
Cldn-4
Ctrl
IL-17A
h
IL-17F
Protein expression in % of Ctrl
150
100
50
0
***
Angulin-1
Tricellulin
Cldn-2
Cldn-4
Ctrl
IL-17F

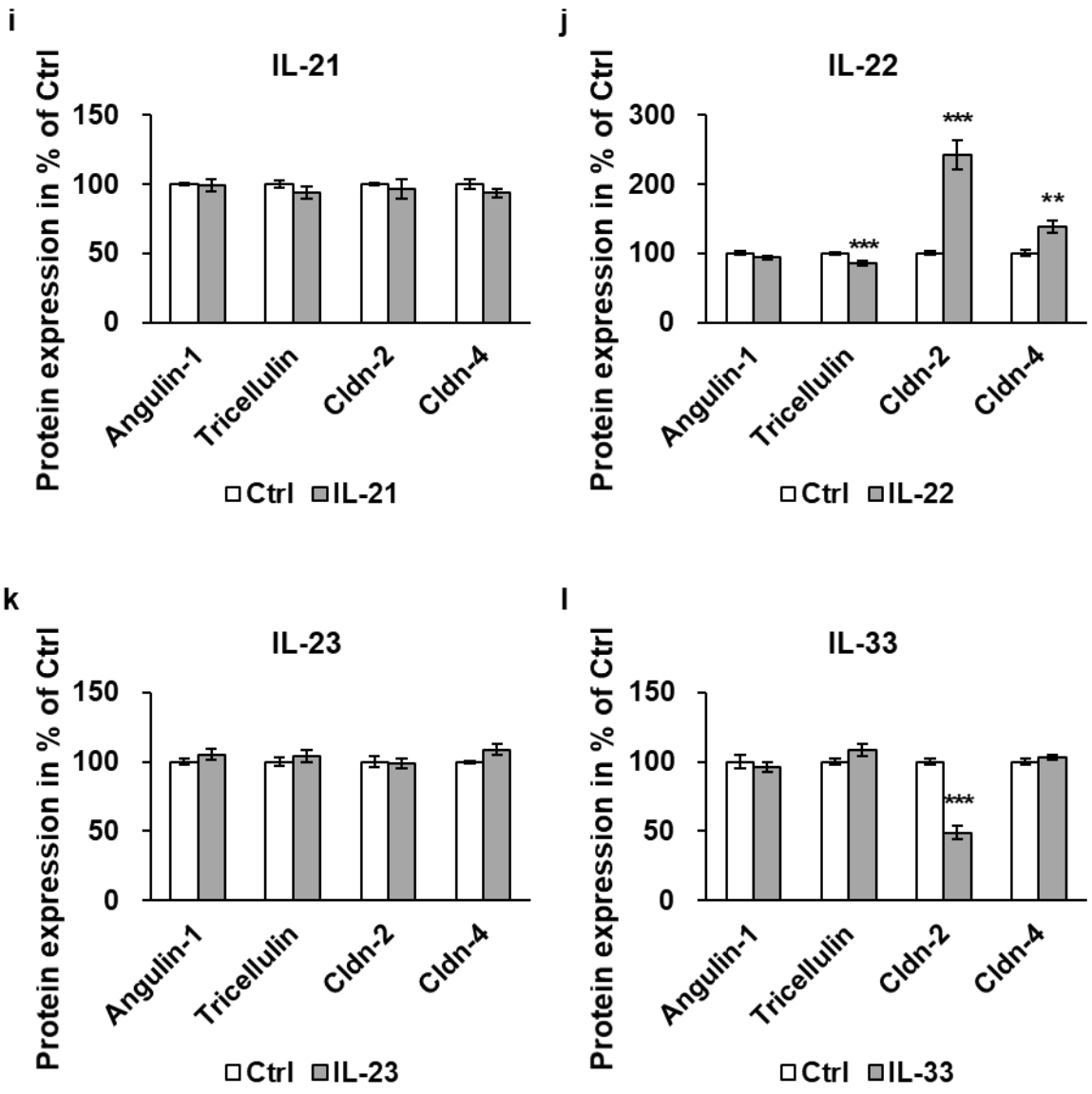

Figure 12 *Cytokines effect on TJ protein expression in T84 cells. Densitometric analysis revealed that leptin led to a downregulation of angulin-1 to 81.11 ± 2.07 % of untreated Ctrl after 48 h (**c**, ***p < 0.001, n = 12), while other cytokines did not affect angulin-1 expression. Tricellulin expression was reduced by 48 h of IL-22 treatment (**j**, ***p < 0.001, n = 12) while elevated by 48 h of IL-6 treatment (**e**, *p < 0.05, n = 12).*

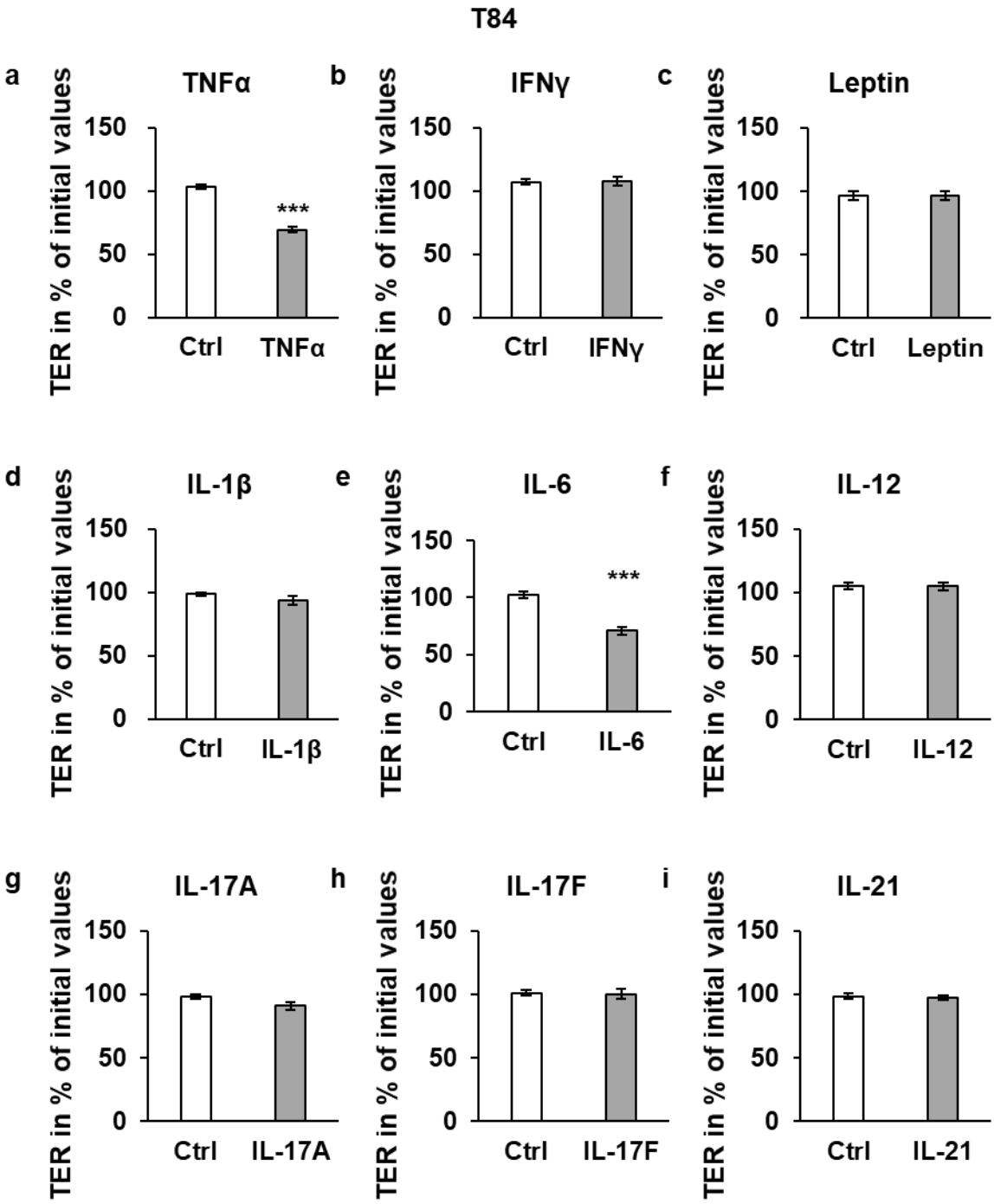
T84
a
TNFα
b
IFNγ
c
Leptin
d
IL-1β
e
IL-6
f
IL-12
g
IL-17A
h
IL-17F
i
IL-21
TER in % of initial values
150
100
50
0
***
Ctrl
TNFα
IFNγ
Leptin
IL-1β
IL-6
IL-12
IL-17A
IL-17F
IL-21

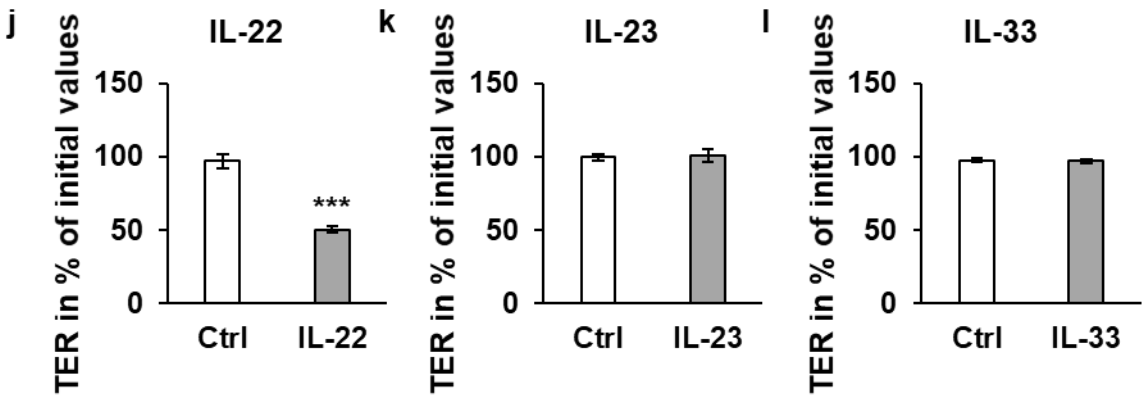

Figure 13 *Cytokines effect on TER in T84 cells. 24 h of TNF-α treatment, 48 h of IL-6 or IL-22 reduced the TER to 69.37 ± 1.93 % (**a**, ***p < 0.001, n = 9), 71.12 ± 3.45 % (**e**, ***p < 0.001, n = 9), and 50.42 ± 2.22 % (**j**, ***p < 0.001, n = 9) respectively.*

In Caco-2 cells, leptin was also the only cytokine that led to a downregulation of angulin-1 (**Figure 14c**, ****p* < 0.001). A slight increase of angulin-1 was observed after the treatment with TNF-α (**Figure 14a**, ***p* < 0.01) or IL-17F (**Figure14h**, **p* < 0.05). All the cytokines tested resulted in non-significant change of tricellulin protein expression (**Figure 14**). Cldn-2 was upregulated by TNF-α (**Figure 14a**, ****p* < 0.001), IL-6 (**Figure 14e**, ****p* < 0.001), IL-17F (**Figure 14h**, **p* < 0.05), IL-22 (**Figure 14j**, ****p* < 0.001), and IL-33 (**Figure 14i**, **p* < 0.05), whereas Cldn-4 protein expression was increased by TNF-α (**Figure 14a**, ****p* < 0.001), IL-6 (**Figure14e**, **p* < 0.05), IL-17F (**Figure14h**, **p* < 0.05), and IL-22 (**Figure14j**, **p* < 0.05). As for TER, there was also no significant change observed after leptin treatment (**Figure 15c**), while TNF-α (**Figure 15a**, ****p* < 0.001) and IL-22 (**Figure 15j**, ***p* < 0.01) could lead to a reduction of TER in Caco-2 cells.

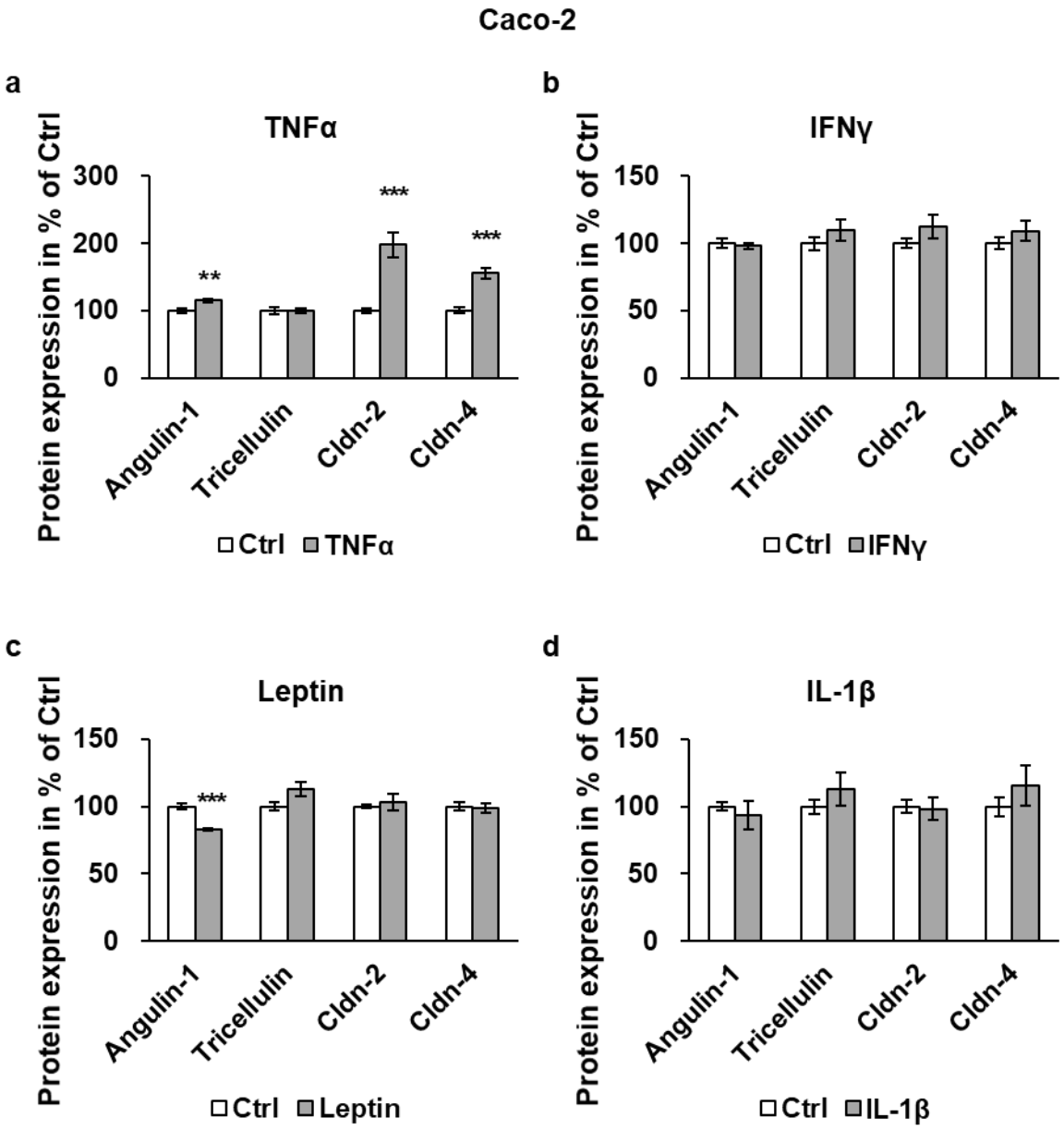
Caco-2
a
TNFα
Protein expression in % of Ctrl
300
200
100
0
**
***
***
Angulin-1
Tricellulin
Cldn-2
Cldn-4
Ctrl
TNFα
b
IFNγ
Protein expression in % of Ctrl
150
100
50
0
Angulin-1
Tricellulin
Cldn-2
Cldn-4
Ctrl
IFNγ
c
Leptin
Protein expression in % of Ctrl
150
100
50
0
***
Angulin-1
Tricellulin
Cldn-2
Cldn-4
Ctrl
Leptin
d
IL-1β
Protein expression in % of Ctrl
150
100
50
0
Angulin-1
Tricellulin
Cldn-2
Cldn-4
Ctrl
IL-1β

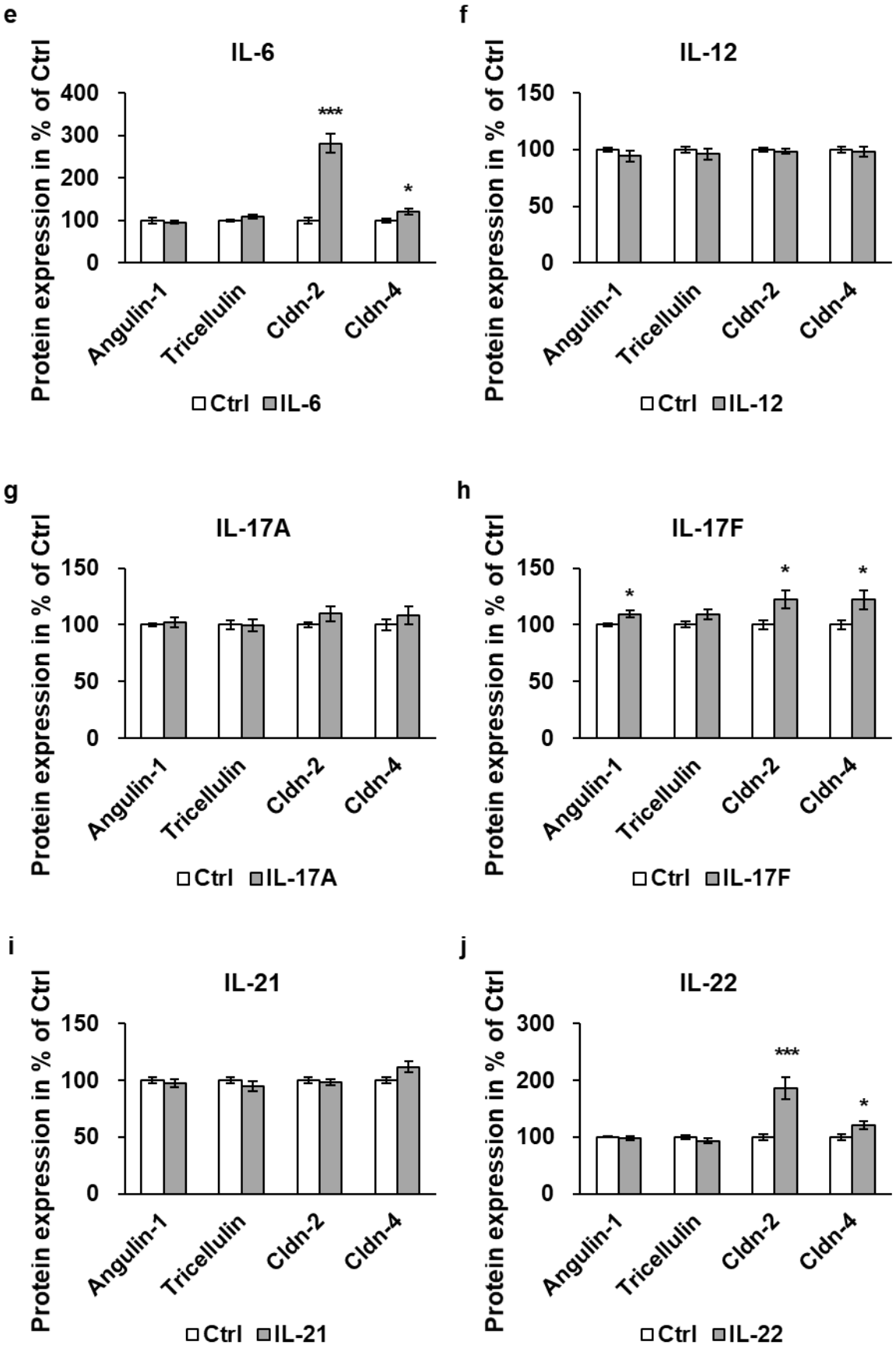
e
IL-6
Protein expression in % of Ctrl
400
300
200
100
0
***
*
Angulin-1
Tricellulin
Cldn-2
Cldn-4
Ctrl
IL-6
f
IL-12
Protein expression in % of Ctrl
150
100
50
0
Angulin-1
Tricellulin
Cldn-2
Cldn-4
Ctrl
IL-12
g
IL-17A
Protein expression in % of Ctrl
150
100
50
0
Angulin-1
Tricellulin
Cldn-2
Cldn-4
Ctrl
IL-17A
h
IL-17F
Protein expression in % of Ctrl
150
100
50
0
*
*
*
Angulin-1
Tricellulin
Cldn-2
Cldn-4
Ctrl
IL-17F
i
IL-21
Protein expression in % of Ctrl
150
100
50
0
Angulin-1
Tricellulin
Cldn-2
Cldn-4
Ctrl
IL-21
j
IL-22
Protein expression in % of Ctrl
300
200
100
0
***
*
Angulin-1
Tricellulin
Cldn-2
Cldn-4
Ctrl
IL-22

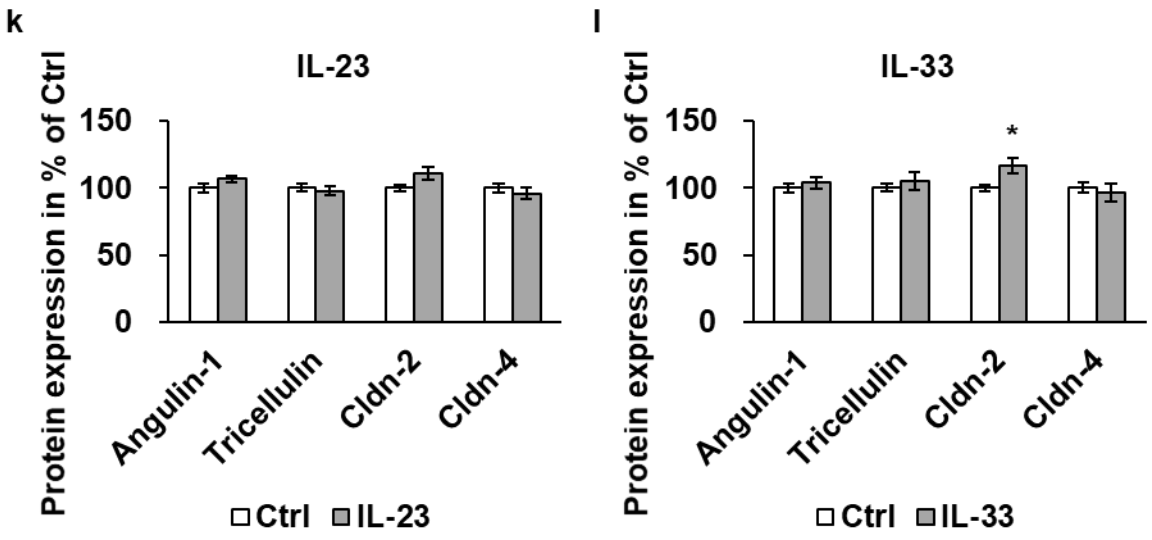

Figure 14 *Cytokines effect on TJ protein expression in Caco-2 cells. After 48 h treatment of leptin, angulin-1 was downregulated to 82.38 ± 1.03 % (**c**, ***p < 0.001, n = 12). On the contrary, TNF-α and IL-17F could slightly upregulate angulin-1 after 24 h (**a**, **p < 0.01, n = 12; **h**, *p < 0.05, n = 9).*

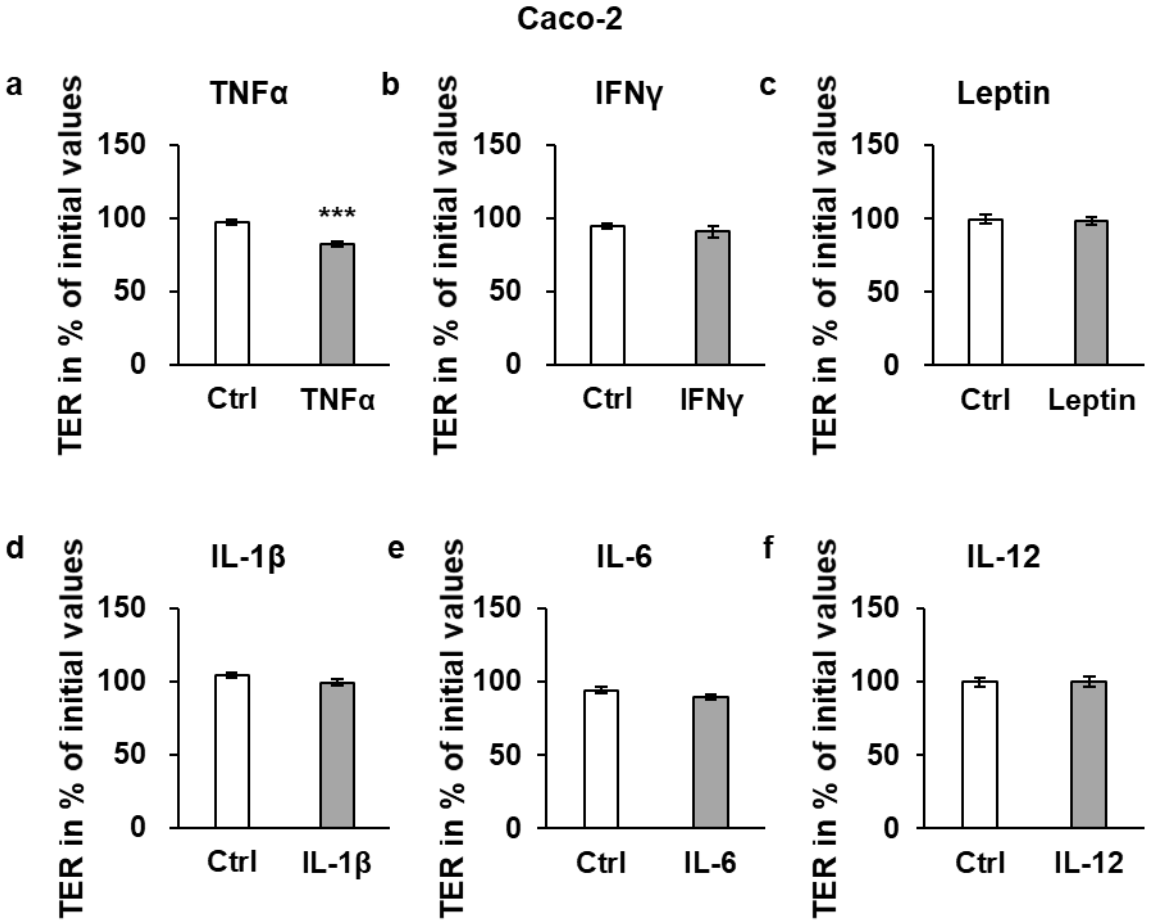

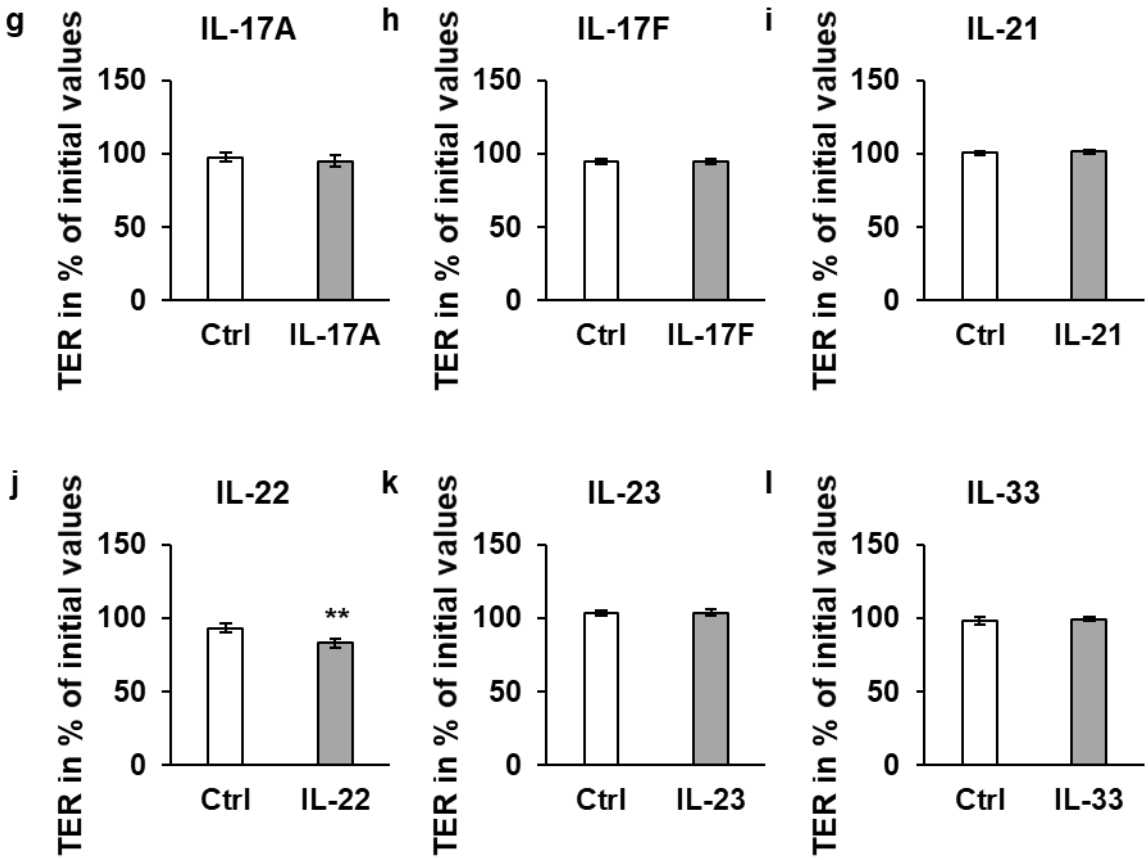

Figure 15 *Cytokines effect on TER in Caco-2 cells. The TER of Caco-2 cells was decreased after 24 h of TNF-α treatment (**a**, ***p < 0.001, n = 9) as well as 48 h treated with IL-22 (**j**, **p = 0.001, n = 9).*

In HT-29/B6 cells, unlike T84 or Caco-2 cells, angulin-1 protein expression was not affected by 48 h of leptin treatment (**Figure 16c**) but was slightly increased by IL-33 (**Figure 16l**, ****p* < 0.001). Like T84 cells, a decreased tricellulin protein level was exhibited after IL-22 treatment (**Figure 16j**, ***p* < 0.01); in addition to IL-6 (**Figure 16e**, ***p* < 0.01), tricellulin could also be upregulated by IL-21 (**Figure 16i**, ***p* < 0.01). Cldn-2 was raised due to TNF-α (**Figure 16a**, ****p* < 0.001), IL-17A (**Figure 16g**, ****p* < 0.001), IL-21 (**Figure 16i**, ****p* < 0.001), IL-22 (**Figure 16j**, ****p* < 0.001), and IL-23 treatment (**Figure 16k**, **p* < 0.05), whereas decreased by IFN-γ and IL-33 (**Figure 16b and l**, ****p* < 0.001). TNF-α, IFN-γ and IL-22 decreased TER in HT-29/B6 cells (**Figure 16 a, b, and j**, ****p* < 0.001).

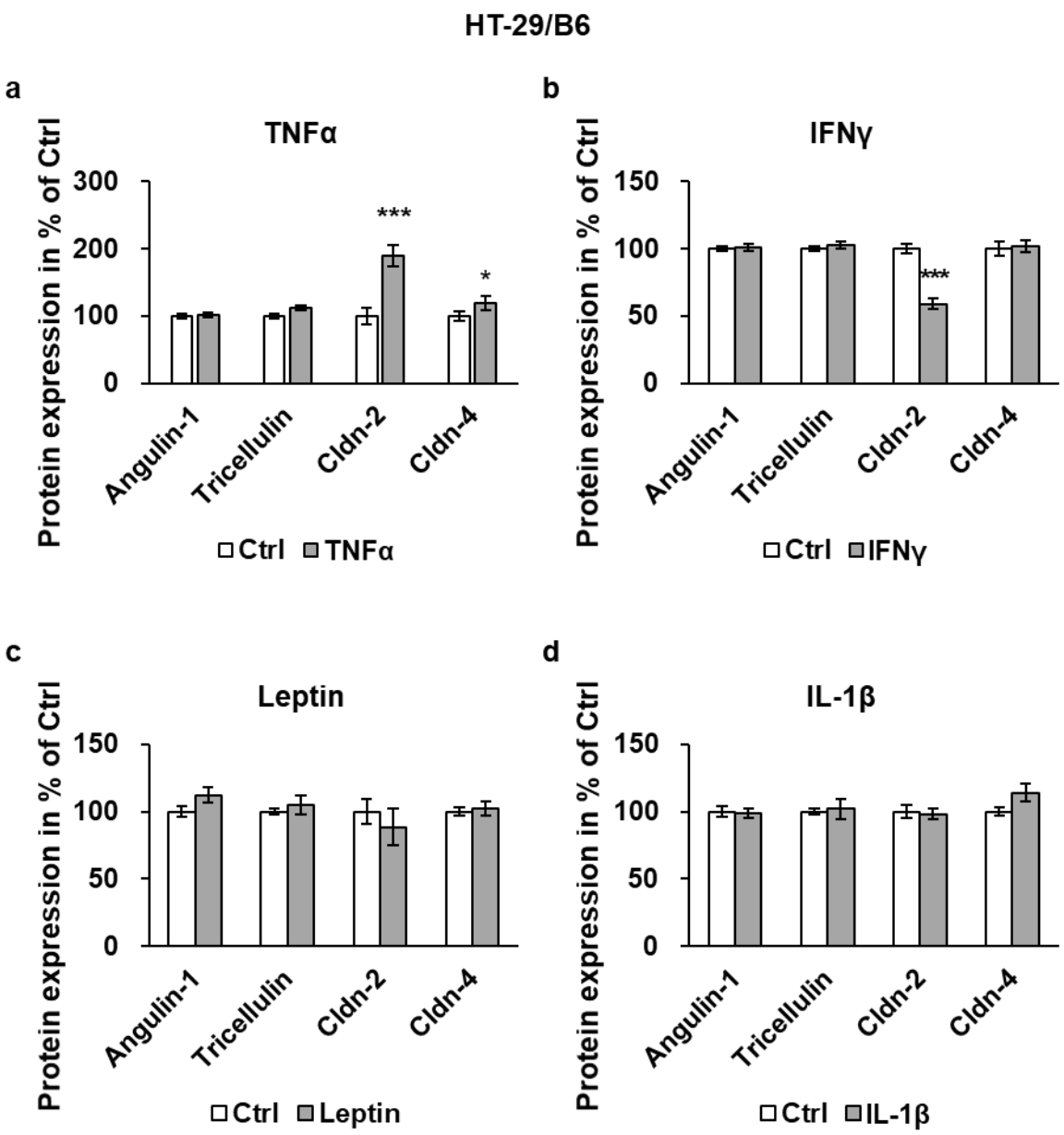
HT-29/B6
a
TNFα
Protein expression in % of Ctrl
300
200
100
0
***
*
Angulin-1
Tricellulin
Cldn-2
Cldn-4
Ctrl
TNFα
b
IFNγ
Protein expression in % of Ctrl
150
100
50
0
***
Angulin-1
Tricellulin
Cldn-2
Cldn-4
Ctrl
IFNγ
c
Leptin
Protein expression in % of Ctrl
150
100
50
0
Angulin-1
Tricellulin
Cldn-2
Cldn-4
Ctrl
Leptin
d
IL-1β
Protein expression in % of Ctrl
150
100
50
0
Angulin-1
Tricellulin
Cldn-2
Cldn-4
Ctrl
IL-1β

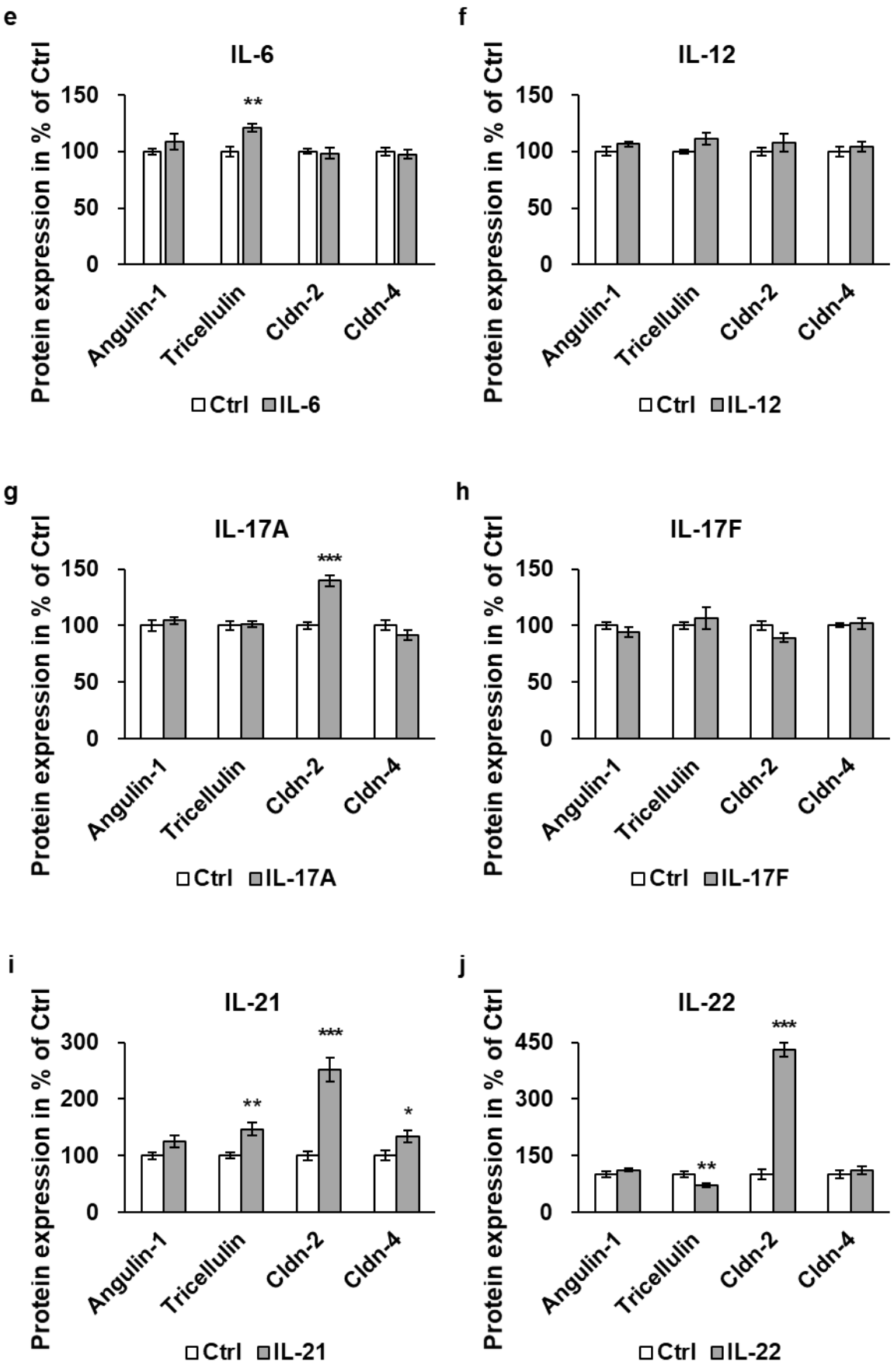
e
IL-6
Protein expression in % of Ctrl
150
100
50
0
**
Angulin-1
Tricellulin
Cldn-2
Cldn-4
Ctrl
IL-6
f
IL-12
Protein expression in % of Ctrl
150
100
50
0
Angulin-1
Tricellulin
Cldn-2
Cldn-4
Ctrl
IL-12
g
IL-17A
Protein expression in % of Ctrl
150
100
50
0
***
Angulin-1
Tricellulin
Cldn-2
Cldn-4
Ctrl
IL-17A
h
IL-17F
Protein expression in % of Ctrl
150
100
50
0
Angulin-1
Tricellulin
Cldn-2
Cldn-4
Ctrl
IL-17F
i
IL-21
Protein expression in % of Ctrl
300
200
100
0
**
***
*
Angulin-1
Tricellulin
Cldn-2
Cldn-4
Ctrl
IL-21
j
IL-22
Protein expression in % of Ctrl
450
300
150
0
**
***
Angulin-1
Tricellulin
Cldn-2
Cldn-4
Ctrl
IL-22

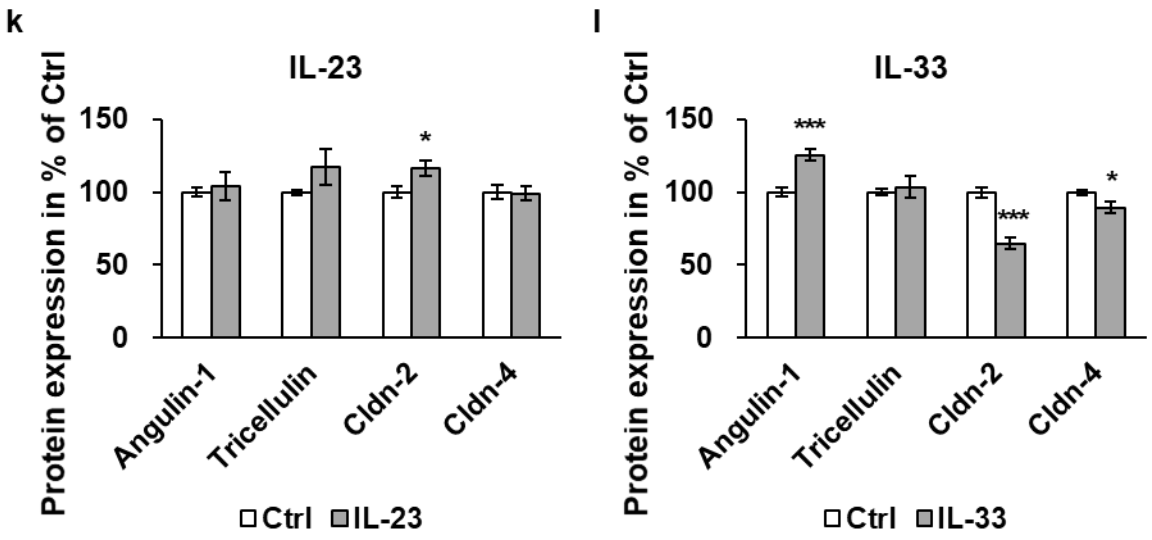

Figure 16 *Cytokines effect on TJ protein expression in HT-29/B6. Angulin-1 was upregulated to 125.38 ± 3.97 % of untreated Ctrl after 48 h IL-33 treatment (**l**, ***p < 0.001, n = 9). Tricellulin was decreased by IL-22 to 69.98 ± 5.28 % (**j**, **p < 0.01, n = 9) but increased by IL-6 to 120.84 ± 3.32 % (**e**, **p < 0.01, n = 11) and IL-21 to 146.62 ± 11.67 % (**l**, **p < 0.01, n = 8).*

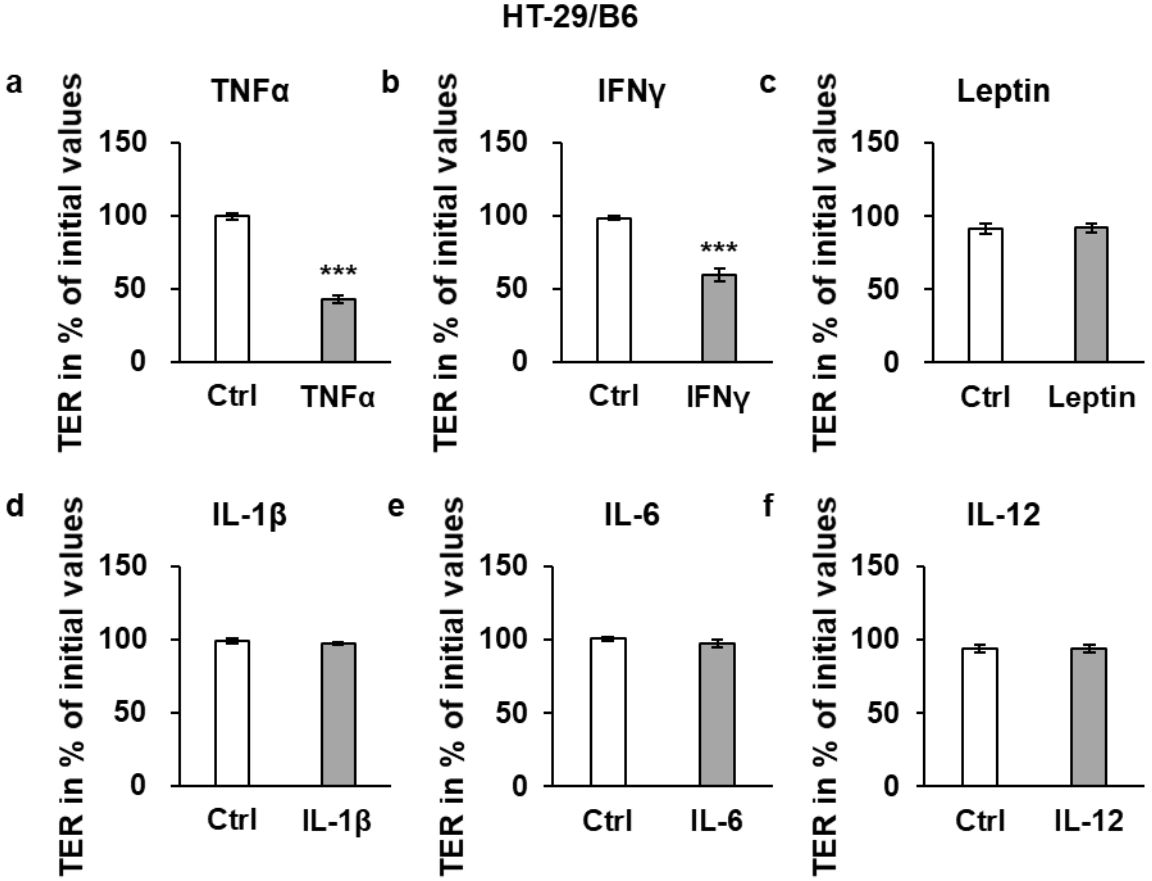

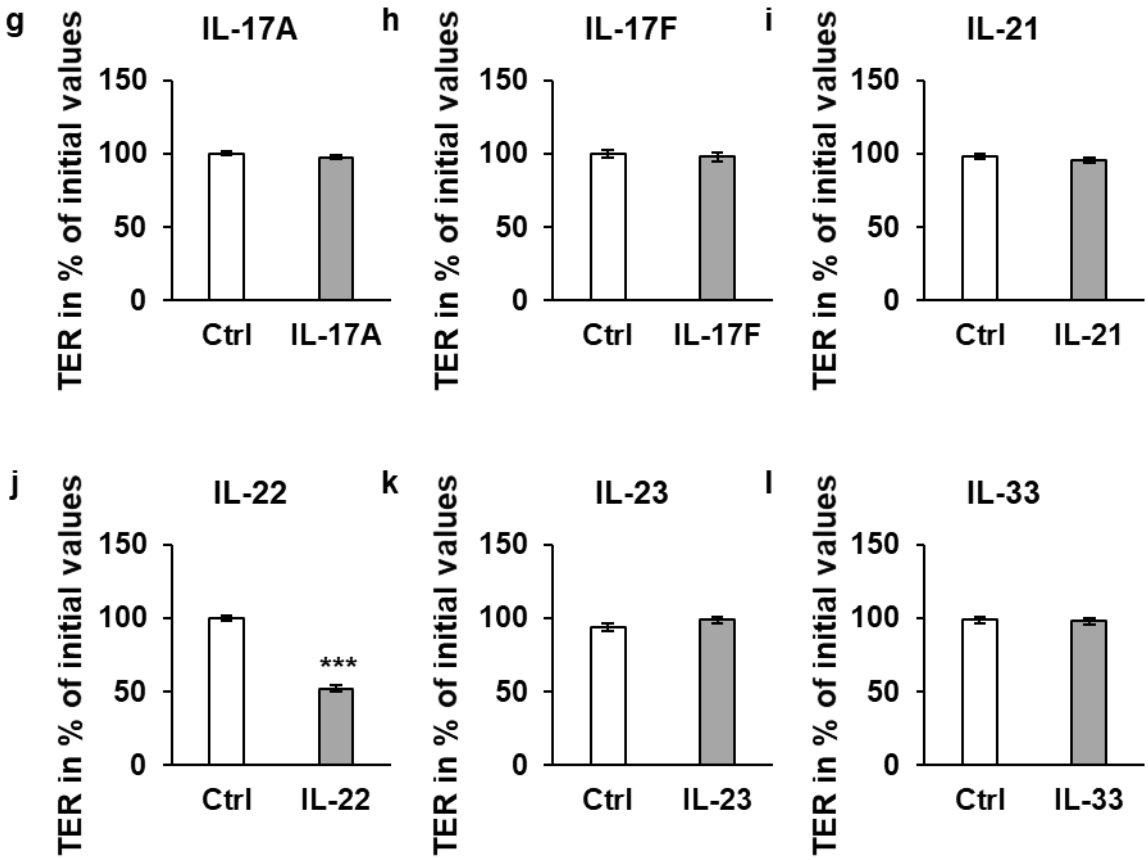

Figure 17 *Cytokines effect on TER in HT-29/B6. TER was reduced to 42.66 ± 2.30 % by TNF-α (**a**, ***p < 0.001, n = 9), 59.31 ± 4.03 % by IFN-γ (**b**, ***p < 0.001, n = 9), and 51.88 ± 2.22 % by IL-22 (**j**, ***p < 0.001, n = 9).*

Then, leptin treatment for different time periods (24 h, 48 h and 96 h) was applied and the protein expression of angulin-1 and tricellulin was investigated. In T84 cells, angulin-1 only showed a tendency of decrease after 24 h of treatment (**Figure 18a**, n = 6) whereas 96 h of leptin treatment led to nearly 50 % of angulin-1 downregulation (**Figure 18a**, ****p* < 0.001, n = 12). The protein expression of tricellulin was comparable at these three time points compared to untreated Ctrl (**Figure 18b**).

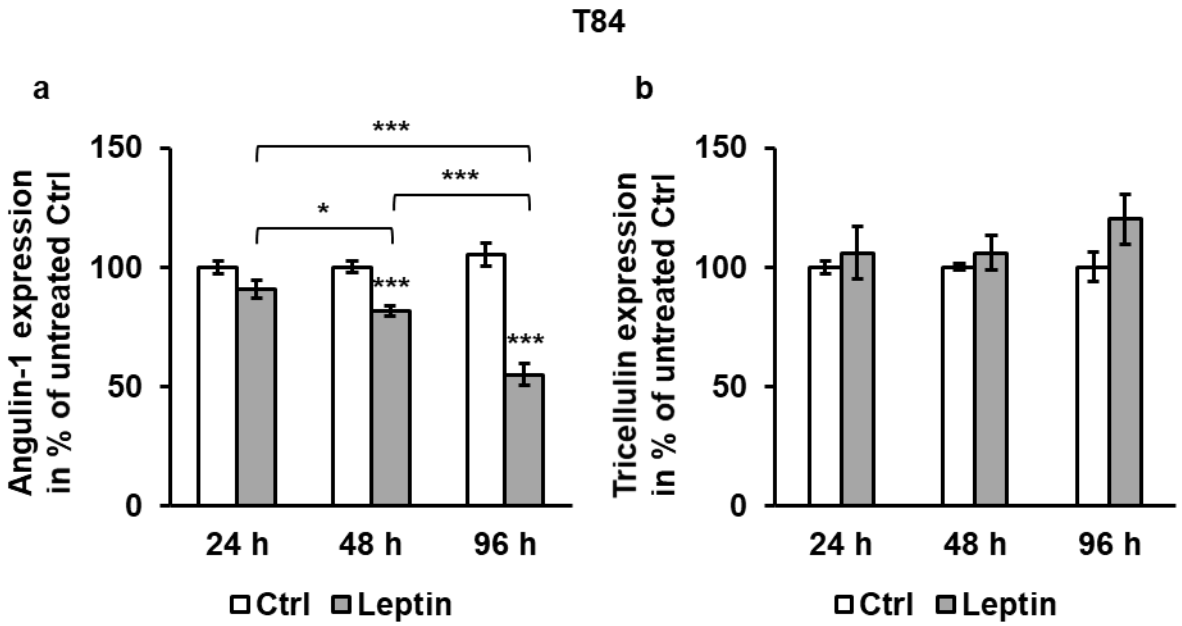

Figure 18 *Protein expression effect of leptin at different time point in T84 cells.* ***(a)*** *Densitometric analysis showed angulin-1 expression to be 90.68 ± 3.83 % at 24 h (n = 6), 81.11 ± 2.07 % at 48 h (***p < 0.001, n = 12), and 58.66 ± 2.62 % at 96 h (***p < 0.001, n = 12) compared to untreated Ctrl. The protein expression at 96 h was decreased compared to both 24 h (***p < 0.001) and 48 h (***p < 0.001). At 48 h, angulin-1 expression was also lower than 24 h (*p < 0.05).* ***(b)*** *Tricellulin expression level had no difference between 24 h (n = 6), 48 h (n = 12), and 96 h (n = 6).*

In Caco-2 cells, angulin-1 protein expression demonstrated a similar time-dependent pattern and was downregulated to a larger extent after 96 h of leptin treatment compared to untreated Ctrl (**Figure 19a**, ****p* < 0.001, n = 12) as well as treatment for 24 h (**Figure 19a**, ****p* < 0.001, n = 6) or 48 h (**Figure 19a**, ****p* < 0.001, n = 12). Likewise, there was no difference on tricellulin expression at different time points investigated (**Figure 19b**).

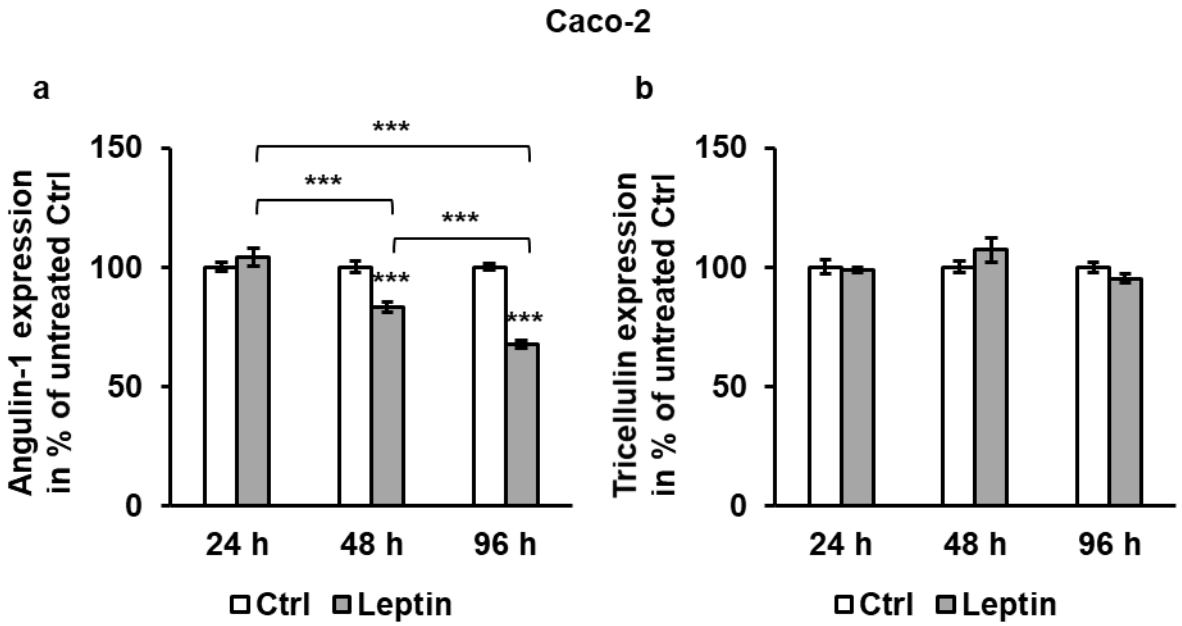

Figure 19 *Protein expression effect of leptin at different time point in Caco-2 cells.* ***(a)*** *Angulin-1 expression level exhibited reduction at 48 h (82.38 ± 1.03 %, ***p < 0.001, n = 12) and 96 h (67.71 ± 1.68 %, ***p < 0.001, n = 12) of leptin treatment compared to untreated Ctrl. There was significant difference between 24 h and 48 h (***p < 0.001), 48 h (***p < 0.001) and 96 h (***p < 0.001), and 24 h and 96h.* ***(b)*** *Tricellulin expression was not affected by leptin at 24 h, 48 h, nor 96 h.*

4.1.4 Barrier function of T84 and Caco-2 cells treated with leptin

To determine whether this expressional change of angulin-1 could lead to alteration of macromolecule passage, TER as well as permeability for the macromolecule marker FITC-dextran 4 kDa (FD4) was investigated in T84 and Caco-2 cells treated with leptin. In both cell lines, the TER values remained at a similar level after incubation with leptin compared with Ctrl (**Figure 20a, c**). As for the permeability for FD4, the results between Ctrl and leptin group were comparable in T84 cells (**Figure 20b**), whereas in Caco-2 cells, permeability for FD4 was increased (**Figure 20d**, *$p < 0.05$).

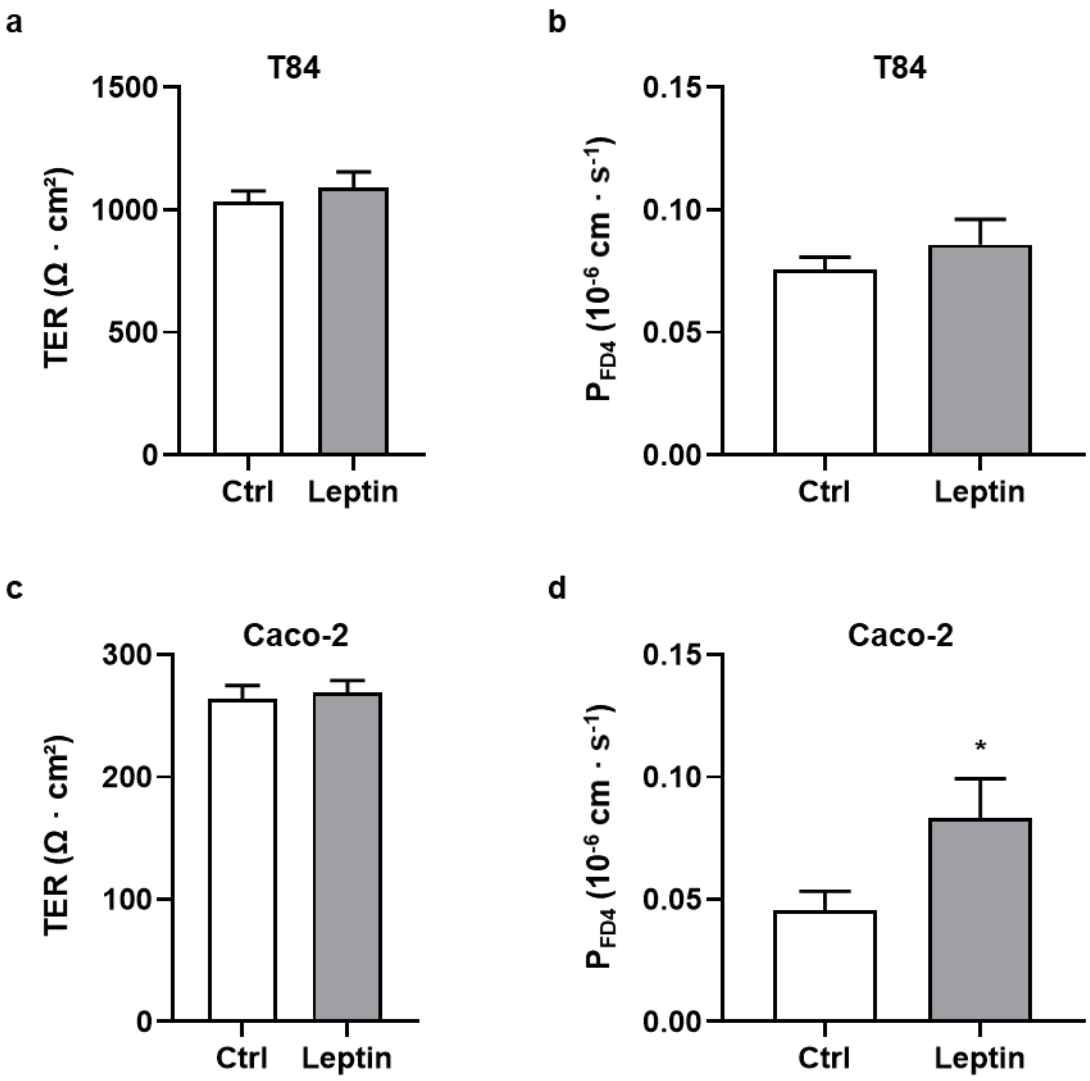

Figure 20 *Functional analysis in T84 and Caco-2 cells.* ***(a)*** *Transepithelial resistance in T84 cells.* ***(b)*** *Permeability for FITC-dextran 4 kDa in T84 cells: Ctrl = 0.075 ± 0.005 · 10^{-6} cm · s^{-1}, n = 9; Leptin = 0.086 ± 0.01 · 10^{-6} cm · s^{-1}, n = 8.* ***(c)*** *Transepithelial resistance in T84 cells.* ***(d)*** *Permeability for FITC-dextran 4 kDa in Caco-2 cells: Ctrl = 0.045 ± 0.008 · 10^{-6} cm · s^{-1}, n = 9; Leptin = 0.083 ± 0.016 · 10^{-6} cm · s^{-1}, n = 11, *p < 0.05.*

4.1.5 Tricellulin localization after leptin treatment

Immunofluorescent staining was then carrier out in order to investigate whether a shifted localization of tricellulin could also be induced by leptin treatment. The localization of tricellulin was not changed and remained at tTJs in both T84 and Caco-2 cells treated with leptin (**Figure 21**).

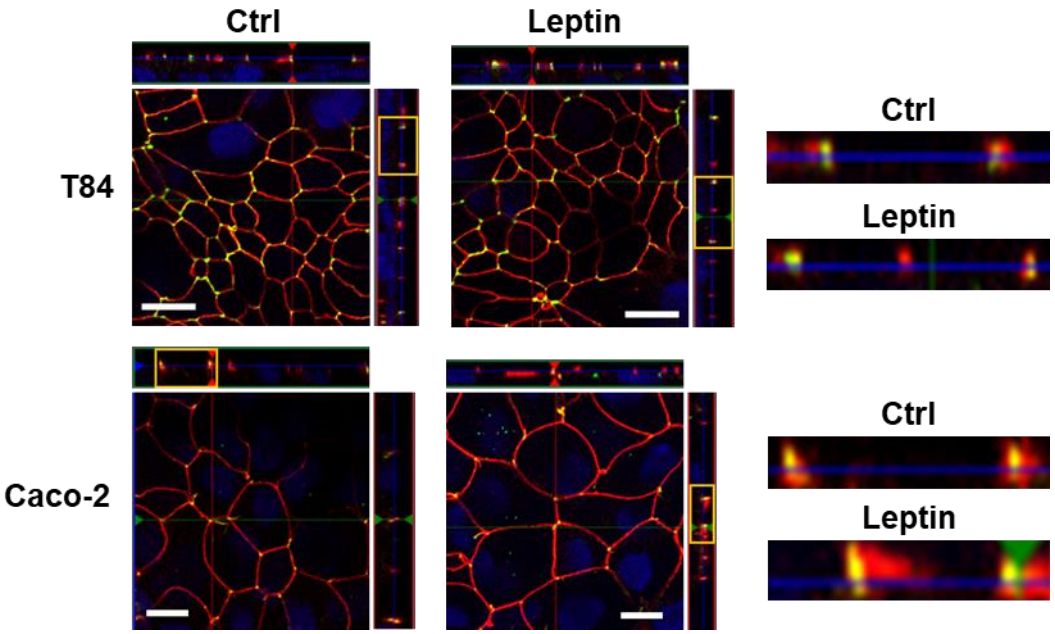

Figure 21 *Representative immunofluorescent staining of tricellulin (green) and ZO-1 (red) in human intestinal cell lines. Nuclei were stained using DAPI (blue). With the TJ indicator ZO-1, the localization of tricellulin at tTJs are demonstrated. The selected Z-scans (yellow box) are magnified on the right, indicating that there were no localization shifts in lateral direction. Bars = 10 µm.*

4.1.6 Signaling pathway of leptin

Regarding the signaling pathways of leptin, JAK2 (Myers et al., 2008), STAT3 (Shimada et al., 2016a), ERK1/2 (Banks et al., 2000), and PI3K (Plum et al., 2007) were reported in literature. Therefore, their corresponding inhibitors were applied 1 h prior to leptin treatment in order to figure out the potential responsible signaling pathways for angulin-1 downregulation induced by leptin. JAK2 was supposed to be the upstream pathway but in both T84 and Caco-2 cells its inhibitor AG490 only partially blocked the decrease of angulin-1 (**Figure 22a, b**, $*p < 0.05$, n = 6). STAT3 inhibitors Stattic and WP1066 on the other hand could completely inhibit this effect in both cell lines (**Figure 22a, b**, $***p < 0.001$, n = 6).

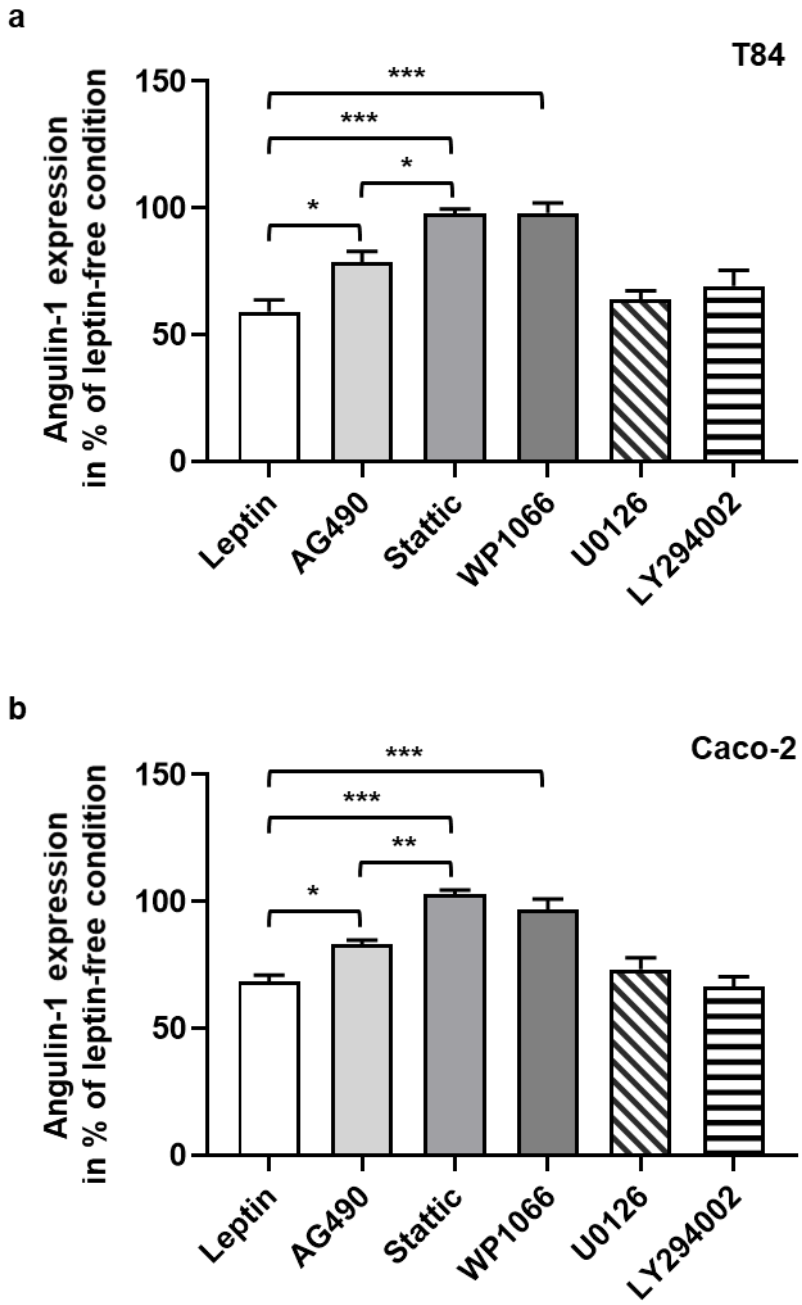

Figure 22 *Densitometric analysis of angulin-1 expression pre-treated with different inhibitors in T84 cells* ***(a)*** *and in Caco-2 cells* ***(b)****. JAK2 inhibitor AG490 was able to partially restore the expression of angulin-1 (*p < 0.05, n = 6). STAT3 inhibitors Stattic and WP1066 block the downregulation of leptin (***p < 0.001, n = 6, respectively). ERK1/2 inhibitor U0126 and PI3K inhibitor LY294002 showed no effect on angulin-1 downregulation.*

Next, phosphorylation protein analysis was performed in order to further illuminate STAT3 regulation. A significant change of STAT3 phosphorylation was observed after 30 min incubation with leptin in T84 cells (**Figure 23a**, $^{**}p < 0.01$, n = 7) and in Caco-2 cells (**Figure 23b**, $^{**}p < 0.01$, n = 6) and peaked after 60 min of leptin treatment in T84 cells (**Figure 23a**, $^{***}p < 0.001$, n = 11) and in Caco-2 cells (**Figure 23b**, $^{**}p < 0.01$, n = 9).

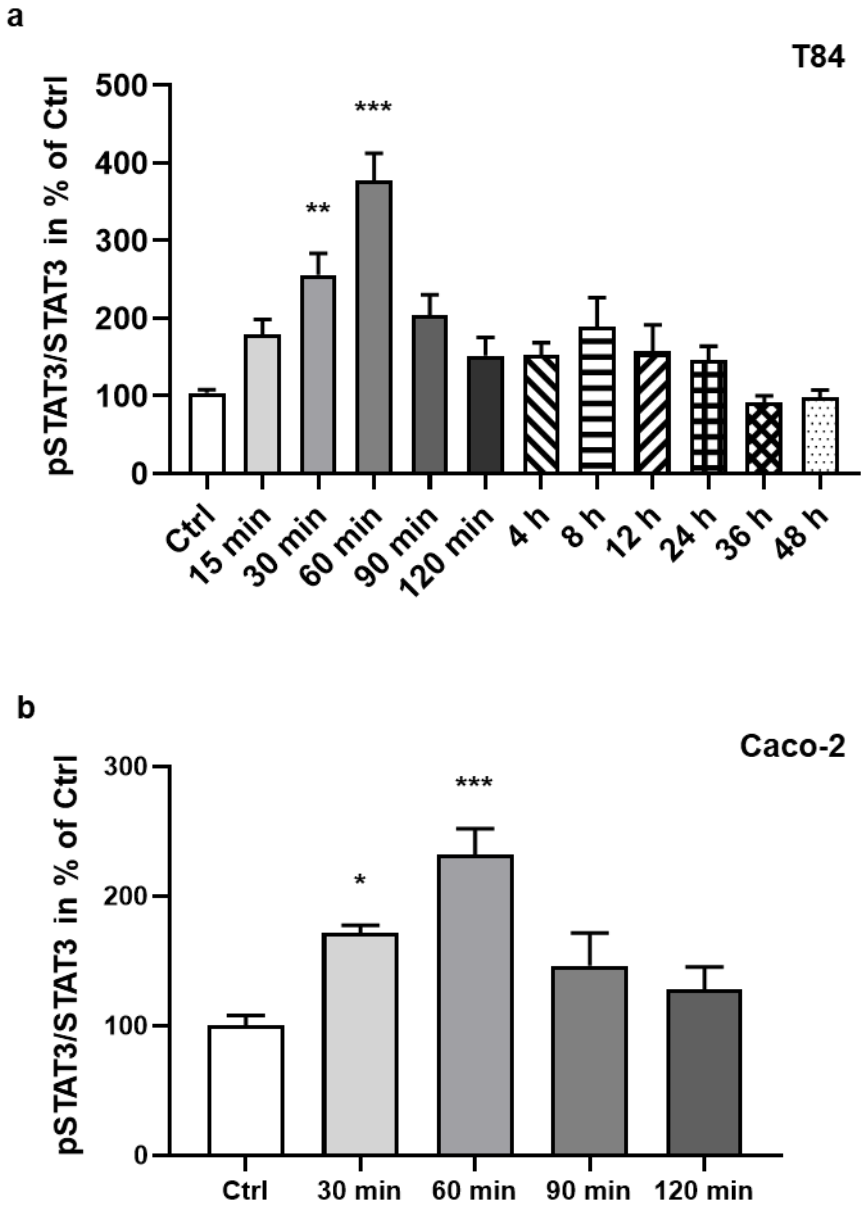

Figure 23 *Phosphorylated STAT3 to total STAT3 ratio at different time points of leptin treatment in T84* ***(a)*** *and Caco-2 cells* ***(b)****. The phosphorylation of STAT3 reached significancy after 30 min of leptin treatment and peaks at 60 min in both cell lines. *p < 0.05, **p < 0.01, ***p < 0.001, n = 6 – 11.*

With 1 h of pre-incubation with JAK2 inhibitor AG490, a partial blockage of STAT3 phosphorylation was demonstrated in T84 cells (**Figure 24a**, $^{**}p < 0.01$, n = 8) and in Caco-2 cells (**Figure 24b**, $^{*}p < 0.05$, n = 6). Akin to the inhibitors finding on angulin-1 protein expression, the phosphorylation of STAT3 was fully inhibited by the treatment of Stattic or WP1066 in both cell lines (**Figure 24a, b**, $^{***}p < 0.001$, n = 6 - 8).

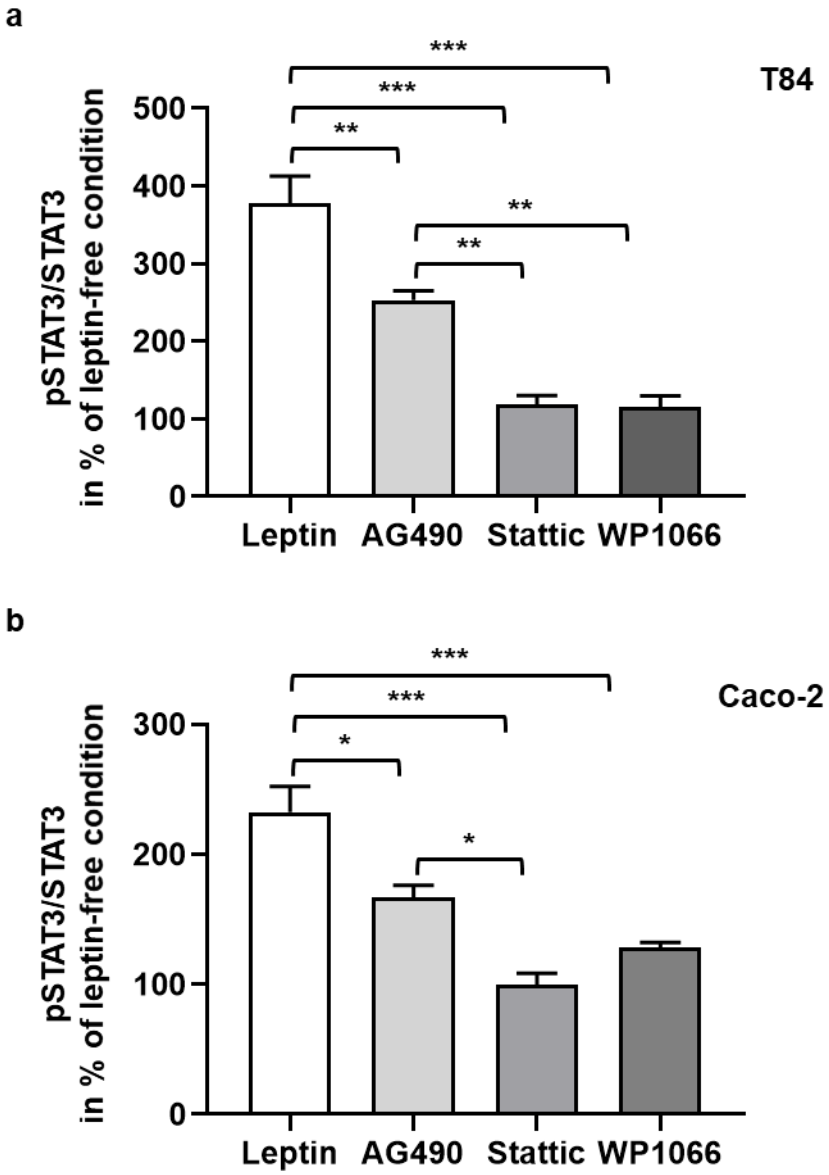

Figure 24 *Effect of inhibitors on phosphorylated STAT3 to total STAT3 ratio in T84* ***(a)*** *and in Caco-2 cells* ***(b)****. The phosphorylation of STAT3 was reduced to leptin-free condition after the application of Stattic or WP1066 (***p < 0.001, n = 6, respectively). AG490 was only able to incompletely inhibit STAT3 pathway. *p < 0.05, **p < 0.01, ***p < 0.001, n = 6 – 8.*

4.2 Potential role of tricellulin in remission of UC

4.2.1 Patients features

From 2017 to 2020, 14 UC patients and 24 controls (patients without intestinal diseases who had colonoscopy examination) were enrolled to the project (**Table 2**). The diagnosis of UC follows the latest guideline Ungaro et al. (2017). In total, 36 pieces of biopsies were collected from the 14 UC patients from different time of follow-up. The Mayo endoscopic subscore was used to evaluate disease activity (Schroeder et al., 1987). Remission of UC was defined according to the clinical presentation and to the normal Mayo endoscopic subscore while active patients were those with mild, moderate, or severe disease activity.

Table 2 Characteristics of the enrolled patients

Characteristic	Control (n = 24)	UC (n = 14)
Age (median, range)	54 (24-66)	50 (35-60)
Gender (male/female)	8/16	5/9
Mayo endoscopic subscore (n)		
normal	-	10
active	-	4

4.2.2 Tricellulin expression in remission of UC

Using the collected biopsies, the expression of tricellulin along with several other TJ proteins was analysed on both mRNA and protein level. First, on mRNA expression level, tricellulin in remission patients of UC (UC_{Rem}) was not changed compared with controls (Ctrl) (**Figure 25a**), consistent with a recent research from Kjærgaard et al. (2020). Previous study investigated claudin-2 (Cldn-2) and claudin-4 (Cldn-4) protein expression in active patients of UC (Krug et al., 2018), thus here the mRNA expression level of these two proteins was also analysed in order to be comparable. In UC_{Rem}, Cldn-2 and Cldn-4 mRNA expression were unaltered in comparison with Ctrl (**Figure 25b, c**). As for the other component of the tTJ, the angulin family (angulin-1, -2, -3) which played a role in CD without alteration of tricellulin expression (Hu et al., 2020) also showed comparable mRNA expression in UC_{Rem} and Ctrl (**Figure 25d–f**).

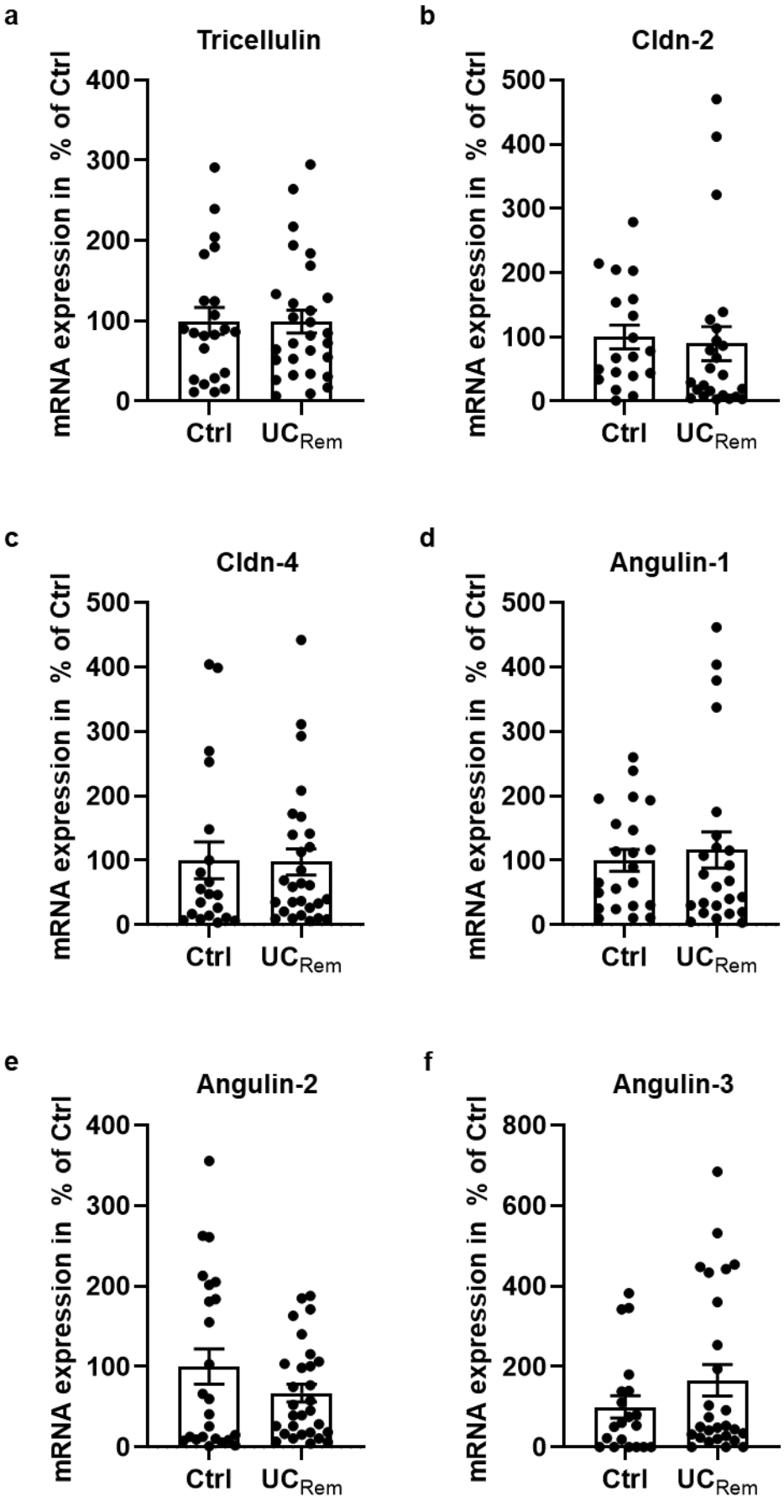
a
Tricellulin
mRNA expression in % of Ctrl
400
300
200
100
0
Ctrl
UCRem
b
Cldn-2
mRNA expression in % of Ctrl
500
400
300
200
100
0
Ctrl
UCRem
c
Cldn-4
mRNA expression in % of Ctrl
500
400
300
200
100
0
Ctrl
UCRem
d
Angulin-1
mRNA expression in % of Ctrl
500
400
300
200
100
0
Ctrl
UCRem
e
Angulin-2
mRNA expression in % of Ctrl
400
300
200
100
0
Ctrl
UCRem
f
Angulin-3
mRNA expression in % of Ctrl
800
600
400
200
0
Ctrl
UCRem

Figure 25 *Scatterplot with bar of mRNA expression analysis of TJ proteins in human colon biopsies. Mean value of Ctrl was set to 100 %.* ***(a)*** *Tricellulin: Ctrl = 100 ± 16.75 %, n = 22, UC_{Rem}: 99.25 ± 14.37 %, n = 28.* ***(b)*** *Cldn-2: Ctrl = 100 ± 18.61 %, n = 19; UC_{Rem} = 89.66 ± 26.37 %, n = 24.* ***(c)*** *Cldn-4: Ctrl = 100 ± 28.64 %, n = 20; UC_{Rem} = 97.58 ± 20.27 %, n = 28.* ***(d)*** *Angulin-1: Ctrl = 100 ± 16.81 %, n = 22; UC_{Rem} = 116.13 ± 27.89 %, n = 24.* ***(e)*** *Angulin-2: Ctrl = 100 ± 21.85 %, n = 24; UC_{Rem} = 67.14 ± 10.88 %, n = 29.* ***(f)*** *Angulin-3: Ctrl = 100 ± 27.54 %, n = 20; UC_{Rem} = 165.79 ± 39.05 %, n = 27.*

Next, on protein expression level, tricellulin in UC_{Rem} was at the same range as in Ctrl while in active UC (UC_{Active}) was downregulated, similar to previous finding (Krug et al., 2018) (**Figure 26a, b**, $^{**}p < 0.01$). Cldn-4 in UC_{Rem} also did not change compared with Ctrl while the tendency of reduction in UC_{Active} was in line with the downregulation in previous study (Oshima et al., 2008, Krug et al., 2018) (**Figure 26c, d**). Furthermore, angulin-1 protein expression was unchanged in UC_{Rem} as well (**Figure 26e, f**).

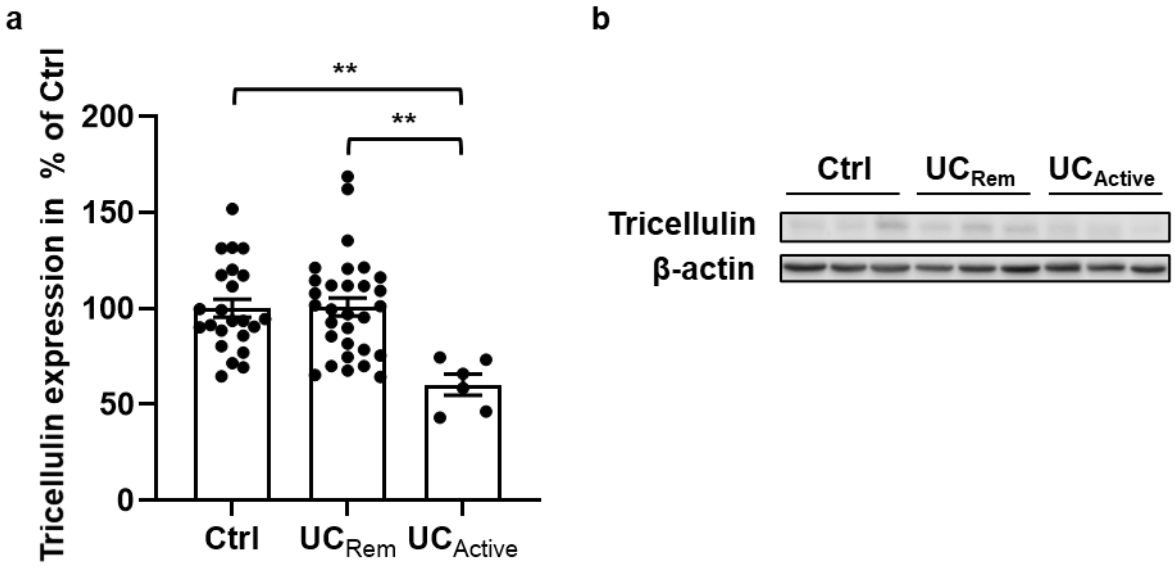

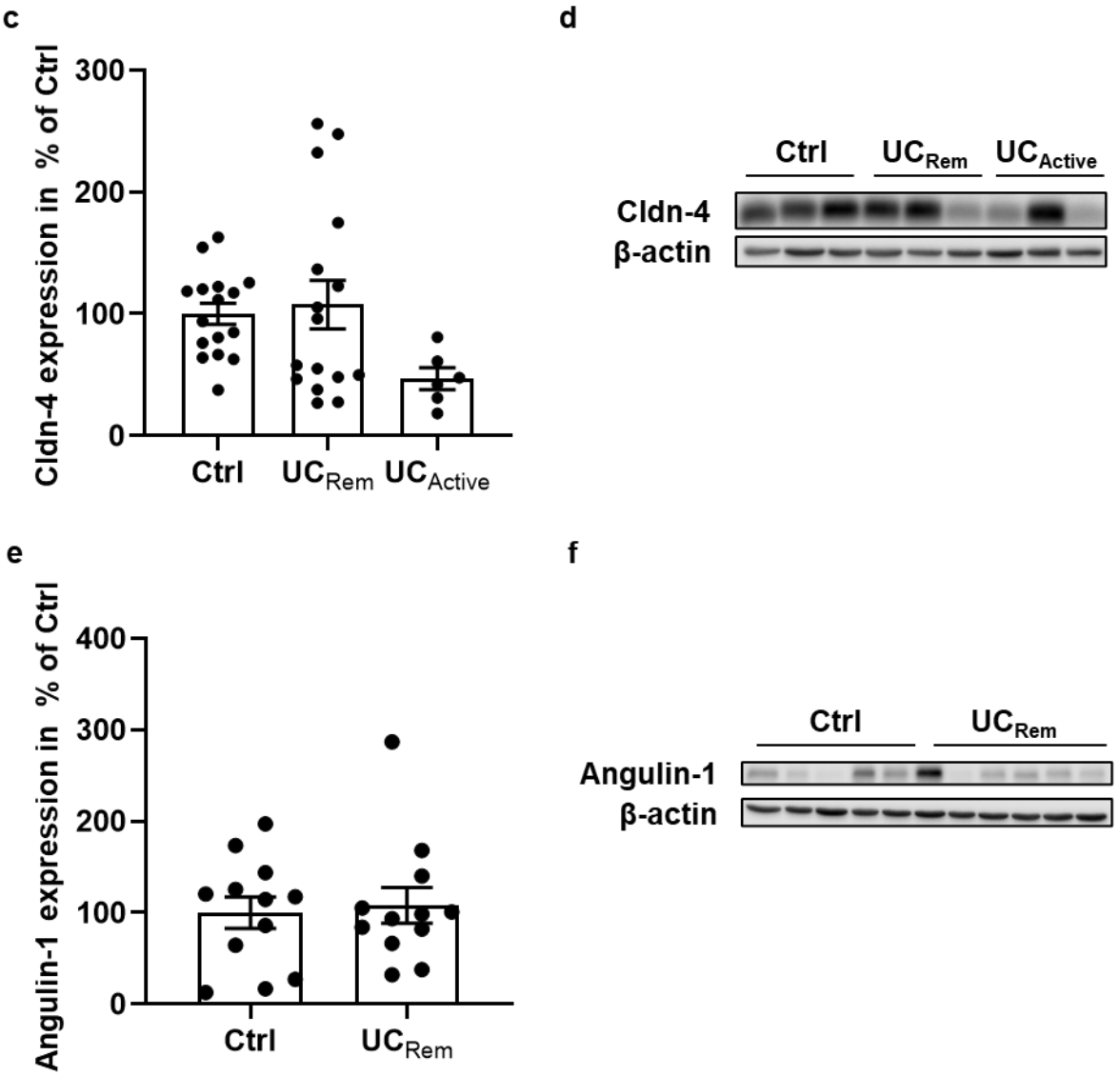

Figure 25 *Analysis of TJ proteins expression in human colon biopsies. Mean value of Ctrl was set to 100 %.* ***(a)*** *Scatterplot with bar of tricellulin of Ctrl, UC_{Rem} and UC_{Active}. Tricellulin of UC_{Rem} retained the same level compared to Ctrl, while in UC_{Active} tricellulin was downregulated compared to both UC_{Rem} and Ctrl (Ctrl: 100 ± 4.75 %, n = 23; UC_{Rem}: 100.69 ± 4.79 %, n = 30; UC_{Active}: 60.22 ± 5.47 %, n = 6, **p < 0.01).* ***(b)*** *Representative western blots of tricellulin from Ctrl, UC_{Rem} and UC_{Active}.* ***(c)*** *Scatterplot with bar of Cldn-4 of Ctrl (100 ± 8.70 %, n = 16), UC_{Rem} (107.63 ± 20.06 %, n = 16) and UC_{Active} (46.89 ± 9.03 %, n = 6).* ***(d)*** *Representative western blots of Cldn-4 from Ctrl, UC_{Rem} and UC_{Active}.* ***(e)*** *Scatterplot with bar of angulin-1 of Ctrl (100 ± 17.32 %, n = 12) and UC_{Rem} (108.01 ± 19.58 %, n = 12).* ***(f)*** *Representative western blots of angulin-1 from Ctrl and UC_{Rem}.*

4.2.3 Electrophysiological properties of colon biopsies in remission of UC

Regarding the intestinal barrier function, impedance spectroscopic analysis of the biopsies exhibited an unchanged transepithelial resistance in UC_{Rem} compared with Ctrl (**Figure 27a**). Permeability for fluorescein was also at the same level as in UC_{Rem} in comparison with Ctrl (**Figure 27b**), consistent with the previous finding that permeability for 400 Da FITC-sulfonic acid was comparable to Ctrl (Vivinus-Nébot et al., 2014). Permeability for macromolecule represented by FD4 in UC_{Rem} remained unaltered compared to Ctrl as well (**Figure 27c**).

As for UC_{Active}, transepithelial resistance (R^t) was within a similar range as in UC_{Rem} and Ctrl, wherein the epithelial resistance (R^{epi}) was reduced and the subepithelial resistance (R^{sub}) tended to raise (**Figure 27a**, $*p < 0.05$). Permeability for both fluorescein and FD4 was increased compared with Ctrl and UC_{Rem} (**Figure 27b, c**, $***p < 0.001$). These results in UC_{Active} were similar to previous findings of Krug et al. (2018).

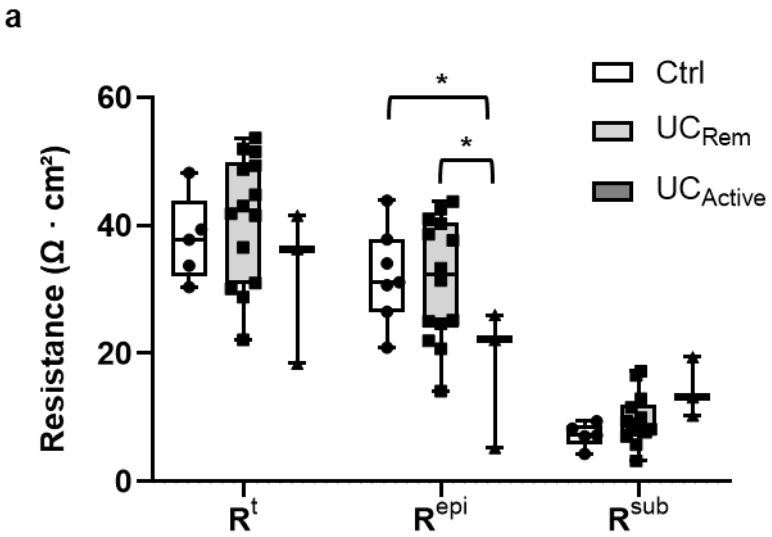

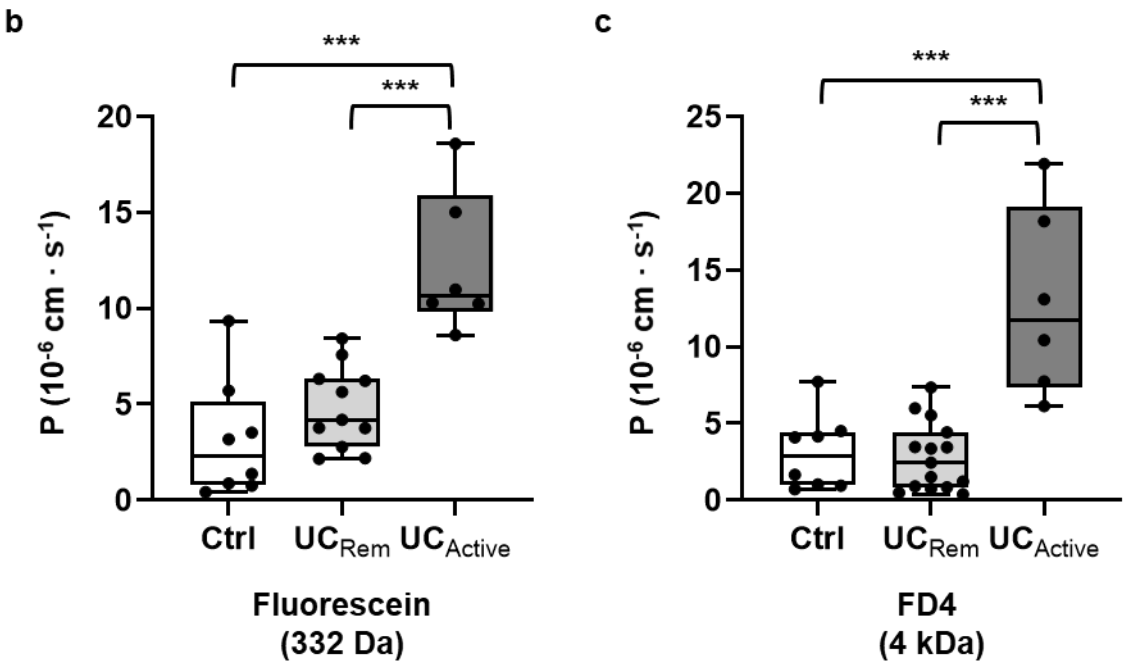

Figure 27 *Electrophysiological and functional analysis of intestinal biopsies in Ctrl, remission and active UC.* ***(a)*** *Electrical resistances of colon biopsies of Ctrl, remission UC (UC_{Rem}), and active UC (UC_{Active}). UC_{Rem} showed the same level of transepithelial resistance (R^t), epithelial (R^{epi}) and subepithelial resistance (R^{sub}) as in Ctrl (Ctrl: $R^t = 37.89 \pm 3.02\ \Omega \cdot cm^2$, $R^{epi} = 30.62 \pm 3.79\ \Omega \cdot cm^2$, $R^{sub} = 7.26 \pm 0.85\ \Omega \cdot cm^2$, n = 5; UC_{Rem}: $R^t = 41.08 \pm 2.65\ \Omega \cdot cm^2$, $R^{epi} = 31.45 \pm 2.53\ \Omega \cdot cm^2$, $R^{sub} = 9.63 \pm 1.03\ \Omega \cdot cm^2$, n = 14). UC_{Active} has lower R^{epi} ($17.8 \pm 2.53\ \Omega \cdot cm^2$, n = 3) compared with Ctrl (*p < 0.05) and UC_{Rem} (*p < 0.05), together with an increasing tendency of R^{sub} ($14.29 \pm 2.69\ \Omega \cdot cm^2$, n = 3) leading to the same level of R^t ($32.09 \pm 7.00\ \Omega \cdot cm^2$, n = 3).* ***(b)*** *Permeability for fluorescein. In Ctrl and UC_{Rem}, the permeability stayed at the same range, both of which are lower than UC_{Active} (Ctrl: $3.15 \pm 1.09 \cdot 10^{-6}$ cm · s^{-1}, n = 8; UC_{Rem}: $4.82 \pm 0.65 \cdot 10^{-6}$ cm · s^{-1}, n = 11; UC_{Active}: $12.29 \pm 1.53 \cdot 10^{-6}$ cm · s^{-1}, n = 6, ***p < 0.001).* ***(c)*** *Permeability for FITC-dextran 4 kDa. Similar results were observed that UC_{Active} had higher permeability than Ctrl and UC_{Rem} (Ctrl: $3.10 \pm 0.87 \cdot 10^{-6}$ cm · s^{-1}, n = 8; UC_{Rem}: $2.81 \pm 0.57 \cdot 10^{-6}$ cm · s^{-1}, n = 15; UC_{Active}: $12.91 \pm 2.50 \cdot 10^{-6}$ cm · s^{-1}, n = 6, ***p < 0.001).*

4.3 AP-1-involved IL-13-mediated tricellulin downregulation in UC

4.3.1 Recognition of potential AP-1 binding sites involved

Based on the previous investigation that sub-proteins of AP-1, Jun and Fos family proteins, were involved in IL-13-mediated tricellulin downregulation in UC (Krug et al., 2018), potential binding sites of these two protein families were searched in an online database ISMARA (**I**ntegrated **S**ystem for **M**otif **A**ctivity **R**esponse **A**nalysis) (Balwierz et al., 2014) and literature (Van Lint et al., 1991, Hess et al., 2004, Ji et al., 2012, Gray et al., 2012, Kim et al., 1997, Carroll et al., 2006), then recognised on a region of 5.1 kbp upstream of the start codon of tricellulin, assuming that this region might cover the whole or most important regions of the tricellulin promoter, with the focus on Jun and Fos (**Figure 28a**).

Next, in attempts to facilitate the following experiments, the 5114 bp tricellulin promoter was shortened to 3925 bp (**Figure 28b**). In addition, a 2189 bp-length promoter that did not contain Jun or Fos motif of higher affinity was also constructed in order to preliminarily screen whether these binding sites should be analysed in more detail (**Figure 28c**). All three promoters were inserted onto a firefly luciferase vector pGL4.10 and then transiently transfected to human intestinal epithelial cell line HT-29/B6 which was used in previous research (Krug et al., 2018), along with a *Renilla* luciferase vector pGL4.19 served as an internal control of the system. However, the firefly luciferase value of both shortened promoters was much lower than the 5114 bp version as well as the empty vector while the *Renilla* luciferase values were relatively comparable (**Figure 28d**), indicating that although all three promoters were able to transcript, there were important factors, for example enhancers, missing on both shorter promoters. Therefore, the 5114 bp tricellulin promoter (WT) was used as a template to generate mutations.

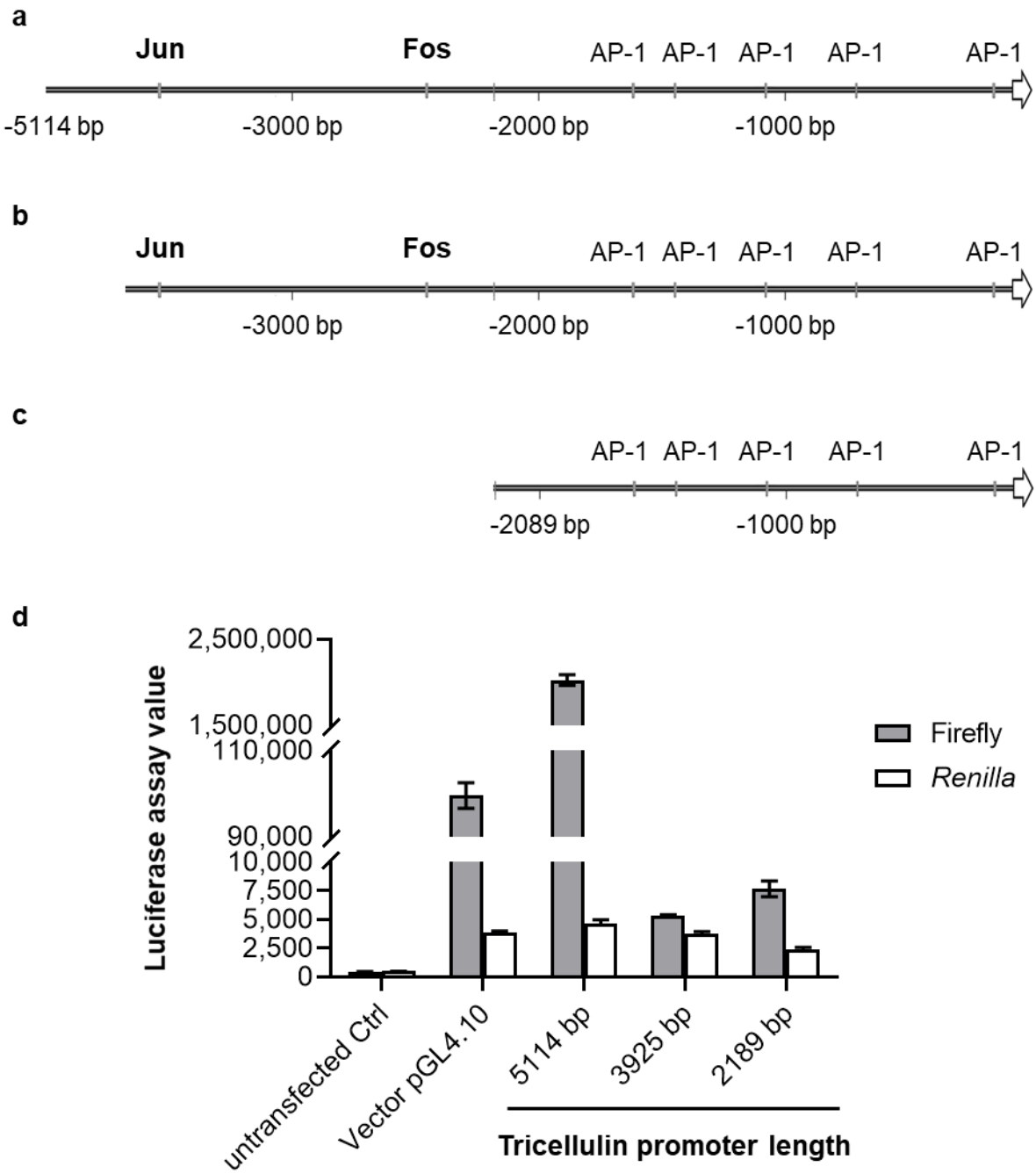

Figure 28 *Schematic representation of AP-1 binding sites on tricellulin promoter of 5114 bp* ***(a)****, 3925 bp* ***(b)****, and 2189 bp* ***(c)****.* ***(d)*** *Respective firefly and Renilla luciferase values of different conditions.*

To create a system that properly reflected the change of tricellulin promoter induced by IL-13, the WT promoter was transfected in parallel on 12-well plate or Millicell-PCF inserts, followed by a 48-h treatment with IL-13. Although the protein expression of

tricellulin was downregulated in both conditions, the promoter activity could only be reduced when the cells grow on the inserts (**Figure 29**, ****p* < 0.001, n = 11). Thus, the following experiments were performed with this setting.

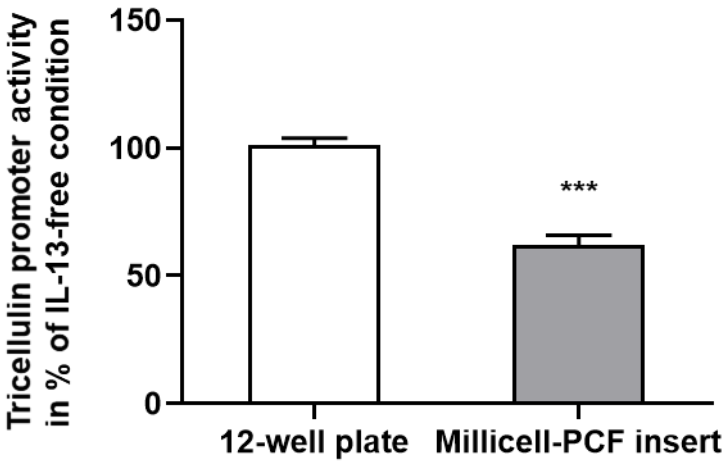

Figure 29 *Tricellulin promoter activity in different transfection conditions. After 48 h of IL-13 treatment, the promoter activity of the cells grown on 12-well plate remained unchanged (100.96 ± 2.88 %, n = 6) while the cells cultured on the Millicell insert decreased to 62.16 ± 3.71 % (***p < 0.001, n = 11).*

4.3.2 Tricellulin promoter activity in each mutation condition

To further investigate the function of Jun and Fos binding site, tricellulin promoter containing Jun, Fos, or both mutated binding sites (**Figure 30a**) were constructed and integrated into the vector pGL4.10. After 48 h of IL-13 treatment, promoter activity showed a decrease in the wildtype promotor as well as the fos-mutated promotor (fos-mut) with the prerequisite of a downregulated tricellulin protein expression (**Figure 30b**, ****p* < 0.001). In addition, no reduction was observed when the jun binding site was mutated, but interestingly, despite different degrees, tricellulin promoter activity was still decreased when both jun and fos binding sites were mutated (**Figure 30b**, ***p* < 0.01).

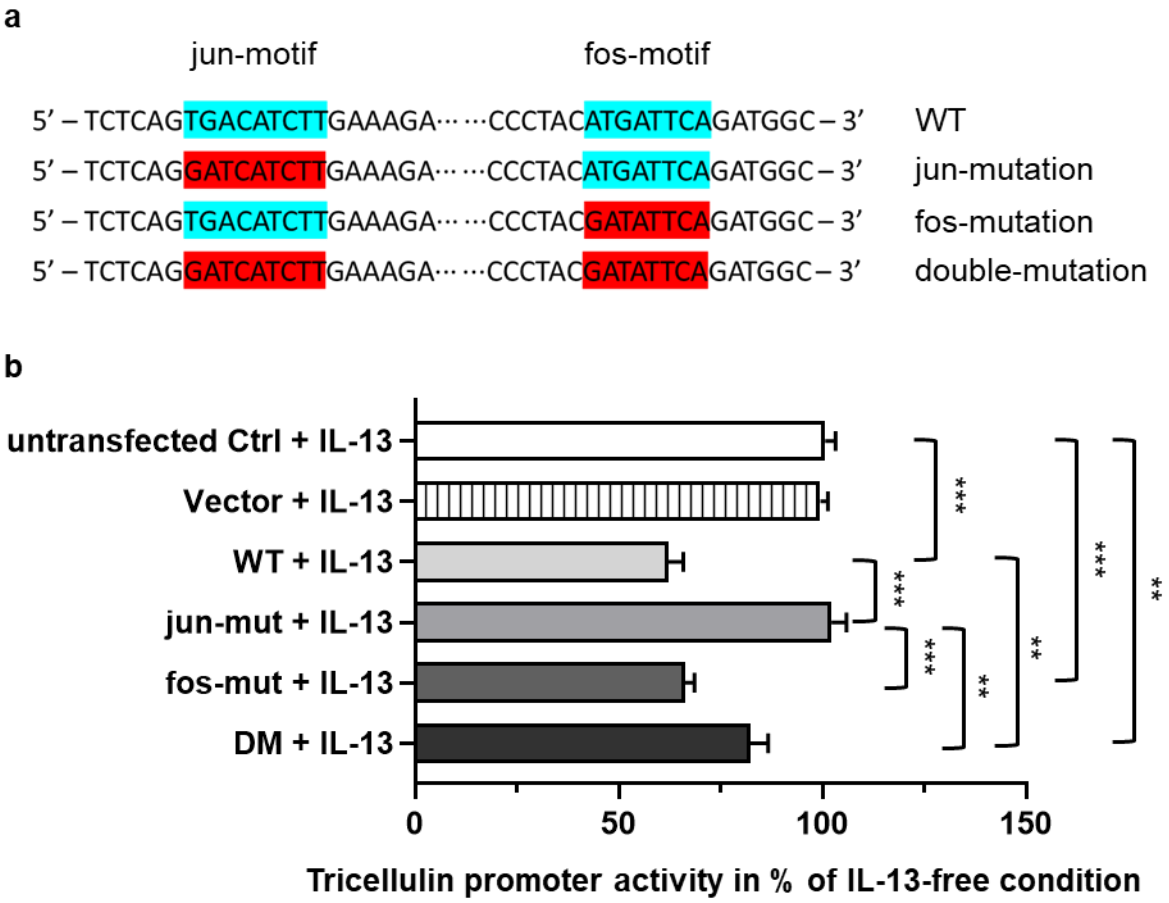

Figure 30 (a) *Schematic representation of jun- and fos-motif domain sequence of each tricellulin promoter mutant. WT = wild type.* ***(b)*** *Effects of mutated binding sites on tricellulin promoter activity. The mean value of IL-13 free condition in each mutation was set to 100 %. Untransfected Ctrl: 100.64 ± 2.61 %, Vector: 99.49 ± 1.88 %, WT: 62.16 ± 3.71 %, jun-mut: 102.21 ± 3.75 %, fos-mut: 66.22 ± 2.35 %, double-mutation (DM): 82.26 ± 4.40 %, n = 7 – 12, **p < 0.01, ***p < 0.001.*

4.3.3 Effects of additional c-jun and c-fos on tricellulin promoter activity

According to the finding of Krug et al. (2018), within jun and fos protein family, c-jun and c-fos were likely to be involved in tricellulin downregulation. Therefore, to clarify the potential role of jun or fos binding site, additional co-transfection was performed

with human c-jun and human c-fos plasmid. No significant change of tricellulin promoter activity was observed after additional transfection of jun, fos, or jun plus fos (**Figure 31**).

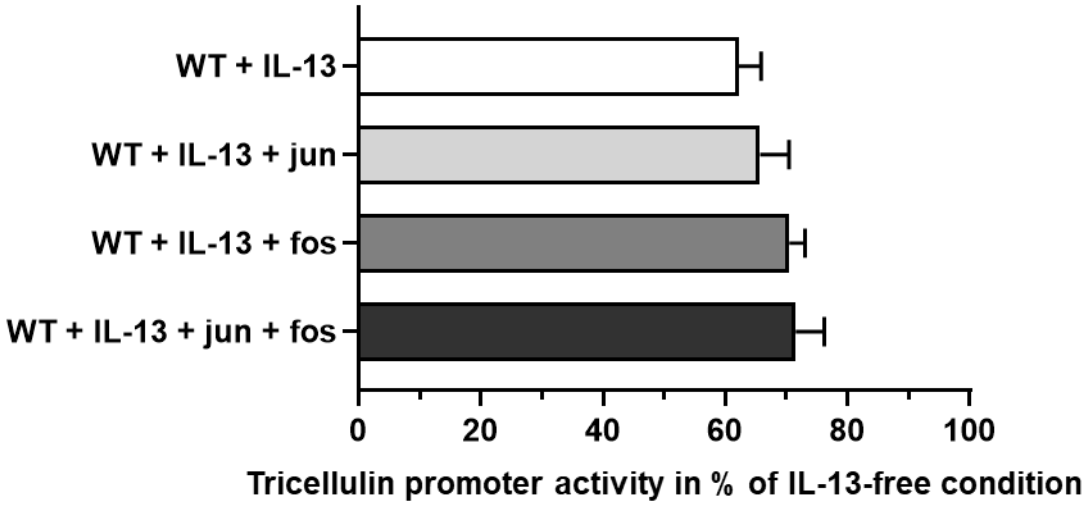

Figure 31 *Tricellulin promoter activity with co-transfection of jun, fos, or jun plus fos. The mean value of IL-13 free condition in each mutation was set to 100 %. WT + IL-13: 62.16 ± 3.71 %, WT + IL-13 + jun: 65.69 ± 4.75 %, WT + IL-13 + fos: 70.49 ± 2.53 %, WT + IL-13 + jun + fos: 72.58 ± 5.50 %, n = 7 – 12.*

5 Discussion

5.1 The involvement of angulins in active CD

The tTJ is the vertical ladder-like meshwork of TJ strands at the regions of where three or more cells encounter, which has been observed and described around fifty years ago (Staehelin et al., 1969). Because of the special tube-like structural arrangement, the tTJ has been assumed to be the weak spot of the paracellular barrier for a long period of time.

However, the first molecular component of the tTJ, tricellulin, was not discovered until 2005 (Ikenouchi et al., 2005). Overexpression experiments to different levels showed that tricellulin formed a barrier at tTJs for macromolecules (Krug et al., 2009a). Afterwards, screening cDNA library of T84 cells by the fluorescence localization-based retrovirus-mediated expression (FL-Rex) method revealed the second role of angulin-1 (still named LSR back then) as a fundamental element of the tTJ and a recruiter of tricellulin to tTJs (Masuda et al., 2011). Two years later, the examination of the other two homologues of angulin-1, angulin-2 and -3 (ILDR1 and ILDR2 at the time), completed the present composition of the tTJ as well as the angulin family (Higashi et al., 2013).

The localization of angulins at tTJs was exhibited by immunofluorescent staining of the mouse epithelial cell line EpH4 as well as in mouse tissues, and further evidenced by its presence along the central tube using immuno-freeze-fracture replica electron microscopy (Masuda et al., 2011, Higashi et al., 2013). In principle, at least one angulin shows expression in the tissues where tricellulin is expressed. In the colon, this role falls on angulin-1 (Higashi et al., 2013).

In a previous study, the tricellulin protein expression level was found to be unchanged in sigmoid colon biopsies of CD patients compared with controls, while the localization of tricellulin interestingly exhibited a shift from crypts towards surface epithelium (Krug et al., 2018). This variation in localization indicated the complex involvement of the upstreaming regulators of tricellulin in CD. Therefore, in this thesis, the expression level of angulins was analysed in CD. Firstly, the analysis of FFPE sections from CD

and controls revealed a downregulation of angulin-1 in CD. Then, to exclude the potential influence from the samples which has been fixed and embedded, fresh endoscopic biopsies from controls, active and remission CD were analysed. The expression of angulin-1 was also downregulated in active CD compared to controls and additionally this decrease was shown to be recovered in remission of CD. Meanwhile, the comparison at mRNA level also returned similar results, indicating that at least the main form of angulins in colon, angulin-1, was involved in the complex regulation of tTJ proteins in CD. Unfortunately, limited by the insufficient reliability of the antibodies available in the laboratory against angulin-2 and -3, only the mRNA expression level of these two proteins was analysed here.

As lack of all three angulins led to the deviation of tricellulin from tTJs and a strong reduction of TER and a sharp rise of permeability to fluorescein (332 Da), FITC-dextran 4, 10, and 40 kDa (Masuda et al., 2011, Higashi et al., 2013), further examination regarding to barrier function in CD needs to be performed.

5.2 Leptin affecting the expression of angulin-1

In the exploration of the underlying mechanisms behind angulin-1 downregulation in CD, leptin was revealed to be the only one that could induce this effect in human intestinal epithelial cell lines T84 and Caco-2 among the tested twelve cytokines commonly involved in CD. The pathophysiological role of leptin is twofold: (i) leptin could enhance the effect of cytokines from T_h1 and T_h17 families and (ii) the hypertrophic MAT in CD could serve as an extra source of leptin releasement (Weidinger et al., 2018).

Regarding the localization of tricellulin in T84 and Caco-2 cells, no shift was observed by immunofluorescent staining, which appeared to be contradictory at first glance to the previous finding that tricellulin was not concentrated at tTJs after knockdown of angulin-1 (Masuda et al., 2011). However, on one hand, that knockdown was to an extreme extent of trace level of angulin-1 while the downregulation of angulin-1 caused by leptin was within the range of 40 to 50 percent. On the other hand, the previous experiment was performed using a cell line which did not express either angulin-2 or -3, but these two proteins that were also able to recruit tricellulin (Higashi et al., 2013) were present in both T84 and Caco-2 cells. Therefore, the unshifted localization of

tricellulin was also reasonable. Although tricellulin was still localized at tTJs, the barrier function already became vulnerable as an increased permeability for FD4 in Caco-2 cells was observed, which was also in consistent with the previous finding that although angulin-2 and -3 could still hold tricellulin in position, but the barrier function could not be fully recovered (Higashi et al., 2013). Further investigation of these two proteins is needed but waits for antibodies of assuring quality to provide expression and localization information.

The functional differences between T84 and Caco-2 cells could be due to the different basic permeability for FD4. In Caco-2 cells, permeability for FD4 after leptin treatment was increased to the untreated level of T84, which might imply the maximum increase ability under the current conditions. This effect of impaired tTJ might be enlarged in a highly balanced circumstance as in vivo than in the experimental simplified cell culture models.

Furthermore, the interaction between tTJ proteins which might be potentially reduced and subsequently vulnerate the barrier, for example tricellulin-tricellulin or tricellulin-angulin interaction, could also not be directly visualized so far and needs exploration in the future.

5.3 Leptin-regulated downregulation of angulin-1 via STAT3 pathway

The signaling of leptin involves three isoforms of leptin receptor (LR). Due to lack of intrinsic kinase activity, the leptin signal requires the binding of Janus kinase (JAK) 2 to form LR/JAK2 complex and phosphorylate certain tyrosine sites in order to transduce (Myers et al., 2008). The long isoform of LR is the only isoform composed of three tyrosine phosphorylation sites, Tyr_{986}, Tyr_{1079} and Tyr_{1141} in human (Schaab and Kratzsch, 2015) or Tyr_{985}, Tyr_{1077} and Tyr_{1138} in rodents (Hekerman et al., 2005), which makes it the one of the most importance.

There are numbers of pathways reported for the leptin signal. ERK pathway could be activated by Src-homology-2 domain protein (SHP-2) after binding to Tyr_{985} and then regulate the message of c-fos (Banks et al., 2000). The STAT5 pathway is stimulated via Tyr_{1077} or Tyr_{1138} and plays a role in reproduction (Hekerman et al., 2005). The STAT3 pathway could be triggered through Tyr_{1138}, which subsequently could be prohibited by suppressor of cytokine signaling 3 (SOCS3) after interacting with Tyr_{985}

(Bjorbak et al., 2000) or JAK2 itself (Sasaki et al., 2000). Moreover, the PI3K pathway was connected to energy consumption in the central nerve system (Plum et al., 2007).

In this thesis, the signaling of leptin were investigated by applying corresponding inhibitors of reported pathways. The cells pre-treated with JAK2 inhibitor AG490 or STAT3 inhibitors Stattic and WP1066 demonstrated the blockage of angulin-1 down-regulation to a different extent. Phosphorylation assay disclosed the activation of STAT3 when treated with leptin. What is in common in these two experiments was the partial blockage of AG490 but total hindrance of Stattic and WP1066, indicating the dispensability of JAK2 (**Figure 31**).

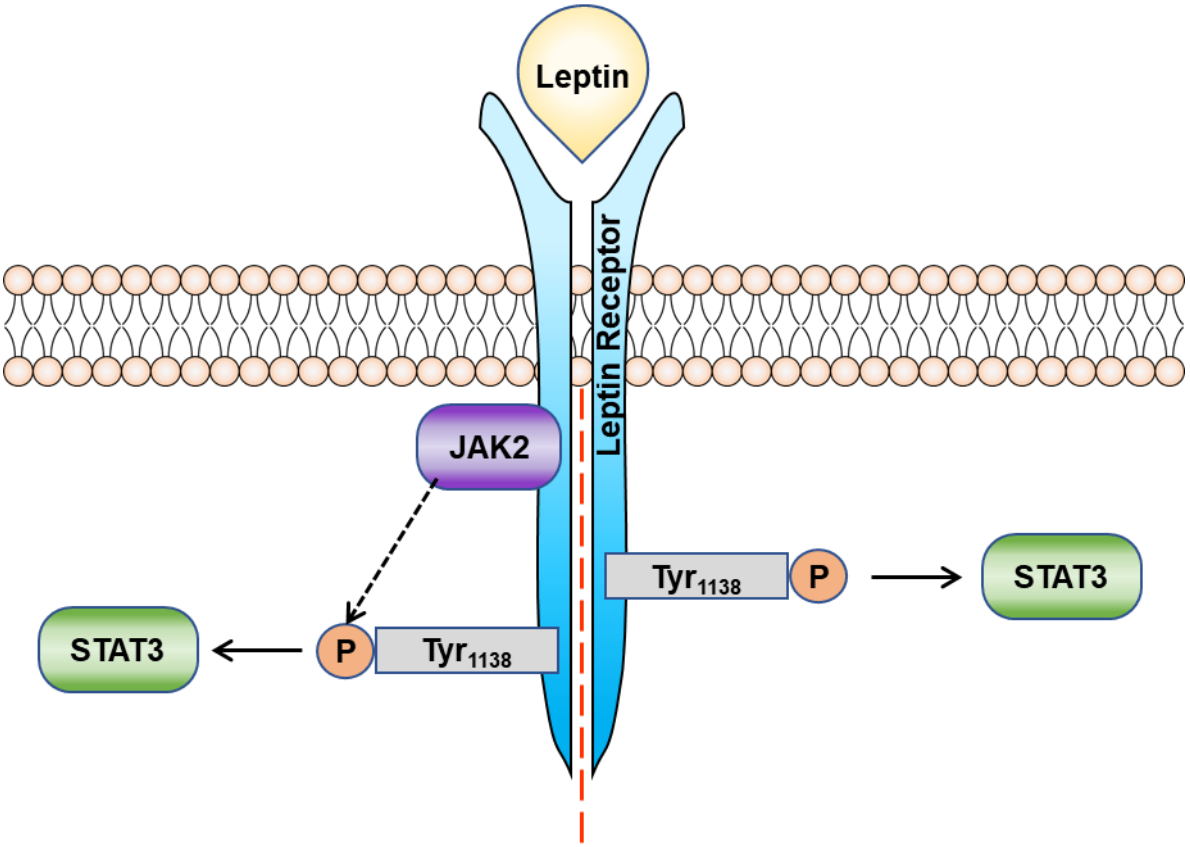

Figure 31 *Scheme of the leptin-STAT3 pathway. Each side of the dashed line represents one access of STAT3 activation with or without binding of JAK2 (modified from Procaccini et al. (2009)).*

In HT-29/B6 cells, leptin was not able to downregulate angulin-1, indicating the involvement of other potential indispensable factor(s) in this regulation, or change of the protein expression of the other two angulins. However, this was impossible to analyse due to present the lack of reliable antibodies.

5.3 Recovered tricellulin expression and barrier function in remission UC

UC is a chronic relapsing and remitting inflammatory disease, the cause of which has been assumed to be the consequence of the miscommunication between the immune system and the intestinal barrier. Tricellulin, a tTJ protein involved in barrier function, could serve as a potential messenger in between due to its liability for the passage of macromolecules. In active UC, tricellulin was shown to be downregulated which was paralleled by an increased paracellular passage of macromolecules compared with control patients (Krug et al., 2018).

These findings imply a possibility to explore the pathogenesis of UC by combing through the causal relation between tricellulin and the impaired barrier function. This also raised the classical hen-or-egg question regarding the initiation of the inflammation in UC. In active inflammatory condition, downregulation of tricellulin resulted in a defected TJ structure and an increased uptake of luminal antigens. Therein, it remains to be determined the role of tricellulin, as an initiation factor or as the consequence of the inflammation. Analysis of tricellulin as well as barrier function in inflammation-free condition of UC patients might provide a chance to answer this question.

For this purpose, colon tissues from UC patients in remission and controls were collected in this thesis. The mRNA and protein expression of tricellulin which were downregulated in active of UC were both recovered in remission patients. These results were consistent with a recent study of quiescent UC that tricellulin was at the same level as in controls (Kjærgaard et al., 2020). Previously, Cldn-4 was shown to be decreased as well in active UC (Oshima et al., 2008). Here, a tendency of Cldn-4 downregulation was pointed out, but because of a rather low number of biopsies, this change was not significant. As for Cldn-4 in remission of UC, the expression remained at the same level as in controls. Additionally, the mRNA expression of Cldn-2 was investi-

gated and demonstrated a similar level in remission of UC compared to controls. Unfortunately, all three Cldn-2 antibodies currently available failed to recognize Cldn-2 in human tissue as the antibodies did not identify signals from active patients that served as positive controls for Cldn-2 upregulation. For that reason, only mRNA expression of Cldn-2 was analysed.

Regarding angulins, the mRNA expression of all three angulins was not altered in remission of UC in comparison with controls. Angulin-1, the major constituent in colon of the angulin family (Higashi et al., 2013) and downregulated factor in CD (Hu et al., 2020), demonstrated an unchanged protein expression level in remission UC. As written in 5.1, the protein expression of angulin-2 and -3 was not investigated due to lack of reliable antibodies.

Meanwhile, the electrophysiological features and paracellular fluxes of the collected biopsies were measured in Ussing chambers. Similar to a previous study (Krug et al., 2018), epithelial resistance was reduced in active UC patients along with enhanced paracellular fluxes of fluorescein and FD4. In remission of UC, epithelial resistance, subepithelial resistance, and the overall transepithelial resistance were all within the same range as in controls. The permeabilities for fluorescein and FD4 were also unchanged, indicating that the barrier function in remission patients was also recovered.

Taken together, tricellulin expression as well as the permeability for macromolecules up to 4 kDa was recovered in remission of UC, by which an ongoing antigen uptake causing the relapse of inflammation could not be verified. The exploration of the relation between tricellulin and the passage of macromolecules in the pathophysiology of UC therefore requires further investigation at more precise time points, for instance shortly before the relapse. However, until now neither the first onset nor the relapse of UC is predictable, which raises the need for long-term follow-up studies to obtain suitable tissues in order to detect a novel predictive factor for relapse.

5.4 c-jun as one main mediator of tricellulin downregulation in active UC

AP-1 was shown to be the common downstreaming transcription factor of JNK and ERK1/2 signaling pathways which were responsible for IL-13-induced tricellulin downregulation (Krug et al., 2018). Using the dual-luciferase reporter assay, we measured

the activity of tricellulin promoter with or without potentially mutated AP-1 binding site(s), which rendered interesting results.

The involvement of jun binding site could be confirmed by the fact of unchanged tricellulin promoter activity after IL-13 treatment when this site alone was mutated. The sole mutation of the fos motif had no influence on tricellulin promoter activity regulated by IL-13. This indicated that IL-13-induced tricellulin downregulation proceeded via the jun binding site, and that although AP-1 could bind to tricellulin promoter via fos in absence of the jun motif, the promoter activity was affected by IL-13 treatment. Surprisingly however, the mutation of both jun and for sites together did not lead to unchanged promoter activity as one would expect, because the jun site was mutated here, too.

One explanation for this could be that the other AP-1 binding motifs (as marked in Figure 1), which were less specific for fos or jun were able to function when the promoter lacks both higher affinitive jun and fos sites. It is possible that these sites bind to jun protein, despite relatively weaker, but could lead to signaling to a less extent. To explore this in more detail, all the remaining potential sites for AP-1 should be mutated and analysed.

The regulation of AP-1 could draw into great complexity due to (i) the various combinations of AP-1 subunits; (ii) the different binding affinity and specificity; (iii) the interaction with other regulators; and (iv) the diversity of expression and activity among individual cell types, which leads to the variation of abundance, stability, and activity of AP-1 and its component proteins (Landschulz et al., 1988, Karin et al., 1997, Behre et al., 1999, Meng and Xia, 2011).

AP-1 is a dimeric structure mainly composed of jun and fos family proteins, however, activating transcription factor (ATF) family protein (Ziff, 1990), musculoaponeurotic fibrosarcoma (Maf) family protein (Nishizawa et al., 1989), neural retina leucine zipper (Nrl) (Swaroop et al., 1992, Kerppola and Curran, 1994), and Jun-dimerizing proteins (JDPs) (Aronheim et al., 1997) are also reported to form AP-1 dimers. For example, ATF family proteins were also shown to be involved in JNK (Wang et al., 2020, Zhou et al., 2020, Kashyap et al., 2019) and ERK1/2 pathways (Kitanaka et al., 2019, Buzzi et al., 2010, Du et al., 2019). This growing number of proteins known to be participated in the formation of AP-1 largely increases the number of possible combinations of AP-

1 subunits and in addition the complexity of regulatory mechanisms. Therefore, with the absence of jun and fos binding sites, the possibility that these proteins are able to bind to DNA, which might have another structural orientation due the lack of the binding sites, and transduce signals, should not be neglected.

Secondly, different dimer combinations of AP-1 lead to different binding preferences. Jun-Jun as well as Jun-Fos exhibits higher affinity for the phorbol 12-O-tetradecanoate-13-acetate (TPA)-responsive element (TRE), while Jun-ATF preferentially binds to the cyclic adenosine monophosphate (cAMP)-responsive element (CRE) (Hai and Curran, 1991). Other combinations are also able to interact with DNA sequences apart from these two common elements (Meng and Xia, 2011), which provides a further explanation why the double-mutated tricellulin promoter showed a decreased activity.

Besides the influence from the AP-1 protein family, interaction with external factors could also exert impact on transcription activity. An example for this is that Ras protein could upregulate c-Jun expression and enhance AP-1 activity by phosphorylating c-Jun via JNK as well as inducing c-Fos transcription via ERK1/2 (Behre et al., 1999, Deng and Karin, 1994). Another example is the inhibitory effect caused by the physical interaction between leucine zipper domain of jun and the helix-loop-helix region of MyoD (Bengal et al., 1992).

Furthermore, the regulation of AP-1 also involves the stability of jun and fos, represented by the increased stability and transcriptional activity of phosphorylated c-Jun by JNK (Musti et al., 1997, Smeal et al., 1994) and by the degradation of c-Fos resulting from the phosphorylation of c-Jun by various protein kinases like mitogen-activated protein kinase (MAPK) (Tsurumi et al., 1995).

In addition, the result that the promoter assay did not work on 12-well plates but only on cell inserts in spite of tricellulin downregulation (**Figure 32**) might imply a complex regulation downstream of IL13Rα2 itself. The cell inserts could provide the condition for directional growth by allowing access and exchange of media solutes from the basal site, indicating that a proper cellular polarity in the regulation of the AP-1- and IL-13-mediated tricellulin downregulation might be of importance.

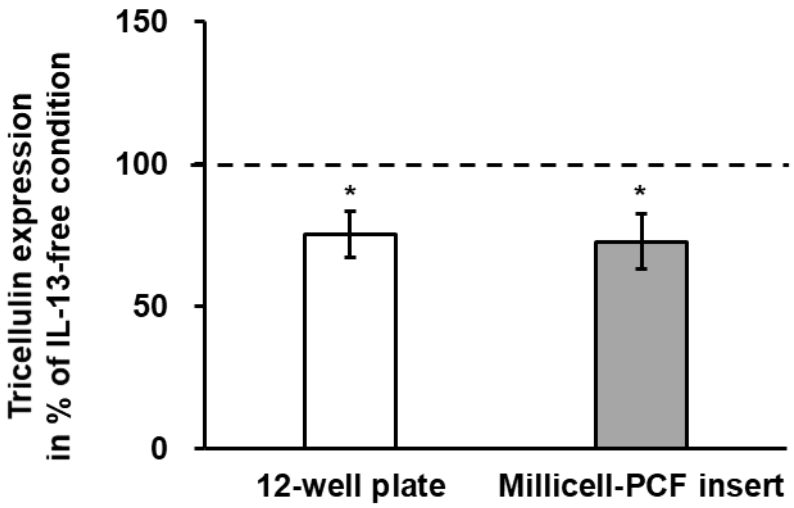

Figure 32 *Tricellulin expression in different transfection conditions. After 48 h of IL-13 treatment, tricellulin was downregulated both on 12-well plates (75.25 ± 7.93 %, *p < 0.05, n = 3) and on the Millicell inserts (72.77 ± 9.78 %, *p < 0.05, n = 3).*

These findings suggest the possibility of using a jun motif-specific anti-peptide to block the binding of AP-1 via jun and hence the downregulation of tricellulin. On the other hand, to avoid the complexity as well as broad involvement of AP-1, further investigation targeting JNK pathway alone, but not ERK1/2 pathway, might also be promising. It is worth noting that both Cldn-2 upregulation and tricellulin downregulation effects induced by IL-13 are linked to JNK signaling, as shown in previous studies. There, the increase of Cldn-2 could be blocked by inhibitor U0126, which targets the upstreaming ERK1/2 of JNK, and that the decrease of tricellulin could be prevented by targeting JNK1/2/3 (Meng and Xia, 2011, Krug et al., 2018). However, one needs to keep in mind that all these factors, AP-1, ERK1/2, and JNK, are very common signaling proteins involved in many regulatory processes and that inhibition of these therefore has to be designed in a very specific way for Cldn-2 and tricellulin.

6 Summary

The tight junction (TJ) protects the intestinal barrier function and controls the paracellular transport of water, ions, small water-soluble molecules, and macromolecules. The structure of the TJ comprises the belt-like meshwork of the TJ strands between two epithelial cells, called the bicellular TJ (bTJ), and the vertically converged central tube by the most apical bTJs in the region where three or more cells meet, termed tricellular TJ (tTJ). The tTJ is assumed to be a weak spot of the intestinal epithelial barrier due to the presumed space left in the central tube. Major components of the tTJ are tricellulin and the three members of the angulin family. Tricellulin regulates the passage of macromolecules and therefore acts a crucial part in preventing an uncontrolled uptake of pathogens and immunogens from the gut lumen. Angulin-1, -2, and -3 share the ability to recruit tricellulin to the tTJ. In each epithelium, at least one angulin localizes at the tTJ and in colon the major role falls on angulin-1.

Dysregulation of TJ proteins could cause or could be caused by corresponding diseases due to altered paracellular passage. Inflammatory bowel diseases (IBD) are possibly caused by a dysregulated communication between intestinal epithelial cells and the immune system. IBD has two major subtypes, Crohn's disease (CD) and ulcerative colitis (UC). In CD, tricellulin was found to have a shifted localization with unaltered expression level while in UC, it was downregulated by IL-13.

In this thesis, several aspects dealing with the tTJ and the related regulation in IBD were investigated.

First, the expression of angulin-1 was analysed in IBD. Angulin-1 was downregulated in active CD at both mRNA and protein expression levels. For the exploration of the mechanisms behind, three intestinal epithelial cell lines were investigated using cytokines treatments, inhibitors treatments, phosphorylation analysis, and electrophysiological and flux measurements. It turned out that leptin could induce the downregulation of angulin-1 in T84 and Caco-2 cells, and that STAT3 and its upstreaming pathway JAK2 were responsible signaling mechanisms of this regulation. Incomplete blockage of STAT3 activation by the JAK2 inhibitor AG490 suggested an independent pathway bypassing JAK2. An observed increase of permeability for FITC-dextran 4 kDa (FD4)

in Caco-2 cells indicated the potency of macromolecular passage caused by angulin-1 downregulation. Findings of this subproject have been published (Hu et al., 2020).

In a second project, it was studied whether tricellulin might still be altered in remission of UC at expression level, which subsequently might increase potential antigen uptake and lead to relapse of the inflammation. Intestinal biopsies from patients in UC remission were analysed for the expression of tricellulin as well as for electrophysiological and flux properties. Tricellulin expression in remission UC was not significantly different to controls at both mRNA and protein expression levels. In line with this, transepithelial resistance, epithelial resistance, and subepithelial resistance were all similar between remission UC and healthy controls, along with the comparable permeability for fluorescein and FD4. Analysis of timepoints shortly before occurrence of relapse might show different expression. However, this remains a hypothesis and needs to be further elucidated.

A third project focused on the downregulation of tricellulin by IL-13 via AP-1. Promoter studies were performed to analyse the responsible binding sites for this downregulation. Mutation analysis found that the jun binding site – 3473 bp before the start codon – was essential for the regulation.

In conclusion, several aspects of the tTJ proteins in IBD were studied and lead to new findings which might serve as basis for therapeutic intervention.

7 Zusammenfassung

Die Tight Junction (TJ) gewährleistet die intestinale Barrierefunktion und reguliert den parazellulären Transport von Wasser, Ionen, kleinen Soluten und Makromolekülen. Die Struktur der TJ besteht aus der bizellulären TJ (bTJ), dem gürtelartigen Netzwerk von Strängen zwischen zwei Epithelzellen, und der trizellulären TJ (tTJ). Die tTJ bildet einen vertikal konvergierenden „central tube“ von den apikalsten bTJs der Region, in der drei oder mehr Zellen aufeinandertreffen. Es wird angenommen, dass die tTJ eine potentielle Schwachstelle der intestinalen Barriere aufgrund ihrer röhrenartigen Struktur darstellt. Tricellulin und die drei Mitglieder der Angulinfamilie sind die Haupt-Proteinbestandteile der tTJ. Tricellulin reguliert in reziproker Weise die Passage von Makromolekülen und spielt dadurch im Darm eine entscheidende Rolle bei der Verhinderung der unkontrollierten Aufnahme von Antigenen aus dem Lumen. Die Angulin-1, -2 und -3 besitzen die Fähigkeit, Tricellulin zur tTJ zu rekrutieren. In allen tTJs ist mindestens ein Angulin lokalisiert und im Kolon spielt Angulin-1 die Hauptrolle.

Eine Dysregulation von TJ-Proteinen könnte entsprechende Erkrankungen aufgrund einer veränderten parazellulären Passage verursachen oder durch diese verursacht werden. Chronisch-entzündliche Darmerkrankungen (CED) werden möglicherweise durch eine dysregulierte Kommunikation zwischen Darmepithelzellen und dem Immunsystem verursacht. Die zwei Haupttypen der CED sind Morbus Crohn (MC) und Colitis ulcerosa (CU). Bei MC wurde eine veränderte Lokalisation von Tricellulin bei unverändertem Expressionsniveau gefunden, während es bei CU durch Interleukin-13 (IL-13) in der Expression herunterreguliert wurde.

In dieser Arbeit wurden verschiedene Aspekte, die sich mit der tTJ und der damit relevante Regulierung in der CED befassen, untersucht.

Zunächst wurde die Expression von Angulin-1 bei CED analysiert. Angulin-1 wurde in der aktiven MC sowohl auf mRNA- als auch auf Proteinexpressionsebene herunterreguliert. Zur Erforschung der zugrunde liegenden Mechanismen wurden drei Darmepithelzelllinien verwendet, wobei Zytokin- und Inhibitorbehandlungen, Phosphorylierungsanalysen sowie Elektrophysiologische- und Fluxmessungen durchgeführt wurden. Es stellte sich heraus, dass Leptin die Herunterregulierung von Angulin-1 in T84-

und in Caco-2-Zellen induzieren konnte und dass STAT3 und sein Upstream-Signalweg JAK2 für die Signalmechanismen dieser Regulation verantwortlich waren. Die unvollständige Blockierung der STAT3-Aktivierung durch den JAK2-Inhibitor AG490 deutete auf einen unabhängigen Signalweg hin, der JAK2 umgeht. Ein beobachteter Anstieg der Permeabilität für FITC-Dextran 4 kDa (FD4) in Caco-2-Zellen zeigte die Potenz der makromolekularen Passage an, die durch die Herunterregulierung von Angulin-1 verursacht wird. Die Ergebnisse dieses Teilprojekts wurden publiziert (Hu et al., 2020).

In einem zweiten Projekt wurde untersucht, ob Tricellulin bei der Remission von CU auf Expressionsebene noch verändert sein könnte, und ob die potenzielle Antigenaufnahme anschließend erhöht und durch die einem Schub der Entzündung verursacht wird. Darmbiopsate von Patienten in Remission einer CU wurden auf die Expression von Tricellulin sowie mittels elektrophysiologischen und Fluxmessungen untersucht. Die Expression von Tricellulin in Remission der CU war sowohl auf mRNA- als auch auf Proteinexpressionsebene nicht signifikant von gesunden Kontrollen verschieden. Dementsprechend waren der transepitheliale Widerstand, der epitheliale Widerstand und der subepitheliale Widerstand zwischen Remission der CU und gesunden Kontrollen ähnlich, ebenso wie die Permeabilität für Fluorescein und für FD4. Zeitpunkte kurz vor dem Schub konnten im Rahmen dieser Arbeit nicht untersucht werden. Ob sich zu diesem Zeitpunkt unterschiedliche Ausprägungen zeigen, muss daher noch aufgeklärt werden.

Ein drittes Projekt konzentrierte sich auf die bereits beschriebene Herunterregulierung von Tricellulin durch IL-13 über AP-1. Um die verantwortlichen Bindungsstellen für diese Herunterregulierung zu analysieren, wurden Promotorstudien durchgeführt. Mutationsanalysen ergaben, dass die jun-Bindungsstelle – 3473 bp vor dem Startcodon – für die Regulation wichtig war.

Zusammenfassend ist zu sagen, dass mehrere Aspekte der tTJ-Proteine bei der CED untersucht wurden und zu neuen Erkenntnissen führten, die als Grundlage für eine therapeutische Intervention gelten könnten.

8 References

Abella, V., Scotece, M., Conde, J., Pino, J., Gonzalez-Gay, M. A., Gómez-Reino, J. J., Mera, A., Lago, F., Gómez, R. & Gualillo, O. 2017. Leptin in the interplay of inflammation, metabolism and immune system disorders. *Nature Reviews Rheumatology,* 13**,** 100-109.

Akbar, S., Pinçon, A., Lanhers, M.-C., Claudepierre, T., Corbier, C., Gregory-Pauron, L., Malaplate-Armand, C., Visvikis, A., Oster, T. & Yen, F. T. 2016. Expression profile of hepatic genes related to lipid homeostasis in LSR heterozygous mice contributes to their increased response to high-fat diet. *Physiological genomics,* 48**,** 928-935.

Ananthakrishnan, A. N. 2015. Epidemiology and risk factors for IBD. *Nat Rev Gastroenterol Hepatol,* 12**,** 205-17.

Ananthakrishnan, A. N., Khalili, H., Konijeti, G. G., Higuchi, L. M., De Silva, P., Korzenik, J. R., Fuchs, C. S., Willett, W. C., Richter, J. M. & Chan, A. T. 2013. A prospective study of long-term intake of dietary fiber and risk of Crohn's disease and ulcerative colitis. *Gastroenterology,* 145**,** 970-7.

Ananthakrishnan, A. N., Luo, C., Yajnik, V., Khalili, H., Garber, J. J., Stevens, B. W., Cleland, T. & Xavier, R. J. 2017. Gut Microbiome Function Predicts Response to Anti-integrin Biologic Therapy in Inflammatory Bowel Diseases. *Cell Host Microbe,* 21**,** 603-610.e3.

Aniwan, S., Harmsen, W. S., Tremaine, W. J., Kane, S. V. & Loftus, E. V., Jr. 2018. Overall and Cause-Specific Mortality of Inflammatory Bowel Disease in Olmsted County, Minnesota, From 1970 Through 2016. *Mayo Clin Proc,* 93**,** 1415-1422.

Aronheim, A., Zandi, E., Hennemann, H., Elledge, S. J. & Karin, M. 1997. Isolation of an AP-1 repressor by a novel method for detecting protein-protein interactions. *Mol Cell Biol,* 17**,** 3094-102.

Atreya, R., Mudter, J., Finotto, S., Mullberg, J., Jostock, T., Wirtz, S., Schutz, M., Bartsch, B., Holtmann, M., Becker, C., Strand, D., Czaja, J., Schlaak, J. F., Lehr, H. A., Autschbach, F., Schurmann, G., Nishimoto, N., Yoshizaki, K., Ito, H., Kishimoto, T., Galle, P. R., Rose-John, S. & Neurath, M. F. 2000. Blockade of interleukin 6 trans signaling suppresses T-cell resistance against apoptosis in chronic intestinal inflammation: evidence in crohn disease and experimental colitis in vivo. *Nat Med,* 6**,** 583-8.

Balwierz, P. J., Pachkov, M., Arnold, P., Gruber, A. J., Zavolan, M. & Van Nimwegen, E. 2014. ISMARA: automated modeling of genomic signals as a democracy of regulatory motifs. *Genome Res,* 24**,** 869-84.

Banks, A. S., Davis, S. M., Bates, S. H. & Myers, M. G., Jr. 2000. Activation of downstream signals by the long form of the leptin receptor. *J Biol Chem,* 275**,** 14563-72.

Barbier, M., Vidal, H., Desreumaux, P., Dubuquoy, L., Bourreille, A., Colombel, J.-F., Cherbut, C. & Galmiche, J.-P. 2003. Overexpression of leptin mRNA in mesenteric adipose tissue in inflammatory bowel diseases. *Gastroentérologie clinique et biologique,* 27**,** 987-991.

Behre, G., Whitmarsh, A. J., Coghlan, M. P., Hoang, T., Carpenter, C. L., Zhang, D. E., Davis, R. J. & Tenen, D. G. 1999. c-Jun is a JNK-independent coactivator of the PU.1 transcription factor. *J Biol Chem,* 274**,** 4939-46.

Bengal, E., Ransone, L., Scharfmann, R., Dwarki, V. J., Tapscott, S. J., Weintraub, H. & Verma, I. M. 1992. Functional antagonism between c-Jun and MyoD proteins: a direct physical association. *Cell,* 68**,** 507-19.

Bewtra, M., Kaiser, L. M., Tenhave, T. & Lewis, J. D. 2013. Crohn's disease and ulcerative colitis are associated with elevated standardized mortality ratios: a meta-analysis. *Inflamm Bowel Dis,* 19**,** 599-613.

Bjorbak, C., Lavery, H. J., Bates, S. H., Olson, R. K., Davis, S. M., Flier, J. S. & Myers, M. G., Jr. 2000. SOCS3 mediates feedback inhibition of the leptin receptor via Tyr985. *J Biol Chem,* 275**,** 40649-57.

Borck, G., Ur Rehman, A., Lee, K., Pogoda, H.-M., Kakar, N., Von Ameln, S., Grillet, N., Hildebrand, M. S., Ahmed, Z. M., Nürnberg, G., Ansar, M., Basit, S., Javed, Q., Morell, R. J., Nasreen, N., Shearer, A. E., Ahmad, A., Kahrizi, K., Shaikh, R. S., Ali, R. A., Khan, S. N., Goebel, I., Meyer, N. C., Kimberling, W. J., Webster, J. A., Stephan, D. A., Schiller, M. R., Bahlo, M., Najmabadi, H., Gillespie, P. G., Nürnberg, P., Wollnik, B., Riazuddin, S., Smith, R. J. H., Ahmad, W., Müller, U., Hammerschmidt, M., Friedman, T. B., Riazuddin, S., Leal, S. M., Ahmad, J. & Kubisch, C. 2011. Loss-of-function mutations of ILDR1 cause autosomal-recessive hearing impairment DFNB42. *American journal of human genetics,* 88**,** 127-137.

Brown, K. D., Zurawski, S. M., Mosmann, T. R. & Zurawski, G. 1989. A family of small inducible proteins secreted by leukocytes are members of a new superfamily that includes leukocyte and fibroblast-derived inflammatory agents, growth factors, and indicators of various activation processes. *J Immunol,* 142**,** 679-87.

Bruewer, M., Luegering, A., Kucharzik, T., Parkos, C. A., Madara, J. L., Hopkins, A. M. & Nusrat, A. 2003. Proinflammatory cytokines disrupt epithelial barrier function by apoptosis-independent mechanisms. *J Immunol,* 171**,** 6164-72.

Burisch, J. & Munkholm, P. 2015. The epidemiology of inflammatory bowel disease. *Scand J Gastroenterol,* 50**,** 942-51.

Buzzi, N., Boland, R. & Russo De Boland, A. 2010. Signal transduction pathways associated with ATP-induced proliferation of colon adenocarcinoma cells. *Biochim Biophys Acta,* 1800**,** 946-55.

Canavan, C., Abrams, K. R. & Mayberry, J. F. 2007. Meta-analysis: mortality in Crohn's disease. *Aliment Pharmacol Ther,* 25**,** 861-70.

Carroll, J. S., Meyer, C. A., Song, J., Li, W., Geistlinger, T. R., Eeckhoute, J., Brodsky, A. S., Keeton, E. K., Fertuck, K. C., Hall, G. F., Wang, Q., Bekiranov, S., Sementchenko, V., Fox, E. A., Silver, P. A., Gingeras, T. R., Liu, X. S. & Brown, M. 2006. Genome-wide analysis of estrogen receptor binding sites. *Nat Genet,* 38**,** 1289-97.

Carroll, M. W., Kuenzig, M. E., Mack, D. R., Otley, A. R., Griffiths, A. M., Kaplan, G. G., Bernstein, C. N., Bitton, A., Murthy, S. K., Nguyen, G. C., Lee, K., Cooke-Lauder, J. & Benchimol, E. I. 2019. The Impact of Inflammatory Bowel Disease in Canada 2018: Children and Adolescents with IBD. *Journal of the Canadian Association of Gastroenterology,* 2**,** S49-S67.

Casini-Raggi, V., Kam, L., Chong, Y. J., Fiocchi, C., Pizarro, T. T. & Cominelli, F. 1995. Mucosal imbalance of IL-1 and IL-1 receptor antagonist in inflammatory bowel disease. A novel mechanism of chronic intestinal inflammation. *J Immunol,* 154**,** 2434-40.

Ciapponi, A., Virgilio, S. A., Berrueta, M., Soto, N. C., Ciganda, A., Rojas Illanes, M. F., Rubio Martinez, B., Gamba, J., Gonzalez Salazar, C. A., Rocha Rodriguez, J. N., Scarpellini, B., Bravo Perdomo, A. M., Machnicki, G., Aldunate, L., De Paula, J. & Bardach, A. 2020. Epidemiology of inflammatory bowel disease in Mexico and Colombia: Analysis of health databases, mathematical modelling and a case-series study. *PLoS One,* 15**,** e0228256.

Claude, P. & Goodenough, D. A. 1973. Fracture faces of zonulae occludentes from "tight" and "leaky" epithelia. *J Cell Biol,* 58**,** 390-400.

Cornish, J. A., Tan, E., Simillis, C., Clark, S. K., Teare, J. & Tekkis, P. P. 2008. The risk of oral contraceptives in the etiology of inflammatory bowel disease: a meta-analysis. *Am J Gastroenterol,* 103**,** 2394-400.

Crohn, B. B., Ginzburg, L. & Oppenheimer, G. D. 1932. REGIONAL ILEITIS: A PATHOLOGIC AND CLINICAL ENTITY. *Journal of the American Medical Association,* 99**,** 1323-1329.

Crohn, B. B., Ginzburg, L. & Oppenheimer, G. D. 1952. Regional ileitis: A pathologic and clinical entity. *The American Journal of Medicine,* 13**,** 583-590.

Daley, E., Emson, C., Guignabert, C., De Waal Malefyt, R., Louten, J., Kurup, V. P., Hogaboam, C., Taraseviciene-Stewart, L., Voelkel, N. F., Rabinovitch, M., Grunig, E. & Grunig, G. 2008. Pulmonary arterial remodeling induced by a Th2 immune response. *J Exp Med,* 205**,** 361-72.

Danese, S., Rudzinski, J., Brandt, W., Dupas, J. L., Peyrin-Biroulet, L., Bouhnik, Y., Kleczkowski, D., Uebel, P., Lukas, M., Knutsson, M., Erlandsson, F., Hansen, M. B. & Keshav, S. 2015. Tralokinumab for moderate-to-severe UC: a randomised, double-blind, placebo-controlled, phase IIa study. *Gut,* 64**,** 243-9.

Daperno, M., D'haens, G., Van Assche, G., Baert, F., Bulois, P., Maunoury, V., Sostegni, R., Rocca, R., Pera, A., Gevers, A., Mary, J. Y., Colombel, J. F. & Rutgeerts, P. 2004. Development and validation of a new, simplified endoscopic activity score for Crohn's disease: the SES-CD. *Gastrointest Endosc,* 60**,** 505-12.

Deng, T. & Karin, M. 1994. c-Fos transcriptional activity stimulated by H-Ras-activated protein kinase distinct from JNK and ERK. *Nature,* 371**,** 171-5.

Denker, B. M. & Nigam, S. K. 1998. Molecular structure and assembly of the tight junction. *Am J Physiol,* 274**,** F1-9.

Diamond, J. M. 1977. Twenty-first Bowditch lecture. The epithelial junction: bridge, gate, and fence. *Physiologist,* 20**,** 10-8.

Diaz-Horta, O., Duman, D., Foster, J., 2nd, Sirmaci, A., Gonzalez, M., Mahdieh, N., Fotouhi, N., Bonyadi, M., Cengiz, F. B., Menendez, I., Ulloa, R. H., Edwards, Y. J., Zuchner, S., Blanton, S. & Tekin, M. 2012. Whole-exome sequencing efficiently detects rare mutations in autosomal recessive nonsyndromic hearing loss. *PLoS One,* 7**,** e50628.

Dokmanovic-Chouinard, M., Chung, W. K., Chevre, J. C., Watson, E., Yonan, J., Wiegand, B., Bromberg, Y., Wakae, N., Wright, C. V., Overton, J., Ghosh, S., Sathe, G. M., Ammala, C. E., Brown, K. K., Ito, R., Leduc, C., Solomon, K., Fischer, S. G. & Leibel, R. L. 2008. Positional cloning of "Lisch-Like", a candidate modifier of susceptibility to type 2 diabetes in mice. *PLoS Genet,* 4**,** e1000137.

Dosh, R. H., Jordan-Mahy, N., Sammon, C. & Le Maitre, C. 2019. Interleukin 1 is a key driver of inflammatory bowel disease-demonstration in a murine IL-1Ra knockout model. *Oncotarget,* 10**,** 3559-3575.

Du, M., Wang, Y., Liu, Z., Wang, L., Cao, Z., Zhang, C., Hao, Y. & He, H. 2019. Effects of IL-1β on MMP-9 Expression in Cementoblast-Derived Cell Line and MMP-Mediated Degradation of Type I Collagen. *Inflammation,* 42**,** 413-425.

Duricova, D., Pedersen, N., Elkjaer, M., Gamborg, M., Munkholm, P. & Jess, T. 2010. Overall and cause-specific mortality in Crohn's disease: a meta-analysis of population-based studies. *Inflamm Bowel Dis,* 16**,** 347-53.

Ebert, E. C., Wright, S. H., Lipshutz, W. H. & Hauptman, S. P. 1984. T-cell abnormalities in inflammatory bowel disease are mediated by interleukin 2. *Clinical Immunology and Immunopathology,* 33**,** 232-244.

Eglinton, T. W., Barclay, M. L., Gearry, R. B. & Frizelle, F. A. 2012. The spectrum of perianal Crohn's disease in a population-based cohort. *Dis Colon Rectum,* 55**,** 773-7.

El Hajj, A., Yen, F. T., Oster, T., Malaplate, C., Pauron, L., Corbier, C., Lanhers, M.-C. & Claudepierre, T. 2019. Age-related changes in regiospecific expression of Lipolysis Stimulated Receptor (LSR) in mice brain. *PloS one,* 14**,** e0218812-e0218812.

Engle, M. J., Goetz, G. S. & Alpers, D. H. 1998. Caco-2 cells express a combination of colonocyte and enterocyte phenotypes. *J Cell Physiol,* 174**,** 362-9.

Eum, S. Y., Jaraki, D., Bertrand, L., András, I. E. & Toborek, M. 2014. Disruption of epithelial barrier by quorum-sensing N-3-(oxododecanoyl)-homoserine lactone is mediated by matrix metalloproteinases. *American journal of physiology. Gastrointestinal and liver physiology,* 306**,** G992-G1001.

Farquhar, M. G. & Palade, G. E. 1963. Junctional complexes in various epithelia. *J Cell Biol,* 17**,** 375-412.

Farquhar, M. G. & Palade, G. E. 1965. Cell junctions in amphibian skin. *J Cell Biol,* 26**,** 263-91.

Fogh, J., Fogh, J. M. & Orfeo, T. 1977. One hundred and twenty-seven cultured human tumor cell lines producing tumors in nude mice. *J Natl Cancer Inst,* 59**,** 221-6.

Fogh, J. & Trempe, G. 1975. New human tumor cell lines. *Human tumor cells in vitro.* Springer.

Frivolt, K., Schwerd, T., Schatz, S. B., Freudenberg, F., Prell, C., Werkstetter, K. J., Bufler, P. & Koletzko, S. 2018. Hyperadiponectinemia During Infliximab Induction Therapy in Pediatric Crohn Disease. *J Pediatr Gastroenterol Nutr,* 66**,** 915-919.

Fromm, M., Schulzke, J. D. & Hegel, U. 1985. Epithelial and subepithelial contributions to transmural electrical resistance of intact rat jejunum, in vitro. *Pflugers Arch,* 405**,** 400-2.

Furuse, M., Hirase, T., Itoh, M., Nagafuchi, A., Yonemura, S., Tsukita, S. & Tsukita, S. 1993. Occludin: a novel integral membrane protein localizing at tight junctions. *J Cell Biol,* 123**,** 1777-88.

Fuss, I. J., Heller, F., Boirivant, M., Leon, F., Yoshida, M., Fichtner-Feigl, S., Yang, Z., Exley, M., Kitani, A., Blumberg, R. S., Mannon, P. & Strober, W. 2004. Nonclassical CD1d-restricted NK T cells that produce IL-13 characterize an atypical Th2 response in ulcerative colitis. *J Clin Invest,* 113**,** 1490-7.

García, J. M., Peña, C., García, V., Domínguez, G., Muñoz, C., Silva, J., Millán, I., Diaz, R., Lorenzo, Y., Rodriguez, R. & Bonilla, F. 2007. Prognostic value of LISCH7 mRNA in plasma and tumor of colon cancer patients. *Clinical cancer research : an official journal of the American Association for Cancer Research,* 13**,** 6351-6358.

Ghosh, S., Chaudhary, R., Carpani, M. & Playford, R. 2006. Interfering with interferons in inflammatory bowel disease. *Gut,* 55**,** 1071-3.

Gomollon, F., Dignass, A., Annese, V., Tilg, H., Van Assche, G., Lindsay, J. O., Peyrin-Biroulet, L., Cullen, G. J., Daperno, M., Kucharzik, T., Rieder, F., Almer, S., Armuzzi, A., Harbord, M., Langhorst, J., Sans, M., Chowers, Y., Fiorino, G., Juillerat, P., Mantzaris, G. J., Rizzello, F., Vavricka, S., Gionchetti, P. & Ecco 2017. 3rd European Evidence-based Consensus on the Diagnosis and Management of Crohn's Disease 2016: Part 1: Diagnosis and Medical Management. *J Crohns Colitis,* 11**,** 3-25.

Gong, Y., Himmerkus, N., Sunq, A., Milatz, S., Merkel, C., Bleich, M. & Hou, J. 2017. ILDR1 is important for paracellular water transport and urine concentration mechanism. *Proc Natl Acad Sci U S A,* 114**,** 5271-5276.

Gray, L. T., Fong, K. K., Pavelitz, T. & Weiner, A. M. 2012. Tethering of the conserved piggyBac transposase fusion protein CSB-PGBD3 to chromosomal AP-1 proteins regulates expression of nearby genes in humans. *PLoS Genet,* 8**,** e1002972.

Günzel, D., Krug, S. M., Rosenthal, R. & Fromm, M. 2010. Chapter 3 - Biophysical Methods to Study Tight Junction Permeability. *In:* L. YU, A. S. (ed.) *Current Topics in Membranes.* Academic Press.

Hai, T. & Curran, T. 1991. Cross-family dimerization of transcription factors Fos/Jun and ATF/CREB alters DNA binding specificity. *Proc Natl Acad Sci U S A,* 88**,** 3720-4.

Hasegawa, M., Fujimoto, M., Kikuchi, K. & Takehara, K. 1997. Elevated serum levels of interleukin 4 (IL-4), IL-10, and IL-13 in patients with systemic sclerosis. *J Rheumatol,* 24**,** 328-32.

Hauge, H., Patzke, S., Delabie, J. & Aasheim, H. C. 2004. Characterization of a novel immunoglobulin-like domain containing receptor. *Biochem Biophys Res Commun,* 323**,** 970-8.

Hecht, I., Toporik, A., Podojil, J. R., Vaknin, I., Cojocaru, G., Oren, A., Aizman, E., Liang, S. C., Leung, L., Dicken, Y., Novik, A., Marbach-Bar, N., Elmesmari, A., Tange, C., Gilmour, A., Mcintyre, D., Kurowska-Stolarska, M., Mcnamee, K., Leitner, J., Greenwald, S., Dassa, L., Levine, Z., Steinberger, P., Williams, R. O., Miller, S. D., Mcinnes, I. B., Neria, E. & Rotman, G. 2018. ILDR2 Is a Novel B7-like Protein That Negatively Regulates T Cell Responses. *Journal of immunology (Baltimore, Md. : 1950),* 200**,** 2025-2037.

Hekerman, P., Zeidler, J., Bamberg-Lemper, S., Knobelspies, H., Lavens, D., Tavernier, J., Joost, H. G. & Becker, W. 2005. Pleiotropy of leptin receptor signalling is defined by distinct roles of the intracellular tyrosines. *Febs j,* 272**,** 109-19.

Heller, F., Florian, P., Bojarski, C., Richter, J., Christ, M., Hillenbrand, B., Mankertz, J., Gitter, A. H., Burgel, N., Fromm, M., Zeitz, M., Fuss, I., Strober, W. & Schulzke, J. D. 2005. Interleukin-13 is the key effector Th2 cytokine in ulcerative colitis that affects epithelial tight junctions, apoptosis, and cell restitution. *Gastroenterology,* 129**,** 550-64.

Hemmasi, S., Czulkies, B. A., Schorch, B., Veit, A., Aktories, K. & Papatheodorou, P. 2015. Interaction of the Clostridium difficile Binary Toxin CDT and Its Host Cell Receptor, Lipolysis-stimulated Lipoprotein Receptor (LSR). *The Journal of biological chemistry,* 290**,** 14031-14044.

Hempstock, W., Sugioka, S., Ishizuka, N., Sugawara, T., Furuse, M. & Hayashi, H. 2020. Angulin-2/ILDR1, a tricellular tight junction protein, does not affect water transport in the mouse large intestine. *Sci Rep,* 10**,** 10374.

Hess, J., Angel, P. & Schorpp-Kistner, M. 2004. AP-1 subunits: quarrel and harmony among siblings. *J Cell Sci,* 117**,** 5965-73.

Higashi, T., Tokuda, S., Kitajiri, S., Masuda, S., Nakamura, H., Oda, Y. & Furuse, M. 2013. Analysis of the 'angulin' proteins LSR, ILDR1 and ILDR2--tricellulin recruitment, epithelial barrier function and implication in deafness pathogenesis. *J Cell Sci,* 126**,** 966-77.

Hiramatsu, K., Serada, S., Enomoto, T., Takahashi, Y., Nakagawa, S., Nojima, S., Morimoto, A., Matsuzaki, S., Yokoyama, T., Takahashi, T., Fujimoto, M., Takemori, H., Ueda, Y., Yoshino, K., Morii, E., Kimura, T. & Naka, T. 2018. LSR Antibody Therapy Inhibits Ovarian Epithelial Tumor Growth by Inhibiting Lipid Uptake. *Cancer research,* 78**,** 516-527.

Holm, T. L., Tornehave, D., Sondergaard, H., Kvist, P. H., Sondergaard, B. C., Hansen, L., Hermit, M. B., Holgersen, K., Vergo, S., Frederiksen, K. S., Haase, C. & Lundsgaard, D. 2018. Evaluating IL-21 as a Potential Therapeutic Target in Crohn's Disease. *Gastroenterol Res Pract,* 2018**,** 5962624.

Hu, J. E., Bojarski, C., Branchi, F., Fromm, M. & Krug, S. M. 2020. Leptin Downregulates Angulin-1 in Active Crohn's Disease via STAT3. *Int J Mol Sci,* 21.

Huang, S. K., Xiao, H. Q., Kleine-Tebbe, J., Paciotti, G., Marsh, D. G., Lichtenstein, L. M. & Liu, M. C. 1995. IL-13 expression at the sites of allergen challenge in patients with asthma. *J Immunol,* 155**,** 2688-94.

Ikenouchi, J., Furuse, M., Furuse, K., Sasaki, H., Tsukita, S. & Tsukita, S. 2005. Tricellulin constitutes a novel barrier at tricellular contacts of epithelial cells. *J Cell Biol,* 171**,** 939-45.

Jantchou, P., Morois, S., Clavel-Chapelon, F., Boutron-Ruault, M. C. & Carbonnel, F. 2010. Animal protein intake and risk of inflammatory bowel disease: The E3N prospective study. *Am J Gastroenterol,* 105**,** 2195-201.

Jess, T., Gamborg, M., Munkholm, P. & Sorensen, T. I. 2007. Overall and cause-specific mortality in ulcerative colitis: meta-analysis of population-based inception cohort studies. *Am J Gastroenterol,* 102**,** 609-17.

Ji, Z., Donaldson, I. J., Liu, J., Hayes, A., Zeef, L. A. & Sharrocks, A. D. 2012. The forkhead transcription factor FOXK2 promotes AP-1-mediated transcriptional regulation. *Mol Cell Biol,* 32**,** 385-98.

Jones, G. R., Lyons, M., Plevris, N., Jenkinson, P. W., Bisset, C., Burgess, C., Din, S., Fulforth, J., Henderson, P., Ho, G. T., Kirkwood, K., Noble, C., Shand, A. G., Wilson, D. C., Arnott, I. D. & Lees, C. W. 2019. IBD prevalence in Lothian, Scotland, derived by capture-recapture methodology. *Gut,* 68**,** 1953-1960.

Jostins, L., Ripke, S., Weersma, R. K., Duerr, R. H., Mcgovern, D. P., Hui, K. Y., Lee, J. C., Schumm, L. P., Sharma, Y., Anderson, C. A., Essers, J., Mitrovic, M., Ning, K., Cleynen, I., Theatre, E., Spain, S. L., Raychaudhuri, S., Goyette, P., Wei, Z., Abraham, C., Achkar, J. P., Ahmad, T., Amininejad, L., Ananthakrishnan, A. N., Andersen, V.,

Andrews, J. M., Baidoo, L., Balschun, T., Bampton, P. A., Bitton, A., Boucher, G., Brand, S., Buning, C., Cohain, A., Cichon, S., D'amato, M., De Jong, D., Devaney, K. L., Dubinsky, M., Edwards, C., Ellinghaus, D., Ferguson, L. R., Franchimont, D., Fransen, K., Gearry, R., Georges, M., Gieger, C., Glas, J., Haritunians, T., Hart, A., Hawkey, C., Hedl, M., Hu, X., Karlsen, T. H., Kupcinskas, L., Kugathasan, S., Latiano, A., Laukens, D., Lawrance, I. C., Lees, C. W., Louis, E., Mahy, G., Mansfield, J., Morgan, A. R., Mowat, C., Newman, W., Palmieri, O., Ponsioen, C. Y., Potocnik, U., Prescott, N. J., Regueiro, M., Rotter, J. I., Russell, R. K., Sanderson, J. D., Sans, M., Satsangi, J., Schreiber, S., Simms, L. A., Sventoraityte, J., Targan, S. R., Taylor, K. D., Tremelling, M., Verspaget, H. W., De Vos, M., Wijmenga, C., Wilson, D. C., Winkelmann, J., Xavier, R. J., Zeissig, S., Zhang, B., Zhang, C. K., Zhao, H., Silverberg, M. S., Annese, V., Hakonarson, H., Brant, S. R., Radford-Smith, G., Mathew, C. G., Rioux, J. D., Schadt, E. E., et al. 2012. Host-microbe interactions have shaped the genetic architecture of inflammatory bowel disease. *Nature,* 491**,** 119-24.

Juuti-Uusitalo, K., Klunder, L. J., Sjollema, K. A., Mackovicova, K., Ohgaki, R., Hoekstra, D., Dekker, J. & Van Ijzendoorn, S. C. 2011. Differential effects of TNF (TNFSF2) and IFN-gamma on intestinal epithelial cell morphogenesis and barrier function in three-dimensional culture. *PLoS One,* 6**,** e22967.

Kahraman, R., Calhan, T., Sahin, A., Ozdil, K., Caliskan, Z., Bireller, E. S. & Cakmakoglu, B. 2017. Are adipocytokines inflammatory or metabolic mediators in patients with inflammatory bowel disease? *Therapeutics and clinical risk management,* 13**,** 1295.

Kamanaka, M., Huber, S., Zenewicz, L. A., Gagliani, N., Rathinam, C., O'connor, W., Jr., Wan, Y. Y., Nakae, S., Iwakura, Y., Hao, L. & Flavell, R. A. 2011. Memory/effector (CD45RB(lo)) CD4 T cells are controlled directly by IL-10 and cause IL-22-dependent intestinal pathology. *J Exp Med,* 208**,** 1027-40.

Kaplan, G. G. & Ng, S. C. 2017. Understanding and Preventing the Global Increase of Inflammatory Bowel Disease. *Gastroenterology,* 152**,** 313-321.e2.

Karin, M., Liu, Z. & Zandi, E. 1997. AP-1 function and regulation. *Curr Opin Cell Biol,* 9**,** 240-6.

Karmiris, K., Koutroubakis, I. E., Xidakis, C., Polychronaki, M., Voudouri, T. & Kouroumalis, E. A. 2006. Circulating Levels of Leptin, Adiponectin, Resistin, and Ghrelin in Inflammatory Bowel Disease. *Inflammatory Bowel Diseases,* 12**,** 100-105.

Kashyap, A. S., Fernandez-Rodriguez, L., Zhao, Y., Monaco, G., Trefny, M. P., Yoshida, N., Martin, K., Sharma, A., Olieric, N., Shah, P., Stanczak, M., Kirchhammer, N., Park, S.

M., Wieckowski, S., Laubli, H., Zagani, R., Kasenda, B., Steinmetz, M. O., Reinecker, H. C. & Zippelius, A. 2019. GEF-H1 Signaling upon Microtubule Destabilization Is Required for Dendritic Cell Activation and Specific Anti-tumor Responses. *Cell Rep,* 28**,** 3367-3380.e8.

Keita, A. V., Lindqvist, C. M., Ost, A., Magana, C. D. L., Schoultz, I. & Halfvarson, J. 2018. Gut Barrier Dysfunction-A Primary Defect in Twins with Crohn's Disease Predominantly Caused by Genetic Predisposition. *J Crohns Colitis,* 12**,** 1200-1209.

Kerppola, T. K. & Curran, T. 1994. Maf and Nrl can bind to AP-1 sites and form heterodimers with Fos and Jun. *Oncogene,* 9**,** 675-84.

Khalili, H., Higuchi, L. M., Ananthakrishnan, A. N., Manson, J. E., Feskanich, D., Richter, J. M., Fuchs, C. S. & Chan, A. T. 2012. Hormone therapy increases risk of ulcerative colitis but not Crohn's disease. *Gastroenterology,* 143**,** 1199-1206.

Kim, H., Pennie, W. D., Sun, Y. & Colburn, N. H. 1997. Differential functional significance of AP-1 binding sites in the promoter of the gene encoding mouse tissue inhibitor of metalloproteinases-3. *Biochem J,* 324 (Pt 2)**,** 547-53.

Kitanaka, N., Nakano, R., Sakai, M., Kitanaka, T., Namba, S., Konno, T., Nakayama, T. & Sugiya, H. 2019. ERK1/ATF-2 signaling axis contributes to interleukin-1β-induced MMP-3 expression in dermal fibroblasts. *PLoS One,* 14**,** e0222869.

Kjærgaard, S., Damm, M. M. B., Chang, J., Riis, L. B., Rasmussen, H. B., Hytting-Andreasen, R., Krug, S. M., Schulzke, J. D., Bindslev, N. & Hansen, M. B. 2020. Altered Structural Expression and Enzymatic Activity Parameters in Quiescent Ulcerative Colitis: Are These Potential Normalization Criteria? *Int J Mol Sci,* 21.

Korn, T., Bettelli, E., Gao, W., Awasthi, A., Jäger, A., Strom, T. B., Oukka, M. & Kuchroo, V. K. 2007. IL-21 initiates an alternative pathway to induce proinflammatory TH17 cells. *Nature,* 448**,** 484-487.

Kreusel, K. M., Fromm, M., Schulzke, J. D. & Hegel, U. 1991. Cl- secretion in epithelial monolayers of mucus-forming human colon cells (HT-29/B6). *Am J Physiol,* 261**,** C574-82.

Krug, S. M., Amasheh, S., Richter, J. F., Milatz, S., Gunzel, D., Westphal, J. K., Huber, O., Schulzke, J. D. & Fromm, M. 2009a. Tricellulin forms a barrier to macromolecules in tricellular tight junctions without affecting ion permeability. *Mol Biol Cell,* 20**,** 3713-24.

Krug, S. M., Amasheh, S., Richter, J. F., Milatz, S., Günzel, D., Westphal, J. K., Huber, O., Schulzke, J. D. & Fromm, M. 2009b. Tricellulin forms a barrier to macromolecules in

tricellular tight junctions without affecting ion permeability. *Molecular biology of the cell,* 20**,** 3713-3724.

Krug, S. M., Bojarski, C., Fromm, A., Lee, I. M., Dames, P., Richter, J. F., Turner, J. R., Fromm, M. & Schulzke, J. D. 2018. Tricellulin is regulated via interleukin-13-receptor alpha2, affects macromolecule uptake, and is decreased in ulcerative colitis. *Mucosal Immunol,* 11**,** 345-356.

Krug, S. M., Fromm, M. & Gunzel, D. 2009c. Two-path impedance spectroscopy for measuring paracellular and transcellular epithelial resistance. *Biophys J,* 97**,** 2202-11.

Krug, S. M., Schulzke, J. D. & Fromm, M. 2014. Tight junction, selective permeability, and related diseases. *Semin Cell Dev Biol,* 36**,** 166-76.

Kühn, R., Löhler, J., Rennick, D., Rajewsky, K. & Müller, W. 1993. Interleukin-10-deficient mice develop chronic enterocolitis. *Cell,* 75**,** 263-274.

Landschulz, W. H., Johnson, P. F. & Mcknight, S. L. 1988. The leucine zipper: a hypothetical structure common to a new class of DNA binding proteins. *Science,* 240**,** 1759-64.

Le Drean, G., Haure-Mirande, V., Ferrier, L., Bonnet, C., Hulin, P., De Coppet, P. & Segain, J. P. 2014. Visceral adipose tissue and leptin increase colonic epithelial tight junction permeability via a RhoA-ROCK-dependent pathway. *Faseb j,* 28**,** 1059-70.

Liu, Z., Yadav, P. K., Xu, X., Su, J., Chen, C., Tang, M., Lin, H., Yu, J., Qian, J., Yang, P. C. & Wang, X. 2011. The increased expression of IL-23 in inflammatory bowel disease promotes intraepithelial and lamina propria lymphocyte inflammatory responses and cytotoxicity. *J Leukoc Biol,* 89**,** 597-606.

Lu, Y., Ye, Y., Bao, W., Yang, Q., Wang, J., Liu, Z. & Shi, S. 2017. Genome-wide identification of genes essential for podocyte cytoskeletons based on single-cell RNA sequencing. *Kidney Int,* 92**,** 1119-1129.

Mak, W. Y., Zhao, M., Ng, S. C. & Burisch, J. 2019. The epidemiology of inflammatory bowel disease: East meets west. *J Gastroenterol Hepatol*.

Manninen, P., Karvonen, A. L., Huhtala, H., Rasmussen, M., Salo, M., Mustaniemi, L., Pirttiniemi, I. & Collin, P. 2012. Mortality in ulcerative colitis and Crohn's disease. A population-based study in Finland. *J Crohns Colitis,* 6**,** 524-8.

Markov, A. G., Veshnyakova, A., Fromm, M., Amasheh, M. & Amasheh, S. 2010. Segmental expression of claudin proteins correlates with tight junction barrier properties in rat intestine. *J Comp Physiol B,* 180**,** 591-8.

Markov, A. G., Vishnevskaya, O. N., Okorokova, L. S., Fedorova, A. A., Kruglova, N. M., Rybalchenko, O. V., Aschenbach, J. R. & Amasheh, S. 2019. Cholera toxin perturbs the paracellular barrier in the small intestinal epithelium of rats by affecting claudin-2 and tricellulin. *Pflugers Archiv : European journal of physiology,* 471**,** 1183-1189.

Martin-Padura, I., Lostaglio, S., Schneemann, M., Williams, L., Romano, M., Fruscella, P., Panzeri, C., Stoppacciaro, A., Ruco, L., Villa, A., Simmons, D. & Dejana, E. 1998. Junctional adhesion molecule, a novel member of the immunoglobulin superfamily that distributes at intercellular junctions and modulates monocyte transmigration. *J Cell Biol,* 142**,** 117-27.

Martini, E., Krug, S. M., Siegmund, B., Neurath, M. F. & Becker, C. 2017. Mend Your Fences: The Epithelial Barrier and its Relationship With Mucosal Immunity in Inflammatory Bowel Disease. *Cell Mol Gastroenterol Hepatol,* 4**,** 33-46.

Masuda, S., Oda, Y., Sasaki, H., Ikenouchi, J., Higashi, T., Akashi, M., Nishi, E. & Furuse, M. 2011. LSR defines cell corners for tricellular tight junction formation in epithelial cells. *J Cell Sci,* 124**,** 548-55.

Meng, Q. & Xia, Y. 2011. c-Jun, at the crossroad of the signaling network. *Protein Cell,* 2**,** 889-98.

Mineta, K., Yamamoto, Y., Yamazaki, Y., Tanaka, H., Tada, Y., Saito, K., Tamura, A., Igarashi, M., Endo, T., Takeuchi, K. & Tsukita, S. 2011. Predicted expansion of the claudin multigene family. *FEBS Lett,* 585**,** 606-12.

Mizoguchi, A. 2012. Healing of intestinal inflammation by IL-22. *Inflamm Bowel Dis,* 18**,** 1777-84.

Moller, F. T., Andersen, V., Wohlfahrt, J. & Jess, T. 2015. Familial risk of inflammatory bowel disease: a population-based cohort study 1977-2011. *Am J Gastroenterol,* 110**,** 564-71.

Moninuola, O. O., Milligan, W., Lochhead, P. & Khalili, H. 2018. Systematic review with meta-analysis: association between acetaminophen and nonsteroidal anti-inflammatory drugs (NSAIDs) and risk of Crohn's disease and ulcerative colitis exacerbation. *Aliment Pharmacol Ther,* 47**,** 1428-1439.

Monteleone, G., Biancone, L., Marasco, R., Morrone, G., Marasco, O., Luzza, F. & Pallone, F. 1997. Interleukin 12 is expressed and actively released by Crohn's disease intestinal lamina propria mononuclear cells. *Gastroenterology,* 112**,** 1169-78.

Monteleone, G., Monteleone, I., Fina, D., Vavassori, P., Del Vecchio Blanco, G., Caruso, R., Tersigni, R., Alessandroni, L., Biancone, L., Naccari, G. C., Macdonald, T. T. & Pallone, F. 2005. Interleukin-21 enhances T-helper cell type I signaling and interferon-gamma production in Crohn's disease. *Gastroenterology,* 128**,** 687-94.

Morampudi, V., Graef, F. A., Stahl, M., Dalwadi, U., Conlin, V. S., Huang, T., Vallance, B. A., Yu, H. B. & Jacobson, K. 2016. Tricellular Tight Junction Protein Tricellulin Is Targeted by the Enteropathogenic Escherichia coli Effector EspG1, Leading to Epithelial Barrier Disruption. *Infection and immunity,* 85**,** e00700-16.

Murakami, H. & Masui, H. 1980. Hormonal control of human colon carcinoma cell growth in serum-free medium. *Proc Natl Acad Sci U S A,* 77**,** 3464-8.

Murakami, Y., Nishiwaki, Y., Oba, M. S., Asakura, K., Ohfuji, S., Fukushima, W., Suzuki, Y. & Nakamura, Y. 2019. Estimated prevalence of ulcerative colitis and Crohn's disease in Japan in 2014: an analysis of a nationwide survey. *J Gastroenterol,* 54**,** 1070-1077.

Musti, A. M., Treier, M. & Bohmann, D. 1997. Reduced ubiquitin-dependent degradation of c-Jun after phosphorylation by MAP kinases. *Science,* 275**,** 400-2.

Myers, M. G., Cowley, M. A. & Munzberg, H. 2008. Mechanisms of leptin action and leptin resistance. *Annu Rev Physiol,* 70**,** 537-56.

Nagahama, M., Takehara, M. & Kobayashi, K. 2018. Interaction of Clostridium perfringens Iota Toxin and Lipolysis-Stimulated Lipoprotein Receptor (LSR). *Toxins,* 10**,** 405.

Nagtegaal, A. P., Broer, L., Zilhao, N. R., Jakobsdottir, J., Bishop, C. E., Brumat, M., Christiansen, M. W., Cocca, M., Gao, Y., Heard-Costa, N. L., Evans, D. S., Pankratz, N., Pratt, S. R., Price, T. R., Spankovich, C., Stimson, M. R., Valle, K., Vuckovic, D., Wells, H., Eiriksdottir, G., Fransen, E., Ikram, M. A., Li, C. M., Longstreth, W. T., Jr., Steves, C., Van Camp, G., Correa, A., Cruickshanks, K. J., Gasparini, P., Girotto, G., Kaplan, R. C., Nalls, M., Schweinfurth, J. M., Seshadri, S., Sotoodehnia, N., Tranah, G. J., Uitterlinden, A. G., Wilson, J. G., Gudnason, V., Hoffman, H. J., Williams, F. M. K. & Goedegebure, A. 2019. Genome-wide association meta-analysis identifies five novel loci for age-related hearing impairment. *Sci Rep,* 9**,** 15192.

Neurath, M. F. 2017. Current and emerging therapeutic targets for IBD. *Nat Rev Gastroenterol Hepatol,* 14**,** 269-278.

Neurath, M. F. 2019. Targeting immune cell circuits and trafficking in inflammatory bowel disease. *Nat Immunol,* 20**,** 970-979.

Ng, S. C., Shi, H. Y., Hamidi, N., Underwood, F. E., Tang, W., Benchimol, E. I., Panaccione, R., Ghosh, S., Wu, J. C. Y., Chan, F. K. L., Sung, J. J. Y. & Kaplan, G. G. 2017. Worldwide incidence and prevalence of inflammatory bowel disease in the 21st century: a systematic review of population-based studies. *The Lancet,* 390**,** 2769-2778.

Nishizawa, M., Kataoka, K., Goto, N., Fujiwara, K. T. & Kawai, S. 1989. v-maf, a viral oncogene that encodes a "leucine zipper" motif. *Proc Natl Acad Sci U S A,* 86**,** 7711-5.

Nomura, K., Obata, K., Keira, T., Miyata, R., Hirakawa, S., Takano, K.-I., Kohno, T., Sawada, N., Himi, T. & Kojima, T. 2014. Pseudomonas aeruginosa elastase causes transient disruption of tight junctions and downregulation of PAR-2 in human nasal epithelial cells. *Respiratory research,* 15**,** 21-21.

Oshima, T., Miwa, H. & Joh, T. 2008. Changes in the expression of claudins in active ulcerative colitis. *Journal of Gastroenterology and Hepatology,* 23**,** S146-S150.

Palamides, P., Jodeleit, H., Fohlinger, M., Beigel, F., Herbach, N., Mueller, T., Wolf, E., Siebeck, M. & Gropp, R. 2016. A mouse model for ulcerative colitis based on NOD-scid IL2R gammanull mice reconstituted with peripheral blood mononuclear cells from affected individuals. *Dis Model Mech,* 9**,** 985-97.

Paul, G., Schäffler, A., Neumeier, M., Fürst, A., Bataillle, F., Buechler, C., Müller-Ladner, U., Schölmerich, J., Rogler, G. & Herfarth, H. 2006. Profiling adipocytokine secretion from creeping fat in Crohn's disease. *Inflammatory Bowel Diseases,* 12**,** 471-477.

Persson, P. G., Ahlbom, A. & Hellers, G. 1992. Diet and inflammatory bowel disease: a case-control study. *Epidemiology,* 3**,** 47-52.

Piccioli, P. & Rubartelli, A. 2013. The secretion of IL-1beta and options for release. *Semin Immunol,* 25**,** 425-9.

Pickert, G., Neufert, C., Leppkes, M., Zheng, Y., Wittkopf, N., Warntjen, M., Lehr, H. A., Hirth, S., Weigmann, B., Wirtz, S., Ouyang, W., Neurath, M. F. & Becker, C. 2009. STAT3 links IL-22 signaling in intestinal epithelial cells to mucosal wound healing. *J Exp Med,* 206**,** 1465-72.

Plum, L., Rother, E., Munzberg, H., Wunderlich, F. T., Morgan, D. A., Hampel, B., Shanabrough, M., Janoschek, R., Konner, A. C., Alber, J., Suzuki, A., Krone, W., Horvath, T. L., Rahmouni, K. & Bruning, J. C. 2007. Enhanced leptin-stimulated Pi3k activation in the CNS promotes white adipose tissue transdifferentiation. *Cell Metab,* 6**,** 431-45.

Procaccini, C., Lourenco, E. V., Matarese, G. & La Cava, A. 2009. Leptin signaling: A key pathway in immune responses. *Curr Signal Transduct Ther,* 4**,** 22-30.

Raleigh, D. R., Marchiando, A. M., Zhang, Y., Shen, L., Sasaki, H., Wang, Y., Long, M. & Turner, J. R. 2010. Tight junction-associated MARVEL proteins marveld3, tricellulin, and occludin have distinct but overlapping functions. *Mol Biol Cell,* 21**,** 1200-13.

Reaves, D. K., Fagan-Solis, K. D., Dunphy, K., Oliver, S. D., Scott, D. W. & Fleming, J. M. 2014. The role of lipolysis stimulated lipoprotein receptor in breast cancer and directing breast cancer cell behavior. *PloS one,* 9**,** e91747-e91747.

Reaves, D. K., Hoadley, K. A., Fagan-Solis, K. D., Jima, D. D., Bereman, M., Thorpe, L., Hicks, J., Mcdonald, D., Troester, M. A., Perou, C. M. & Fleming, J. M. 2017. Nuclear Localized LSR: A Novel Regulator of Breast Cancer Behavior and Tumorigenesis. *Molecular cancer research : MCR,* 15**,** 165-178.

Recher, M., Berglund, L. J., Avery, D. T., Cowan, M. J., Gennery, A. R., Smart, J., Peake, J., Wong, M., Pai, S.-Y., Baxi, S., Walter, J. E., Palendira, U., Tangye, G. A., Rice, M., Brothers, S., Al-Herz, W., Oettgen, H., Eibel, H., Puck, J. M., Cattaneo, F., Ziegler, J. B., Giliani, S., Tangye, S. G. & Notarangelo, L. D. 2011. IL-21 is the primary common γ chain-binding cytokine required for human B-cell differentiation in vivo. *Blood,* 118**,** 6824-6835.

Reinecker, H. C., Steffen, M., Witthoeft, T., Pflueger, I., Schreiber, S., Macdermott, R. P. & Raedler, A. 1993. Enhanced secretion of tumour necrosis factor-alpha, IL-6, and IL-1 beta by isolated lamina propria mononuclear cells from patients with ulcerative colitis and Crohn's disease. *Clin Exp Immunol,* 94**,** 174-81.

Reinisch, W., Panes, J., Khurana, S., Toth, G., Hua, F., Comer, G. M., Hinz, M., Page, K., O'toole, M., Moorehead, T. M., Zhu, H., Sun, Y. & Cataldi, F. 2015. Anrukinzumab, an anti-interleukin 13 monoclonal antibody, in active UC: efficacy and safety from a phase IIa randomised multicentre study. *Gut,* 64**,** 894-900.

Rodrigues, V. S., Milanski, M., Fagundes, J. J., Torsoni, A. S., Ayrizono, M. L. S., Nunez, C. E. C., Dias, C. B., Meirelles, L. R., Dalal, S., Coy, C. S. R., Velloso, L. A. & Leal, R. F. 2012. Serum levels and mesenteric fat tissue expression of adiponectin and leptin in patients with Crohn's disease. *Clinical & Experimental Immunology,* 170**,** 358-364.

Roth, M. P., Petersen, G. M., Mcelree, C., Vadheim, C. M., Panish, J. F. & Rotter, J. I. 1989. Familial empiric risk estimates of inflammatory bowel disease in Ashkenazi Jews. *Gastroenterology,* 96**,** 1016-20.

Sadlack, B., Merz, H., Schorle, H., Schimpl, A., Feller, A. C. & Horak, I. 1993. Ulcerative colitis-like disease in mice with a disrupted interleukin-2 gene. *Cell,* 75**,** 253-261.

Sahami, S., Kooij, I. A., Meijer, S. L., Van Den Brink, G. R., Buskens, C. J. & Te Velde, A. A. 2016. The Link between the Appendix and Ulcerative Colitis: Clinical Relevance and Potential Immunological Mechanisms. *Am J Gastroenterol,* 111**,** 163-9.

Samaridis, J., Casorati, G., Traunecker, A., Iglesias, A., Gutierrez, J. C., Muller, U. & Palacios, R. 1991. Development of lymphocytes in interleukin 7-transgenic mice. *Eur J Immunol,* 21**,** 453-60.

Sandle, G. I. 2005. Pathogenesis of Diarrhea in Ulcerative Colitis: New Views on an Old Problem. *Journal of Clinical Gastroenterology,* 39**,** S49-S52.

Sartor, R. B. 2006. Mechanisms of disease: pathogenesis of Crohn's disease and ulcerative colitis. *Nat Clin Pract Gastroenterol Hepatol,* 3**,** 390-407.

Sasaki, A., Yasukawa, H., Shouda, T., Kitamura, T., Dikic, I. & Yoshimura, A. 2000. CIS3/SOCS-3 suppresses erythropoietin (EPO) signaling by binding the EPO receptor and JAK2. *J Biol Chem,* 275**,** 29338-47.

Schaab, M. & Kratzsch, J. 2015. The soluble leptin receptor. *Best Pract Res Clin Endocrinol Metab,* 29**,** 661-70.

Schroeder, K. W., Tremaine, W. J. & Ilstrup, D. M. 1987. Coated oral 5-aminosalicylic acid therapy for mildly to moderately active ulcerative colitis. A randomized study. *N Engl J Med,* 317**,** 1625-9.

Selvaratnam, S., Gullino, S., Shim, L., Lee, E., Lee, A., Paramsothy, S. & Leong, R. W. 2019. Epidemiology of inflammatory bowel disease in South America: A systematic review. *World J Gastroenterol,* 25**,** 6866-6875.

Shimada, H., Abe, S., Kohno, T., Satohisa, S., Konno, T., Takahashi, S., Hatakeyama, T., Arimoto, C., Kakuki, T., Kaneko, Y., Takano, K.-I., Saito, T. & Kojima, T. 2017a. Loss of tricellular tight junction protein LSR promotes cell invasion and migration via upregulation of TEAD1/AREG in human endometrial cancer. *Scientific reports,* 7**,** 37049-37049.

Shimada, H., Satohisa, S., Kohno, T., Konno, T., Takano, K.-I., Takahashi, S., Hatakeyama, T., Arimoto, C., Saito, T. & Kojima, T. 2017b. Downregulation of lipolysis-stimulated lipoprotein receptor promotes cell invasion via claudin-1-mediated matrix metalloproteinases in human endometrial cancer. *Oncology letters,* 14**,** 6776-6782.

Shimada, H., Satohisa, S., Kohno, T., Takahashi, S., Hatakeyama, T., Konno, T., Tsujiwaki, M., Saito, T. & Kojima, T. 2016a. The roles of tricellular tight junction protein lipolysis-stimulated lipoprotein receptor in malignancy of human endometrial cancer cells. *Oncotarget,* 7**,** 27735-52.

Shimada, H., Satohisa, S., Kohno, T., Takahashi, S., Hatakeyama, T., Konno, T., Tsujiwaki, M., Saito, T. & Kojima, T. 2016b. The roles of tricellular tight junction protein lipolysis-stimulated lipoprotein receptor in malignancy of human endometrial cancer cells. *Oncotarget,* 7**,** 27735-27752.

Silverberg, M. S., Satsangi, J., Ahmad, T., Arnott, I. D., Bernstein, C. N., Brant, S. R., Caprilli, R., Colombel, J. F., Gasche, C., Geboes, K., Jewell, D. P., Karban, A., Loftus, E. V., Jr., Pena, A. S., Riddell, R. H., Sachar, D. B., Schreiber, S., Steinhart, A. H., Targan, S. R., Vermeire, S. & Warren, B. F. 2005. Toward an integrated clinical, molecular and serological classification of inflammatory bowel disease: report of a Working Party of the 2005 Montreal World Congress of Gastroenterology. *Can J Gastroenterol,* 19 Suppl A**,** 5a-36a.

Sitaraman, S., Liu, X., Charrier, L., Gu, L. H., Ziegler, T. R., Gewirtz, A. & Merlin, D. 2004. Colonic leptin: source of a novel proinflammatory cytokine involved in IBD. *FASEB J,* 18**,** 696-8.

Smeal, T., Hibi, M. & Karin, M. 1994. Altering the specificity of signal transduction cascades: positive regulation of c-Jun transcriptional activity by protein kinase A. *Embo j,* 13**,** 6006-10.

Smithgall, M. D., Comeau, M. R., Yoon, B. R., Kaufman, D., Armitage, R. & Smith, D. E. 2008. IL-33 amplifies both Th1- and Th2-type responses through its activity on human basophils, allergen-reactive Th2 cells, iNKT and NK cells. *Int Immunol,* 20**,** 1019-30.

Sokol, H., Brot, L., Stefanescu, C., Auzolle, C., Barnich, N., Buisson, A., Fumery, M., Pariente, B., Le Bourhis, L., Treton, X., Nancey, S., Allez, M. & Seksik, P. 2020. Prominence of ileal mucosa-associated microbiota to predict postoperative endoscopic recurrence in Crohn's disease. *Gut,* 69**,** 462-472.

Staehelin, L. A. 1973. Further observations on the fine structure of freeze-cleaved tight junctions. *J Cell Sci,* 13**,** 763-86.

Staehelin, L. A., Mukherjee, T. M. & Williams, A. W. 1969. Freeze-etch appearance of the tight junctions in the epithelium of small and large intestine of mice. *Protoplasma,* 67**,** 165-84.

Steed, E., Rodrigues, N. T., Balda, M. S. & Matter, K. 2009. Identification of MarvelD3 as a tight junction-associated transmembrane protein of the occludin family. *BMC Cell Biol,* 10**,** 95.

Stenger, C., Hanse, M., Pratte, D., Mbala, M. L., Akbar, S., Koziel, V., Escanye, M. C., Kriem, B., Malaplate-Armand, C., Olivier, J. L., Oster, T., Pillot, T. & Yen, F. T. 2010. Up-regulation of hepatic lipolysis stimulated lipoprotein receptor by leptin: a potential lever for controlling lipid clearance during the postprandial phase. *Faseb j,* 24**,** 4218-28.

Stockmann, M., Gitter, A. H., Sorgenfrei, D., Fromm, M. & Schulzke, J. D. 1999. Low edge damage container insert that adjusts intestinal forceps biopsies into Ussing chamber systems. *Pflugers Arch,* 438**,** 107-12.

Sugase, T., Takahashi, T., Serada, S., Fujimoto, M., Ohkawara, T., Hiramatsu, K., Koh, M., Saito, Y., Tanaka, K., Miyazaki, Y., Makino, T., Kurokawa, Y., Yamasaki, M., Nakajima, K., Hanazaki, K., Mori, M., Doki, Y. & Naka, T. 2018. Lipolysis-stimulated lipoprotein receptor overexpression is a novel predictor of poor clinical prognosis and a potential therapeutic target in gastric cancer. *Oncotarget,* 9**,** 32917-32928.

Sugimoto, K., Ogawa, A., Mizoguchi, E., Shimomura, Y., Andoh, A., Bhan, A. K., Blumberg, R. S., Xavier, R. J. & Mizoguchi, A. 2008. IL-22 ameliorates intestinal inflammation in a mouse model of ulcerative colitis. *J Clin Invest,* 118**,** 534-44.

Sutherland, L. R., Ramcharan, S., Bryant, H. & Fick, G. 1990. Effect of cigarette smoking on recurrence of Crohn's disease. *Gastroenterology,* 98**,** 1123-8.

Swaroop, A., Xu, J. Z., Pawar, H., Jackson, A., Skolnick, C. & Agarwal, N. 1992. A conserved retina-specific gene encodes a basic motif/leucine zipper domain. *Proc Natl Acad Sci U S A,* 89**,** 266-70.

Thia, K. T., Sandborn, W. J., Harmsen, W. S., Zinsmeister, A. R. & Loftus, E. V. 2010. Risk Factors Associated With Progression to Intestinal Complications of Crohn's Disease in a Population-Based Cohort. *Gastroenterology,* 139**,** 1147-1155.

To, N., Ford, A. C. & Gracie, D. J. 2016a. Systematic review with meta-analysis: the effect of tobacco smoking on the natural history of ulcerative colitis. *Aliment Pharmacol Ther,* 44**,** 117-26.

To, N., Gracie, D. J. & Ford, A. C. 2016b. Systematic review with meta-analysis: the adverse effects of tobacco smoking on the natural history of Crohn's disease. *Aliment Pharmacol Ther,* 43**,** 549-61.

Toru, H., Pawankar, R., Ra, C., Yata, J. & Nakahata, T. 1998. Human mast cells produce IL-13 by high-affinity IgE receptor cross-linking: enhanced IL-13 production by IL-4-primed human mast cells. *J Allergy Clin Immunol,* 102**,** 491-502.

Trayhurn, P. & Wood, I. S. 2004. Adipokines: inflammation and the pleiotropic role of white adipose tissue. *Br J Nutr,* 92**,** 347-55.

Tsukita, S., Furuse, M. & Itoh, M. 2001. Multifunctional strands in tight junctions. *Nat Rev Mol Cell Biol,* 2**,** 285-93.

Tsurumi, C., Ishida, N., Tamura, T., Kakizuka, A., Nishida, E., Okumura, E., Kishimoto, T., Inagaki, M., Okazaki, K., Sagata, N. & Et Al. 1995. Degradation of c-Fos by the 26S proteasome is accelerated by c-Jun and multiple protein kinases. *Mol Cell Biol,* 15**,** 5682-7.

Ungaro, R., Mehandru, S., Allen, P. B., Peyrin-Biroulet, L. & Colombel, J. F. 2017. Ulcerative colitis. *Lancet,* 389**,** 1756-1770.

Urban, J. F., Jr., Noben-Trauth, N., Donaldson, D. D., Madden, K. B., Morris, S. C., Collins, M. & Finkelman, F. D. 1998. IL-13, IL-4Ralpha, and Stat6 are required for the expulsion of the gastrointestinal nematode parasite Nippostrongylus brasiliensis. *Immunity,* 8**,** 255-64.

Ussing, H. H. & Zerahn, K. 1951. Active transport of sodium as the source of electric current in the short-circuited isolated frog skin. *Acta Physiol Scand,* 23**,** 110-27.

Valentini, L., Wirth, E. K., Schweizer, U., Hengstermann, S., Schaper, L., Koernicke, T., Dietz, E., Norman, K., Buning, C., Winklhofer-Roob, B. M., Lochs, H. & Ockenga, J. 2009. Circulating adipokines and the protective effects of hyperinsulinemia in inflammatory bowel disease. *Nutrition,* 25**,** 172-181.

Van Lint, C., Burny, A. & Verdin, E. 1991. The intragenic enhancer of human immunodeficiency virus type 1 contains functional AP-1 binding sites. *J Virol,* 65**,** 7066-72.

Veltkamp, C., Tonkonogy, S. L., De Jong, Y. P., Albright, C., Grenther, W. B., Balish, E., Terhorst, C. & Sartor, R. B. 2001. Continuous stimulation by normal luminal bacteria is essential for the development and perpetuation of colitis in Tg(epsilon26) mice. *Gastroenterology,* 120**,** 900-13.

Vivinus-Nébot, M., Frin-Mathy, G., Bzioueche, H., Dainese, R., Bernard, G., Anty, R., Filippi, J., Saint-Paul, M. C., Tulic, M. K., Verhasselt, V., Hébuterne, X. & Piche, T. 2014. Functional bowel symptoms in quiescent inflammatory bowel diseases: role of epithelial barrier disruption and low-grade inflammation. *Gut,* 63**,** 744-52.

Wade, J. B. & Karnovsky, M. J. 1974. The structure of the zonula occludens. A single fibril model based on freeze-fracture. *J Cell Biol,* 60**,** 168-80.

Waluga, M., Hartleb, M., Boryczka, G., Kukla, M. & Zwirska-Korczala, K. 2014. Serum adipokines in inflammatory bowel disease. *World J Gastroenterol,* 20**,** 6912-7.

Wang, S., Zhu, W., Ouyang, L., Li, J., Li, S. & Yang, X. 2020. Up-Regulation of Tiam1 Promotes the Radioresistance of Laryngeal Squamous Cell Carcinoma Through Activation of the JNK/ATF-2 Signaling Pathway. *Onco Targets Ther,* 13**,** 7065-7074.

Wang, X., Fan, X., Deng, H., Zhang, X., Zhang, K., Xu, J., Li, N., Han, Q. & Liu, Z. 2019. Use of oral contraceptives and risk of ulcerative colitis - A systematic review and meta-analysis. *Pharmacol Res,* 139**,** 367-374.

Weidinger, C., Ziegler, J. F., Letizia, M., Schmidt, F. & Siegmund, B. 2018. Adipokines and Their Role in Intestinal Inflammation. *Front Immunol,* 9**,** 1974.

Wilks, S. & Moxon, W. 1889. *Lectures on pathological anatomy*, Longmans, Green.

Woerly, G., Lacy, P., Younes, A. B., Roger, N., Loiseau, S., Moqbel, R. & Capron, M. 2002. Human eosinophils express and release IL-13 following CD28-dependent activation. *J Leukoc Biol,* 72**,** 769-79.

Wright, J. F., Guo, Y., Quazi, A., Luxenberg, D. P., Bennett, F., Ross, J. F., Qiu, Y., Whitters, M. J., Tomkinson, K. N., Dunussi-Joannopoulos, K., Carreno, B. M., Collins, M. & Wolfman, N. M. 2007. Identification of an interleukin 17F/17A heterodimer in activated human CD4+ T cells. *J Biol Chem,* 282**,** 13447-55.

Xie, T., Akbar, S., Stathopoulou, M. G., Oster, T., Masson, C., Yen, F. T. & Visvikis-Siest, S. 2018a. Epistatic interaction of apolipoprotein E and lipolysis-stimulated lipoprotein receptor genetic variants is associated with Alzheimer's disease. *Neurobiology of aging,* 69**,** 292.e1-292.e5.

Xie, T., Stathopoulou, M. G., Akbar, S., Oster, T., Siest, G., Yen, F. T. & Visvikis-Siest, S. 2018b. Effect of LSR polymorphism on blood lipid levels and age-specific epistatic interaction with the APOE common polymorphism. *Clinical genetics,* 93**,** 846-852.

Xu, L., Lochhead, P., Ko, Y., Claggett, B., Leong, R. W. & Ananthakrishnan, A. N. 2017. Systematic review with meta-analysis: breastfeeding and the risk of Crohn's disease and ulcerative colitis. *Aliment Pharmacol Ther,* 46**,** 780-789.

Yang , X. O., Chang , S. H., Park , H., Nurieva , R., Shah , B., Acero , L., Wang , Y.-H., Schluns , K. S., Broaddus , R. R., Zhu , Z. & Dong , C. 2008. Regulation of inflammatory responses by IL-17F. *Journal of Experimental Medicine,* 205**,** 1063-1075.

Yen, D., Cheung, J., Scheerens, H., Poulet, F., Mcclanahan, T., Mckenzie, B., Kleinschek, M. A., Owyang, A., Mattson, J., Blumenschein, W., Murphy, E., Sathe, M., Cua, D. J., Kastelein, R. A. & Rennick, D. 2006. IL-23 is essential for T cell-mediated colitis and promotes inflammation via IL-17 and IL-6. *J Clin Invest,* 116**,** 1310-6.

Yen, F. T., Mann, C. J., Guermani, L. M., Hannouche, N. F., Hubert, N., Hornick, C. A., Bordeau, V. N., Agnani, G. & Bihain, B. E. 1994. Identification of a lipolysis-stimulated receptor that is distinct from the LDL receptor and the LDL receptor-related protein. *Biochemistry,* 33**,** 1172-80.

Yilmaz, B., Juillerat, P., Oyas, O., Ramon, C., Bravo, F. D., Franc, Y., Fournier, N., Michetti, P., Mueller, C., Geuking, M., Pittet, V. E. H., Maillard, M. H., Rogler, G., Wiest, R., Stelling, J. & Macpherson, A. J. 2019. Microbial network disturbances in relapsing refractory Crohn's disease. *Nat Med,* 25**,** 323-336.

Zeissig, S., Bojarski, C., Buergel, N., Mankertz, J., Zeitz, M., Fromm, M. & Schulzke, J. D. 2004. Downregulation of epithelial apoptosis and barrier repair in active Crohn's disease by tumour necrosis factor alpha antibody treatment. *Gut,* 53**,** 1295-302.

Zeissig, S., Burgel, N., Gunzel, D., Richter, J., Mankertz, J., Wahnschaffe, U., Kroesen, A. J., Zeitz, M., Fromm, M. & Schulzke, J. D. 2007. Changes in expression and distribution of claudin 2, 5 and 8 lead to discontinuous tight junctions and barrier dysfunction in active Crohn's disease. *Gut,* 56**,** 61-72.

Zhang, J., Chen, S. L. & Li, L. B. 2017. Correlation between intestinal flora and serum inflammatory factors in patients with Crohn's disease. *Eur Rev Med Pharmacol Sci,* 21**,** 4913-4917.

Zhou, C., Huang, Y., Chen, Y., Xie, Y., Wen, H., Tan, W. & Wang, C. 2020. miR-602 Mediates the RASSF1A/JNK Pathway, Thereby Promoting Postoperative Recurrence in Nude Mice with Liver Cancer. *Onco Targets Ther,* 13**,** 6767-6776.

Ziff, E. B. 1990. Transcription factors: a new family gathers at the cAMP response site. *Trends Genet,* 6**,** 69-72.

Zou, Y., Wu, L., Xu, W., Zhou, X., Ye, K., Xiong, H., Song, C. & Xie, Y. 2020. Correlation between antibiotic use in childhood and subsequent inflammatory bowel disease: a systematic review and meta-analysis. *Scand J Gastroenterol,* 55**,** 301-311.

9 Abbreviations

AC	alternating current
AJ	adherens junction
AP-1	activator protein 1
APC	antigen presenting cell
APS	ammonium persulfate
ATF	activating transcription factor
BAT	brown adipose tissue
BCA	bicinchoninic acid
bp	base pair
BSA	bovine serum albumin
bTJ	bicellular tight junction
Caco-2	Cell line cancer coli-2
cAMP	cyclic adenosine monophosphate
CD	Crohn's disease
CD_{Active}	active CD
CD_{Rem}	remission of CD
CDT	*Clostridium difficile* transferase
Cldn	claudin
CRE	cAMP-responsive element
Da	Dalton
DAPI	4’,6-diamidino-2-phenylindole
DC	dendritic cell
DLR	dual luciferase reporter
DMEM	Dulbecco's modified eagle medium
DMSO	dimethyl sulfoxide
DS	desmosome
DSS	dextran sulphate sodium
DTT	dithiothreitol
EDTA	ethylene diamine tetra acetic acid
EGTA	ethylene glycol tetra acetic acid
ERK	extracellular signal-regulated kinases
EtBr	ethidium bromide
FBS	fetal bovine serum
FD	FITC-dextran
FD4	FD 4 kDa

FFPE	formalin-fixed paraffin-embedded
FITC	fluorescein isothiocyanate
GWAS	genome-wide association studies
HRP	horseradish peroxidase
IBD	inflammatory bowel disease
IFN	interferon
Ig-like	immunoglobulin-like domain
IHC	immunohistochemistry
IL	interleukin
IL-13Rα2	IL-13 receptor alpha 2
IL-4Rα	IL-4 receptor α
ILC	innate lymphoid cell
ILDR1	immunoglobulin-like domain-containing receptor 1 (= angulin-2)
ILDR2	immunoglobulin-like domain-containing receptor 2 (= angulin-3)
ISMARA	Integrated System for Motif Activity Response Analysis
JAK	Janus kinase
JAM	junctional adhesion molecule
JDP	Jun-dimerizing protein
JNK	c-Jun N-terminal kinase
kDa	kilodalton
LB	lysogeny broth
LPMC	lamina propria mononuclear cell
LR	leptin receptor
LSR	lipolysis-stimulated lipoprotein receptor (= angulin-1)
Maf	musculoaponeurotic fibrosarcoma
MAPK	mitogen-activated protein kinase
MARVEL	myelin and lymphocyte and related proteins for vesicle trafficking and membrane link (MARVEL D2 = tricellulin)
MAT	mesenteric adipose tissue
MEM	minimum essential medium
MHC	major histocompatibility complex
Mv	microvillus
NK	natural killer cell
nm	nanometer
Nrl	neural retina leucine zipper
OCEL	occludin ELL-like domain
PCR	polymerase chain reaction

PFA	paraformaldehyde
PVDF	polyvinylidene fluoride
PVP	polyvinylpyrrolidone
R^{epi}	epithelial resistance
RPMI	Roswell park memorial institute
R^{sub}	subepithelial resistance
RT-PCR	real-time PCR
SAT	subcutaneous adipose tissue
SDS	sodium dodecyl sulfonate
SDS-PAGE	SDS-polyacrylamide gel electrophoresis
SEM	standard error of the mean
SHP-2	Src-homology-2 domain protein
SMR	standardized mortality ratio
SOCS3	suppressor of cytokine signaling 3
STAT	signal transducer and activator of transcription
TAE	tris-acetate/EDTA
TAMP	TJ-associated MARVEL protein
TBS	tris-buffered saline
TEMED	tetramethyl ethylenediamine
TER	transepithelial resistance
T_h	T helper
TJ	tight junction
TLR	toll-like receptor
TNF	tumor necrosis factor
TPA	12-O-tetradecanoate-13-acetate
TRE	TPA-responsive element
T_{reg}	regulatory T cell
tTJ	tricellular tight junction
UC	ulcerative colitis
UC_{Active}	active UC
UC_{Rem}	remission of UC
UV	ultraviolet
VAT	visceral adipose tissue
WAT	white adipose tissue
WT	wild type
ZO-1	Zonula occludens protein 1

10 List of own publications

- Hu JE, Bojarski C, Branchi F, Fromm M, Krug SM. Leptin Downregulates Angulin-1 in Active Crohn's Disease via STAT3. Int J Mol Sci. 2020 Oct 22;21(21):E7824. doi: 10.3390/ijms21217824. PMID: 33105684.